

## **Copyright Warning & Restrictions**

The copyright law of the United States (Title 17, United States Code) governs the making of photocopies or other reproductions of copyrighted material.

Under certain conditions specified in the law, libraries and archives are authorized to furnish a photocopy or other reproduction. One of these specified conditions is that the photocopy or reproduction is not to be “used for any purpose other than private study, scholarship, or research.” If a user makes a request for, or later uses, a photocopy or reproduction for purposes in excess of “fair use” that user may be liable for copyright infringement,

This institution reserves the right to refuse to accept a copying order if, in its judgment, fulfillment of the order would involve violation of copyright law.

**Please Note: The author retains the copyright while the New Jersey Institute of Technology reserves the right to distribute this thesis or dissertation**

Printing note: If you do not wish to print this page, then select “Pages from: first page # to: last page #” on the print dialog screen

The Van Houten library has removed some of the personal information and all signatures from the approval page and biographical sketches of theses and dissertations in order to protect the identity of NJIT graduates and faculty.

## **ABSTRACT**

### **IMPLEMENTATION OF FORTRAN FINITE ELEMENT ANALYSIS SOURCE CODE WITH APPLICATION: PARTICLE DEPOSITION IN A 90 DEGREE DUCT BEND**

**by  
Pantaleo Loiacono**

Two FORTRAN 77 finite element analysis source codes, by J.N. Reddy, were input into a PC, debugged, executed, and tested successfully. These programs are available to students interested in implementing a good finite element analysis source code on a PC or on a workstation in one or two dimensions. The programs can solve problems relating to heat transfer, stresses, beam analysis, frames, trusses, plane elasticity, plate bending, and laminar viscous incompressible fluids with various node and element combinations.

The two-dimensional program was used to obtain the velocity distributions in a 90 degree duct bend with incoming and exiting fully developed flows so that particle deposition analysis could be studied varying the inertia parameter,  $S$ . It was found that at values of  $S$  below 1.0, the maximum particle deposition occurred at the point where the 90 degree duct bend met the exit vertical section; for  $S=1.0$ , deposition was even throughout the duct; finally, for  $S$  greater than 1.0, maximum particle deposition occurred at the center of the 90 degree turn of the duct. All particles were deposited on the upper wall of the duct. Extra anti-corrosive agents should be placed in the area of maximum particle deposition when the particulate matter is harmful to the duct material.

**IMPLEMENTATION OF FORTRAN  
FINITE ELEMENT ANALYSIS SOURCE CODE  
WITH APPLICATION:  
PARTICLE DEPOSITION IN A 90 DEGREE DUCT BEND**

**by  
Pantaleo Loiacono**

**A Thesis  
Submitted to the Faculty of  
New Jersey Institute of Technology  
in Partial Fulfillment of the Requirements for the Degree of  
Master of Science in Mechanical Engineering**

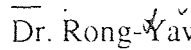
**Department of Mechanical Engineering**

**October 1996**

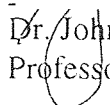
**APPROVAL PAGE**

**IMPLEMENTATION OF FORTRAN  
FINITE ELEMENT ANALYSIS SOURCE CODE  
WITH APPLICATION:  
PARTICLE DEPOSITION IN A 90 DEGREE DUCT BEND**

**Pantaleo Loiacono**

  
Dr. Rong-Yaw Chen, Thesis Advisor  
Professor of Mechanical Engineering, NJIT

Date

  
Dr. John V. Droughton  
Professor of Mechanical Engineering, NJIT

Date

Dr. Ernest S. Geskin  
Professor of Mechanical Engineering, NJIT

Date

## **BIOGRAPHICAL SKETCH**

**Author:** Pantaleo Loiacono

**Degree:** Master of Science

**Place of Birth:** Hoboken, New Jersey

### **Undergraduate and Graduate Education:**

- Master of Science in Mechanical Engineering,  
New Jersey Institute of Technology, Newark, NJ, 1996
- Bachelor of Science in Mechanical Engineering,  
Rutgers University, College of Engineering, New Brunswick, NJ, 1994

**Major:** Mechanical Engineering

To my beloved family

## **ACKNOWLEDGMENT**

I would like to express my sincere gratitude to Dr. Rong-Yaw Chen for advising me throughout this thesis. His suggestions and advice were very helpful during this study. Special thanks to Dr. John V. Droughton and Dr. Ernest S. Geskin for participating in my committee.

I would also like to thank the staff at the University Learning Center for supporting me for three semesters as a graduate assistant. I would especially like to thank Sheridan O. Quarless and Heather M. Rochester who were my supervisors and friends at the ULC.



## TABLE OF CONTENTS

Chapter	Page
1 INTRODUCTION.....	1
1.1 Background Information.....	1
1.2 Objective.....	3
2 LITERATURE SURVEY.....	4
2.1 FORTRAN Source Code.....	4
2.1.1 Alternate Programs.....	4
2.1.2 Entering Reddy's Source Code.....	5
2.2 Applications of the Source Code.....	6
2.2.1 Type of Particle Deposition to be Studied.....	6
2.2.2 Practical Application of Particle Deposition Analysis.....	7
3 PROGRAMMING DISCUSSION.....	9
3.1 Introduction to the Finite Element Method.....	9
3.2 One-Dimensional Analysis.....	10
3.2.1 Development of the Element Equations in One Dimension.....	10
3.2.2 Computer Implementation of One-Dimensional Problems.....	12
3.2.3 Illustrative Example of FEM1DV2: Steady Heat Transfer in a Fin.....	16
3.3 Two-Dimensional Analysis.....	17
3.3.1 The Two-Dimensional Finite Element Model.....	18
3.3.2 Viscous Incompressible Fluid Flow.....	23
3.3.3 Computer Implementation of Two-Dimensional Problems.....	26

## TABLE OF CONTENTS (Continued)

Chapter	Page
3.3.4 Illustrative Example of FEM2DV2: Viscous Fluid Squeezed Between Plates.....	30
3.3.5 Use of FEM2DV2 to Obtain Velocity Distributions for a 90 Degree Duct Bend.....	32
4 PARTICLE DEPOSITION ANALYSIS.....	44
4.1 Governing Equations.....	44
4.2 Method of Solution.....	47
4.2.1 Program “particles.f” Used to Analyze Particle Motion.....	51
4.2.2 Program “particlesout.f” Used to Analyze Particle Deposition.....	63
5 RESULTS AND DISCUSSION OF PARTICLE DEPOSITION.....	68
5.1 Results of Particle Deposition.....	68
5.2 Discussion of Particle Deposition.....	74
6 CONCLUSION.....	77
7 RECOMMENDATIONS.....	79
APPENDIX A EXAMPLE INPUT FILE TO FEM1DV2.....	80
APPENDIX B EXAMPLE OUTPUT FILE FROM FEM2DV2.....	84
APPENDIX C OUTPUT FILE FROM FEM2DV2 FOR FIGURE 3.6 ANALYSIS.	93
APPENDIX D INPUT FILE TO FEM2DV2 FOR MESH OF FIGURE 3.7.....	102
APPENDIX E PROGRAM “nodgen.f”.....	113
APPENDIX F PROGRAM “meshgencurve.f”.....	114
APPENDIX G PROGRAM “particles.f”.....	117

# TABLE OF CONTENTS

## (Continued)

Chapter	Page
APPENDIX H PROGRAM “particlesout.f” WITH OUTPUT “particles.output”.....	140
APPENDIX I PARTICLE DEPOSITION PERCENTAGE VALUES FOR FIGURE 5.2.....	153
APPENDIX J VELOCITY DISTRIBUTION FOR THE 128 ELEMENT MESH OF FIGURE 3.9.....	154
REFERENCES.....	165

## LIST OF TABLES

Table	Page
5.1 Velocity Distributions at Selected Locations from Figure 5.3.....	73
5.2 Typical Radius of a Spherical Particle at Varying Inertia Parameter Values.....	75

## LIST OF FIGURES

Figure	Page
3.1 Flow chart of the computer program FEM1DV2 along with subroutines.....	14
3.2 Finite elements in two dimensions: (a) a three-node element; (b)-(c) four node elements; (d) a five node element; (e) a six-node element.....	20
3.3 Flow chart of the computer program FEM2DV2 along with the subroutines.....	27
3.4 Boundary conditions and finite element meshes for the problem of an incompressible viscous fluid squeezed between plates; (a) geometry of the flow domain; (b) finite element mesh of a quadrant.....	31
3.5 The 90 degree duct bend with entrance and exit velocity distributions, dimensions, and global origin.....	33
3.6 Straight section of the duct used to determine the distance at which a uniform flow will become fully developed.....	35
3.7 A sample 21 element mesh used for the velocity distribution analysis; nine nodes per quadrilateral element.....	38
3.8 The first element of the 21 element mesh showing the node numbers demonstrating the connectivity of an element for the input file of FEM2DV2.....	40
3.9 128 element mesh used to obtain the velocity distributions from the program FEM2DV2; nine nodes per quadrilateral element for a total of 561 nodes.....	42
4.1 Flowchart for the program “particles.f”; the program is listed completely in appendix G.....	52
4.2 Determining the four closest nodes to the particle based upon which nodes lie above and below it at the entrance when the particle is in the 90 degree turn.....	55
4.3 Interpolating to get the velocity of the particle from the four closest nodes; this particle is in the 90 degree turn of the duct.....	57

## LIST OF FIGURES (Continued)

Figure	Page
4.4 Interpolating to get the velocity of the particle from the four closest nodes; computing the velocities at the top and bottom of the section enclosing the particle (the particle is in the 90 degree turn of the duct).....	60
4.5 Interpolating to get the velocity of the particle in the exit vertical section of the duct.....	62
4.6 Flowchart for the program “particlesout.f”; the program is listed completely in appendix H.....	64
4.7 Particle deposition in the 90 degree turn of the duct; particles are deposited in the current section when their location angle $\theta$ is greater than the section angle $\phi$ ..	67
5.1 Section numbers used for determining the particle deposition in the duct; these numbers correspond to the x axis of figure 5.2.....	70
5.2 Particle deposition in the 90 degree duct bend as a function of the $S$ parameter.....	71
5.3 Node numbers and locations of the velocity distribution discussion throughout the duct.....	72

# **CHAPTER 1**

## **INTRODUCTION**

### **1.1 Background Information**

There are many complicated problems in the mechanical engineering field which cannot be solved by direct mathematical formulation and analysis. It is often the case that numerical analysis of the mathematical model must be used in order to solve difficult and otherwise very complex problems. In many of these cases, there are no exact solutions; approximations must be made. The finite element method (FEM) is one technique of numerical analysis of physical processes which has become a very popular and powerful tool in engineering analysis. It was first developed in the 1960's and is used today in many computer-aided design softwares such as I-DEAS, ProEngineer, and AutoCad.

The finite element method divides a given domain into a set of simple subdomains, called finite elements. The collection of these finite elements is called the finite element mesh. Over each of these finite elements the physical process is approximated by polynomial or other functions and algebraic equations are developed, which relate physical quantities at selective points, called nodes. The element equations are combined using continuity of the physical quantities.

This numerical technique has many applications in mechanical engineering, including plane elasticity, flows of viscous incompressible fluids, and bending of elastic plates, among others. The accuracy of this computational method can be increased by increasing the number of elements and nodes which the geometric shape is divided into. Increasing the number of elements and nodes requires more computational time and more

powerful computers, but today's advanced workstations and mainframes can handle most, if not all, of the necessary requirements. In the cases where there are exact mathematical solutions to problems, the finite element method provides better accuracy as the meshes get finer and finer.

Users of most of the popular CAD/CAM software packages which are available in the market today have access to finite element analysis. These software packages are often very simple to use, requiring only the geometric shape and boundary/initial conditions. The meshes can be generated by the computer, under the user's command. There are some cases, though, in which the implementation of a comprehensive source code is desired. One such application is the study of a viscous incompressible fluid through a ninety degree turn in a duct. Given the profile of the flow at the inlet and outlet of this system, along with the boundary conditions dictated by the physical processes of fluid mechanics, the velocity distribution can be obtained using a finite element method source code. This analysis was performed in this thesis with a FORTRAN 77 source code by J.N. Reddy (Reddy, 1993).

With the computed velocity distribution throughout the duct bend, a fluid-solid particle suspension flow can be analyzed. For example, in an air induction system with a ninety degree turn, particulate pollutants flowing with the air characterize a two-phase flow. The particulates may be deposited in the duct bend, causing the system to become infiltrated with particulate matter, resulting in problems ranging from decreased air flow to erosion. Other cases in which this may occur are exhaust systems, ventilation systems,



dust collectors, and valves in the human body involving the flow of blood with undesirable matter such as cholesterol.

This ninety degree bend in a duct was analyzed in this thesis. The inertia force parameter was varied with the velocity distribution remaining constant so that some analysis could be done based upon a varying size of the particulate matter in a steady viscous incompressible flow.

## **1.2 Objective**

The objective of this thesis is to input and debug a FORTRAN source code for finite element analysis and to implement its use in one and two-dimensional cases. The implementation of the two-dimensional case is used to analyze practical problems in fluid mechanics. The problem studied is the deposition of particles in a steady viscous incompressible flow through a ninety degree duct bend, varying the inertia force parameter.

Chapter 2 will focus on the literature survey which was done describing why this particular program was chosen and the decision to implement its use on a specific type of particle deposition; chapter 3 will be a programming discussion showing the basic finite element method procedures used to develop the programs and their actual implementation; chapter 4 will analyze particle deposition from the governing equations to the method of solution; chapter 5 will show the results and provide some discussion of the particle deposition analysis; chapter 6 will conclude this thesis; and finally, chapter 7 discusses some recommendations for future study on related topics.

## CHAPTER 2

### LITERATURE SURVEY

#### 2.1 FORTRAN Source Code

After choosing the topic of finite element analysis, a source code was needed. There are some source codes written in BASIC, C, C++, and FORTRAN, but FORTRAN was chosen because of the familiarity of this high-level programming language in the engineering field. Many of the mechanical engineering textbooks today use FORTRAN for their source code listings for all types of programs.

Having taken the graduate level course "Introduction to the Finite Element Method" at the New Jersey Institute of Technology in the fall of 1994, I became very familiar with the book used in the course, An Introduction to the Finite Element Method, second edition, by John N. Reddy (1993). The book has very in-depth and comprehensive FORTRAN programs listed in the appendices for finite element analysis of one-dimensional and two-dimensional cases. This source code, however, was written for a main frame computer. Implementation of these programs on a personal computer (such as an IBM PC) which is used by most students is highly desirable and well worth the effort.

##### 2.1.1 Alternate Programs

Some other programs were examined as possible substitutes for the implementation of computational finite element analysis. Several authors of these programs were Chandrupalla, Akin, and Ross. One major disadvantage of most of the programs which

were examined was that they were often listed in sections throughout the textbook instead of in one appendix, as in Reddy's program. Reddy's program is all together in one appendix so that it can be examined in its entirety without flipping through the entire book to piece sections together. Most of the other programs can do simple one-dimensional problems such as trusses, beams, frame structures, and plane elasticity only, but Reddy's can do more as described below.

Reddy's programs examine many different cases with two separate source codes. The first program (FEM1DV2) is a one-dimensional analysis, and the second program (FEM2DV2) is a two-dimensional analysis. Both programs can be used to examine many different cases from circular disk plane stresses and strains, Timoshenko beams and plates, Euler-Bernoulli beams and circular plates (1-D), to viscous incompressible flows, plane elasticity, and plate bending problems (2-D). The programs can do static or transient analysis, and many different types of nodes and element types can be used.

### **2.1.2 Entering Reddy's Source Code**

After the decision was made to use Reddy's source code, there was a major obstacle: the software was not included with the textbook, as it is with other similar textbooks. In the preface to the second edition, Reddy talks about the second edition of this book being 60% larger than the first edition because of extensive changes. Due to the fact that he wanted to keep the cost of the book within "reasonable limits", the executable programs were not included with the purchase of the text. Instead, he describes how they can be obtained from the author. The cost of the programs was over \$200. It was decided that it would be more economical and educational to enter the program into the computer using

a scanner, after which the programs would have to be checked line-by-line to ensure that every detail was correct. The programs were scanned, checked, executed, and tested. This was the first portion of the thesis. The programs are available on disks and they can be used by anyone who is interested in doing computational finite element analysis with a FORTRAN source code on an IBM PC or compatible, or on a workstation.

## **2.2 Applications of the Source Code**

After inputting Reddy's source code, there was a desire to do some applications with this sophisticated program. It was decided that computational fluid mechanics would be studied using the finite element method. The two-dimensional program had to be used for this analysis (FEM2DV2) because a steady two-dimensional viscous incompressible flow was to be examined.

The inputs to the 2-D program included the geometry of the domain, information about the type of analysis, number of elements/nodes/etc., and the initial/boundary conditions, as well as information about the fluid parameters. The program analysis produced information about the pressure and stresses, as well as the velocities in the  $x$  and  $y$  directions (denoted as  $u$  and  $v$ , respectively), throughout the region. It was determined that particle deposition could be studied with the computed velocity distributions.

### **2.2.1 Type of Particle Deposition to be Studied**

While the decision was made to study particle deposition, the specifics were vague. Something which was not very well examined was sought. Therefore, a library search was performed on other theses which were done on the topic of particle deposition. It was

discovered that the equations of motion for particle deposition which was being studied had been used in other theses and doctoral dissertations before. Theses were found about particle deposition between a horizontal parallel plate channel (Chu, 1983), in a cylindrical chamber (Shah, 1984), in inclined channels (Chu, 1984), and in convergent channels (Hui, 1986), (Chiou, 1993). It was decided that the focus would be on particle deposition in a ninety degree turn through a duct system, a topic on which there was not much information on in the theses, dissertations, or textbooks which were examined.

The decision was made to concentrate only on one specific parameter in the governing equations (developed and discussed in chapter 4). Several parameters affect particle deposition: inertia, image, and gravity forces. The focus of this study is the inertia force. Only this parameter was varied due to the time constraints and the application of the finite element method to one specific case in particle deposition analysis.

### **2.2.2 Practical Application of Particle Deposition Analysis**

One practical application of the analysis performed on the deposition of particles in a ninety degree turn is the determination of where the particles are mostly deposited. An analysis can be performed determining the most likely target of particle deposition with this type of flow. An air flow with harmful and corrosive particulate pollutants can damage the duct due to settling of the particles, so there is a need to determine where the duct would most likely erode. If there is a large portion of particles deposited in one particular section, then that section should be reinforced in some way to deter the damage incurred by such a deposition.

While in some cases the duct can be entirely reinforced uniformly, it may be more economical to reinforce the duct in the area most likely to undergo damage due to deposition. This is dependent on the particle size, which is directly related to the inertia parameter, as will be shown in chapter 4.

## CHAPTER 3

### PROGRAMMING DISCUSSION

Chapter 2 presented a literature survey determining which finite element method source code was to be used in this thesis and the type of application which the source code will be used for. In this chapter, the finite element method is discussed in further detail, and the source code is implemented.

#### 3.1 Introduction to the Finite Element Method

As was discussed in the introduction (chapter 1), the finite element method is a numerical simulation of a physical process used to evaluate a mathematical model. The finite element method consists of (Reddy, p.15):

1. the domain of the problem represented by a collection of simple subdomains, called finite elements: the collection of these finite elements being called the finite element mesh
2. approximation of the physical process by functions of a desired type (e.g. polynomials), and algebraic equations relating physical quantities at certain points, referred to as nodes, of the element are developed
3. the element equations are organized using continuity of physical quantities

In the finite element method, in general, an approximate solution  $u$  is sought to the differential equation of the form

$$u \approx \sum_{j=1}^n u_j \psi_j + \sum_{j=1}^m c_j \phi_j \quad (3.1)$$

where  $u_j$  are the values of  $u$  at the element nodes,  $\psi_j$  are the interpolation functions,  $c_j$  are the nodeless coefficients, and  $\phi_j$  are the associated approximation functions.

### 3.2 One-Dimensional Analysis

A typical model boundary value problem which arises in a one-dimensional analysis considers solving for  $u(x)$  in the differential equation

$$-\frac{d}{dx}\left(a\frac{du}{dx}\right) + cu - q = 0 \quad \text{for} \quad 0 < x < L \quad (3.2)$$

and the boundary conditions

$$u(0) = u_0, \quad \left(a\frac{du}{dx}\right)\bigg|_{x=L} = Q_0 \quad (3.3)$$

where  $a=a(x)$ ,  $c=c(x)$ ,  $q=q(x)$ ,  $u_0$ , and  $Q_0$  are the data (the known quantities) of the problem. Equation (3.2) arises in many physical processes, including conduction and convection heat transfer in a plane wall or fin (one-dimensional heat transfer), flow through channels and pipes, transverse deflections of cables, axial deformations of bars, and many other physical processes (Reddy, p. 70).

#### 3.2.1 Development of the Element Equations in One Dimension

There are three steps involved in developing the finite element equations:

1. Construction of the weak form of the differential equation
2. Assumption of the form of the approximate solution over a typical finite element
3. Derivation of the finite element equations by substitution of the approximate solution into the weak form



The finite element method seeks an approximate solution to (3.2) over each finite element. The polynomial approximation for a typical finite element  $\Omega^e$  is of the form

$$U^e = \sum_{j=1}^n u_j^e \psi_j^e(x) \quad (3.4)$$

where  $u_j^e$  are the values of the solution at the nodes of the finite element and  $\psi_j^e$  are the approximation functions over the element. The coefficients  $u_j^e$  are determined such that (3.2) is satisfied in a weighted-integral sense.

The approximation solution  $U^e$  must fulfill certain requirements for it to converge to the actual solution  $u$  as the number of elements is increased. The first is that the approximate solution should be continuous over the element and differentiable, as required by the weak form. Next, it should be a complete polynomial, including all lower-order terms up to the highest order used. And finally, it should be an interpolant of the primary variables at the nodes of the finite element (Reddy, p.77).

In order to apply the finite element model based on the weak form, it is not necessary to specify in advance the degree of approximation of  $U^e$ . The model can be developed for an arbitrary degree of interpolation based on (3.4). The weak form can be written as

$$0 = \int_{x_A}^{x_B} \left( a \frac{dw}{dx} \frac{du}{dx} + cwu \right) dx - \int_{x_A}^{x_B} wq dx - \sum_{i=1}^n w(x_i^e) Q_i^e \quad (3.5)$$

where  $x_i^e$  is the global coordinate of the  $i$ th node of element  $\Omega^e$  and  $w$  is the weight function. If nodes 1 and  $n$  denote the endpoints of the element then  $Q_1^e$  and  $Q_n^e$  represent the unknown point sources, and all other  $Q_i^e$  are always known (i.e., applied point

sources). Substituting (3.4) for  $u$  and  $\psi_1^e, \psi_2^e, \dots, \psi_n^e$  for  $w$  into the weak form (3.5),  $n$  algebraic equations are obtained of the form

$$0 = \sum_{j=1}^n K_{ij}^e u_j^e - f_i^e - Q_i^e \quad (i=1,2,\dots,n) \quad (3.6)$$

where

$$K_{ij}^e = \int_{x_A}^{x_B} \left( a \frac{d\psi_i^e}{dx} \frac{d\psi_j^e}{dx} + c \psi_i^e \psi_j^e \right) dx = B(\psi_i^e, \psi_j^e), \quad f_i^e = \int_{x_A}^{x_B} q \psi_i^e dx = l(\psi_i^e) \quad (3.7)$$

In matrix notation, the combination of (3.6) and (3.7) can be written as

$$[K^e] \{u^e\} = \{f^e\} + \{Q^e\} \quad (3.8)$$

The symmetric matrix  $[K^e]$  is called the coefficient matrix (or stiffness matrix in structural mechanics). The column vector  $\{f^e\}$  is the source vector (or force vector in structural mechanics). There exist  $2n$  unknowns in (3.8):  $(u_1^e, u_2^e, \dots, u_n^e)$  and  $(Q_1^e, Q_2^e, \dots, Q_n^e)$ , called primary and secondary element nodal degrees of freedom. There must be given an additional  $n$  conditions in order to solve (3.8). These conditions come from the boundary conditions and by balancing the secondary variables  $Q_i^e$  at nodes common to several elements (Reddy, p.86).

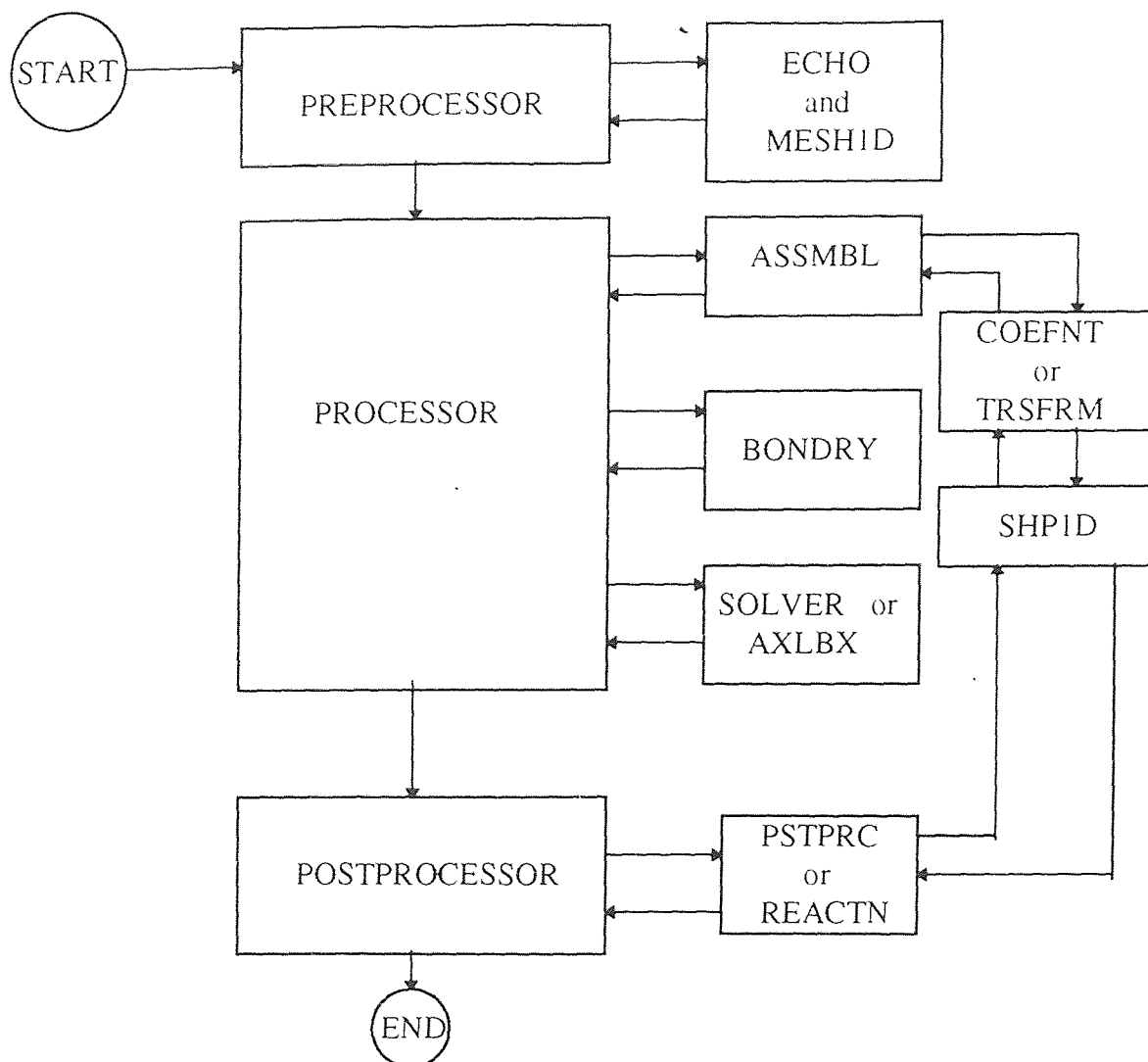
### 3.2.2 Computer Implementation of One-Dimensional Problems

There are three general parts to a finite element program: the preprocessor, processor, and postprocessor. In the preprocessor section of the program, the input data of the problem is read in or generated. Included here are the geometry information, the data of the problem, finite element mesh information, and indicators for various options. In

FEM1DV2, which is J.N. Reddy's one-dimensional finite element analysis program, the input is given to the program through a data file which the program reads when it is executed. The processor part of the program generates the element matrices using numerical integration, assembles the element equations, imposes the boundary conditions, and solves the algebraic equations for the nodal values of the primary variables. Finally, the postprocessor computes the solution by interpolation at points other than nodes, computes the secondary variables that are derivable from the solution, and outputs the data in a desired format for printing and/or plotting.

A flow chart of the program FEM1DV2 is shown in figure 3.1. The preprocessor unit reads the input data and generates the finite element mesh, then prints the data and mesh information. The element type, number of elements used, specified boundary conditions or primary and secondary variables, global coordinates of the nodes, and element properties (like coefficients  $a_e, b_e, c_e, f_e$ , etc.) are read during the preprocessing stage. When a uniform mesh is used, the length of the domain is read in and the global coordinates of the nodes can be generated by the program.

The processor unit of the program FEM1DV2 starts by generating the element matrices. Depending on the type of problem being solved, various subroutines are called to generate the element matrices. The Gauss quadrature is used to evaluate element matrices and vectors, and the arrays are assembled as soon as they are computed. A loop on the number of elements in the mesh is used to compute element matrices and assemble



- ASSMBL:** Subroutine for the assembly of element equations: upper-banded form for static and transient problems; full matrix form for eigenvalue problems.
- AXLBX:** Subroutine for determining eigenvalues and eigenvectors of the equation  $[A]\{X\}=L[B]\{X\}$ .
- BONDRY:** Subroutine for imposing specified boundary conditions of essential, natural, and mixed type.
- COEFNT:** Subroutine for computing element matrices and vectors for all problems except truss and frame problems.
- ECHO:** Subroutine to echo the input file.
- MESH1D:** Subroutine to generate the mesh (i.e. global coordinates of the global nodes and the connectivity array).
- PSTPRC:** Subroutine to postprocess the solution for all problems, except truss and frame problems.
- REACTN:** Subroutine to calculate the reactions for truss and frame problems.
- SHP1D:** Subroutine to compute the shape functions and their derivatives.
- SOLVER:** Subroutine to solve linear algebraic equations.
- TRSFRM:** Subroutine to compute element stiffness matrices and force vectors for truss and frame problems.

**Figure 3.1** Flow chart of the computer program FEM1DV2 along with the subroutines.

them. Based on the specifications of the input variables MODEL and NTYPE, the types of problems which can be solved by this program are as follows:

- all field problems described by model equation (3.2), including radially symmetric heat-transfer-type problems
- radially symmetric elastic disk problems
- the Timoshenko theory of beams
- the Timoshenko theory for bending of circular plates
- the Euler-Bernoulli theory of beams
- the Euler-Bernoulli theory for bending of circular plates
- the two-node truss element
- the two-node Euler-Bernoulli frame element
- the two-node Timoshenko frame element

Static analysis, first-order time derivative problems (parabolic), and second-order time derivative problems (hyperbolic) can be solved according to the specification of the input variable ITEM.

Once all of the input variables are specified (a detailed description of the input variables is given in Reddy, p.274-278), the equations are solved using Gaussian elimination and back-substitution. Postprocessing involves computation of the solution and its gradient at preselected points of the domain. There is increased accuracy with mesh refinement and higher-order elements.

Both of the programs FEM1DV2 and FEM2DV2 were written so that they could be used on a mainframe. However, both programs were implemented on a PC. To do

this, there were virtually no changes to the source code. There were two subroutines in the program FEM2DV2 which had to be copied from FEM1DV2 because the program uses mainframe subroutines to compute eigenvalues and eigenvectors.

### 3.2.3 Illustrative Example of FEM1DV2: Steady Heat Transfer in a Fin

In order to demonstrate how the program FEM1DV2 works, a problem on steady heat transfer in a fin will be analyzed. The problem is governed by

$$-\frac{d^2\theta}{dx^2} + c\theta = 0 \quad \text{for } 0 < x < L \quad (3.9)$$

$$\theta(0) = \theta_0, \quad \left( \frac{d\theta}{dx} \right)_{x=L} = 0 \quad (3.10)$$

where  $\theta$  is the nondimensional temperature, and  $L$ ,  $c$ ,  $\theta_0$  are

$$L=0.25 \text{ m} \quad c=256 \text{ m}^{-2} \quad \theta_0 = 100^\circ \text{C} \quad (3.11)$$

This problem is governed by model equation (3.2). For the input file to the program, the specifications will be MODEL=1, NTYPE=0, and ITEM=0 (for a steady-state solution). Since  $a = a_0 = 1.0$  and  $c = c_0 = 256$ , then ICONT=1, AX0=1.0, and CX0=256.0. All other specifications are zero for this problem. Using a uniform mesh of four linear elements (NEM=4, IELEM=1), the increments DX(I) are

$$\{DX\} = \{0.0, 0.0625, 0.0625, 0.0625, 0.0625\} \quad (3.12)$$

There are no mixed (convection) boundary conditions, so NNBC=0. NSPV=1, NSSV=0, denoting the number of specified primary and secondary variables, respectively. At node 1 and degree of freedom 1, there is a specified boundary condition on the primary variable, so that ISPV(1,1)=1 and ISPV(1,2)=1. The specified value is VSPV(1)=100.0.

The complete input file is given in appendix A as is the output from the program FEM1DV2. This same example is done by Reddy (p.279) and the results which are in appendix A match the printed results in the book, showing that the program works as it is supposed to. The program computes the nondimensional temperature at each of the nodes in this example.

Other examples which were tested successfully were radially symmetric heat transfer in a solid cylinder and the deformation of a rotating disk (Reddy, p. 278-282). While the program FEM1DV2 was run successfully for these three examples, there is no guarantee that it will successfully produce the correct output for the other examples. The program compiles but run-time errors could happen. The user may have to debug the program in certain cases.

### 3.3 Two-Dimensional Analysis

The finite element analysis of two-dimensional problems is similar to that of one-dimensional problems, as discussed in section 3.2. In two-dimensional analysis, the problems are described by partial differential equations over geometrically complex regions. The boundary of a two-dimensional domain is in general a curve, so the finite elements are simple two-dimensional geometric shapes such as triangles and rectangles. An approximate solution to a given problem on a domain is sought; however, the domain is approximated by a suitable finite element mesh. In consequence, there exist approximation errors in a 2-D finite element analysis due to the approximation of the solution *and* the discretization errors due to the approximation of the domain (Reddy, p.

295). Since irregular geometries can be represented by a collection of finite elements, the method is a valuable tool for the solution of boundary, initial, and eigenvalue problems arising in the fields of engineering.

### 3.3.1 The Two-Dimensional Finite Element Model

The model equation for boundary value problems is a second-order partial differential equation. The solution for  $u$  must be found in the equation

$$-\frac{\partial}{\partial x}\left(a_{11}\frac{\partial u}{\partial x}+a_{12}\frac{\partial u}{\partial y}\right)-\frac{\partial}{\partial y}\left(a_{21}\frac{\partial u}{\partial x}+a_{22}\frac{\partial u}{\partial y}\right)+a_{00}u-f=0 \quad (3.13)$$

for given data  $a_{ij}(i, j = 1, 2), a_{00}$  and  $f$ , and specified boundary conditions. As a special case, the Poisson equation results from (3.13) by setting  $a_{11} = a_{22} = a$  and  $a_{12} = a_{21} = a_{00} = 0$

$$-\nabla \cdot (a \nabla u) = f \quad \text{in } \Omega \quad (3.14)$$

where  $\nabla$  is the gradient operator. In Cartesian coordinates, this equation can be written as

$$-\frac{\partial}{\partial x}\left(a\frac{\partial u}{\partial x}\right)-\frac{\partial}{\partial y}\left(a\frac{\partial u}{\partial y}\right)=f \quad (3.15)$$

The major steps of developing the finite element model of equation (3.13) are (Reddy, p.297)

1. Discretization of the domain into a set of finite elements
2. Weak formulation of the governing differential equation
3. Derivation of finite element interpolation functions
4. Development of the finite element model using the weak form



5. Assembly of finite elements to obtain the global system of algebraic equations
6. Imposition of the boundary conditions
7. Solution of equations
8. Post-computation of solution and quantities of interest

More than one simple geometric shape can be selected as a finite element, ranging from triangles and rectangles to quadrilaterals and others. The number of nodes in an element can be varied as well. Typical triangular elements have three, four, or six nodes, while typical quadrilateral elements have four, five, or nine nodes, as shown in figure 3.2. Accuracy considerations and computational requirements are key factors in selecting the type of element and the number of nodes each element will have.

The weak form of (3.13) over the typical element  $\Omega^e$  is written as

$$0 = \int_{\Omega^e} w \left[ -\frac{\partial}{\partial x}(F_1) - \frac{\partial}{\partial y}(F_2) + a_{00}u - f \right] dx dy \quad (3.16)$$

where

$$F_1 = a_{11} \frac{\partial u}{\partial x} + a_{12} \frac{\partial u}{\partial y}, \quad F_2 = a_{21} \frac{\partial u}{\partial x} + a_{22} \frac{\partial u}{\partial y} \quad (3.17)$$

From the gradient theorem,

$$\int_{\Omega^e} \frac{\partial}{\partial x}(wF_1) dx dy = \oint_{\Gamma^e} wF_1 n_x ds \quad (3.18)$$

$$\int_{\Omega^e} \frac{\partial}{\partial y}(wF_2) dx dy = \oint_{\Gamma^e} wF_2 n_y ds \quad (3.19)$$

where  $n_x$  and  $n_y$  are the components (direction cosines) of the unit normal vector

$$\hat{n} = n_x \hat{i} + n_y \hat{j} = \cos \alpha \hat{i} + \sin \alpha \hat{j} \quad (3.20)$$

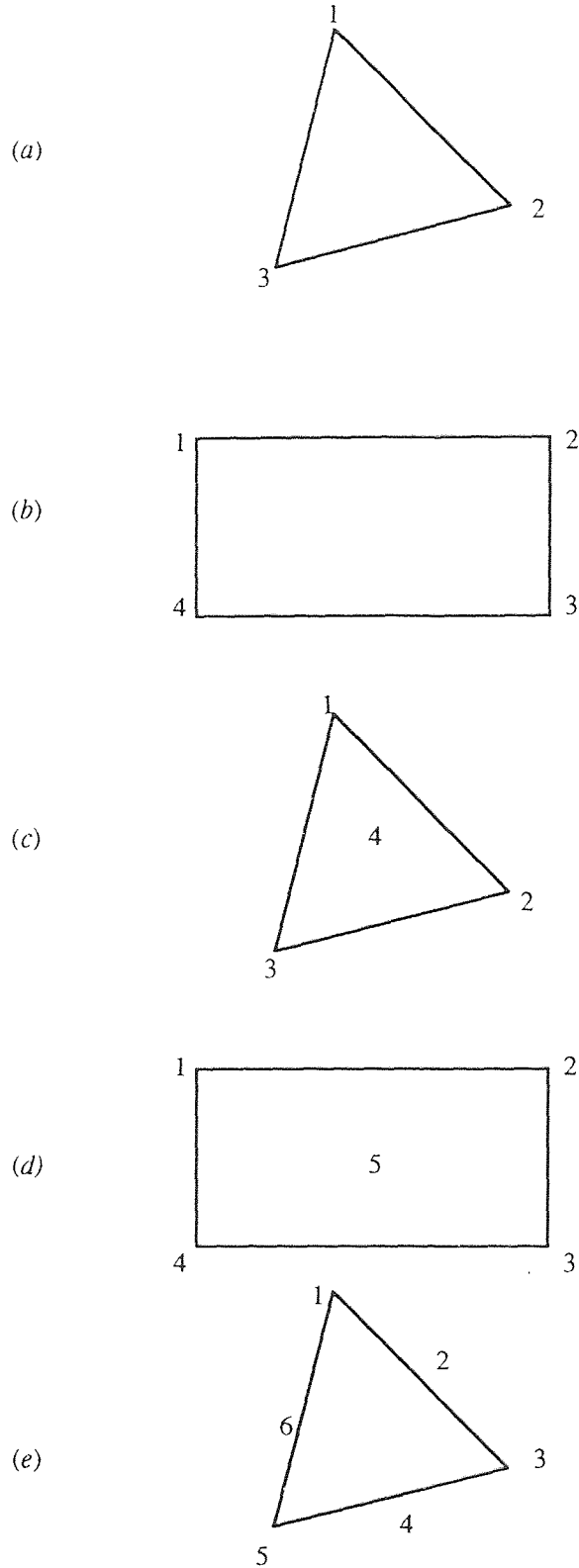


**Figure 3.2** Finite elements in two dimensions: (a) a three-node element; (b)-(c) four node elements; (d) a five node element; (e) a six-node element.

on the boundary  $\Gamma^e$ , and  $ds$  is the arclength of an infinitesimal line element along the boundary. The secondary variable of the formulation,  $q_n$ , is

$$q_n \equiv n_x \left( a_{11} \frac{\partial u}{\partial x} + a_{12} \frac{\partial u}{\partial y} \right) + n_y \left( a_{21} \frac{\partial u}{\partial x} + a_{22} \frac{\partial u}{\partial y} \right) \quad (3.21)$$

Finally, with substitution, (3.16) becomes

$$0 = \int_{\Omega^e} \left[ \frac{\partial w}{\partial x} \left( a_{11} \frac{\partial u}{\partial x} + a_{12} \frac{\partial u}{\partial y} \right) + \frac{\partial w}{\partial y} \left( a_{21} \frac{\partial u}{\partial x} + a_{22} \frac{\partial u}{\partial y} \right) + a_{00} w u - w f \right] dx dy - \oint_{\Gamma^e} w q_n ds \quad (3.22)$$

In the development of the finite element model, the weak form in (3.22) requires that the approximation chosen for  $u$  should be at least linear in both  $x$  and  $y$  so that there are no terms that are equal to zero. The primary variable  $u$  can be approximated over a typical finite element  $\Omega^e$  by the expression

$$u(x, y) \approx U^e(x, y) = \sum_{j=1}^n u_j^e \psi_j^e(x, y) \quad (3.23)$$

where  $u_j^e$  is the value of  $U^e$  at the  $j$ th node  $(x_j, y_j)$  of the element, and  $\psi_j^e$  are the Lagrange interpolation functions with the property

$$\psi_i^e(x_j, y_j) = \delta_{ij} \quad (3.24)$$

The substitution of (3.23) in the weak form (3.22) yields

$$0 = \int_{\Omega'} \left[ \frac{\partial w}{\partial x} \left( a_{11} \sum_{j=1}^n u_j \frac{\partial \psi_j}{\partial x} + a_{12} \sum_{j=1}^n u_j \frac{\partial \psi_j}{\partial y} \right) + \frac{\partial w}{\partial y} \left( a_{21} \sum_{j=1}^n u_j \frac{\partial \psi_j}{\partial x} + a_{22} \sum_{j=1}^n u_j \frac{\partial \psi_j}{\partial y} \right) + a_{00} w \sum_{j=1}^n u_j \psi_j - wf \right] dxdy - \oint_{\Gamma'} w q_n ds \quad (3.25)$$

This equation must hold for any weight function  $w$ . Since there are  $n$  independent algebraic equations needed to solve for the  $n$  unknowns  $u_1, u_2, \dots, u_n$ ,  $n$  independent functions are chosen for  $w$  as  $w = \psi_1, \psi_2, \dots, \psi_n$ . For each  $w$ , an algebraic equation is obtained. The  $i$ th algebraic equation is arrived at by substituting  $w = \psi_i$  into (3.25) and results in

$$0 = \sum_{j=1}^n \left\{ \int_{\Omega'} \left[ \frac{\partial \psi_i}{\partial x} \left( a_{11} \frac{\partial \psi_j}{\partial x} + a_{12} \frac{\partial \psi_j}{\partial y} \right) + \frac{\partial \psi_i}{\partial y} \left( a_{21} \frac{\partial \psi_j}{\partial x} + a_{22} \frac{\partial \psi_j}{\partial y} \right) + a_{00} \psi_i \psi_j \right] dxdy \right\} u_j - \int_{\Omega'} f \psi_i dxdy - \oint_{\Gamma'} \psi_i q_n ds \quad (i=1, 2, \dots, n) \quad (3.26)$$

This equation can be rewritten as

$$\sum_{j=1}^n K_{ij}^e u_j^e = f_i^e + Q_i^e \quad (3.27)$$

where

$$K_{ij}^e = \int_{\Omega'} \left[ \frac{\partial \psi_i}{\partial x} \left( a_{11} \frac{\partial \psi_j}{\partial x} + a_{12} \frac{\partial \psi_j}{\partial y} \right) + \frac{\partial \psi_i}{\partial y} \left( a_{21} \frac{\partial \psi_j}{\partial x} + a_{22} \frac{\partial \psi_j}{\partial y} \right) + a_{00} \psi_i \psi_j \right] dxdy \quad (3.28)$$

$$f_i^e = \int_{\Omega'} f \psi_i^e dxdy, \quad Q_i^e = \oint_{\Gamma'} q_n \psi_i^e ds$$

Finally, this expression can be rewritten in matrix notation as

$$[K^e]\{u^e\} = \{f^e\} + \{Q^e\} \quad (3.29)$$

The matrix  $[K]$  is symmetric when  $a_{12} = a_{21}$ . Equation (3.29) represents the finite element model of (3.13) (Reddy, p.302).

### 3.3.2 Viscous Incompressible Fluid Flow

This section considers the finite element analysis of two-dimensional flows of viscous incompressible fluids. This analysis is relevant because the computer implementation of FEM2DV2 will be based on this type of fluid flow. The governing equations of this analysis is a set of partial differential equations based on the velocity components and pressure. The inertial effects can be neglected when the speed of the flow is low, as in the analysis done in this thesis. This type of flow is known as Stokes flow, with the equations being known as the Stokes equations.

In a closed domain  $\Omega$ , the slow flow of a viscous incompressible fluid is described by

$$\frac{D}{Dt} \equiv \frac{\partial}{\partial t} + V \cdot \nabla \approx \frac{\partial}{\partial t} \quad (3.30)$$

Since the flow is viscous,  $\mu \neq 0$ , where  $\mu$  is the viscosity of the fluid. The fluid is incompressible, so that

$$\frac{D\rho}{Dt} = 0 \quad (\rho = \text{constant}) \quad (3.31)$$

where  $\rho$  is the density of the fluid. The flow is modeled as two-dimensional because the domain is considered to be very long in one direction, namely the  $z$  direction. The governing equations of motion in this case are (Reddy, p.483)

*Conservation of linear momentum*

$$\begin{aligned} \rho \frac{\partial u}{\partial t} - \frac{\partial}{\partial x} \left( 2\mu \frac{\partial u}{\partial x} \right) - \frac{\partial}{\partial y} \left[ \mu \left( \frac{\partial u}{\partial y} + \frac{\partial v}{\partial x} \right) \right] + \frac{\partial P}{\partial x} - f_x &= 0 \\ \rho \frac{\partial v}{\partial t} - \frac{\partial}{\partial x} \left[ \mu \left( \frac{\partial u}{\partial y} + \frac{\partial v}{\partial x} \right) \right] - \frac{\partial}{\partial y} \left( 2\mu \frac{\partial v}{\partial y} \right) + \frac{\partial P}{\partial y} - f_y &= 0 \end{aligned} \quad (3.32)$$

*Conservation of mass*

$$\frac{\partial u}{\partial x} + \frac{\partial v}{\partial y} = 0 \quad (3.33)$$

where  $u$  and  $v$  are the velocity components in the  $x$  and  $y$  directions, respectively,  $P$  is the pressure, and  $f_x$  and  $f_y$  are the components of the body force. And finally, the boundary and initial conditions are

$$\begin{aligned} t_x &\equiv 2\mu \frac{\partial u}{\partial x} n_x + \mu \left( \frac{\partial u}{\partial y} + \frac{\partial v}{\partial x} \right) n_y - P n_x = \hat{t}_x \\ t_y &\equiv \mu \left( \frac{\partial u}{\partial y} + \frac{\partial v}{\partial x} \right) n_x + 2\mu \frac{\partial v}{\partial y} n_y - P n_y = \hat{t}_y \end{aligned} \quad \text{on } \Gamma_1$$

$$u = \hat{u}, \quad v = \hat{v} \quad \text{on } \Gamma_2$$

$$u(x, y, 0) = u_0(x, y), \quad v(x, y, 0) = v_0(x, y) \quad (3.34)$$

The weak forms of (3.32) and (3.33) over an element  $\Omega^e$  can be obtained by multiplying each of the three equations by three different weight functions  $w_1, w_2, w_3$  and integrating over the element (Reddy, p.484):

$$\begin{aligned}
0 &= \int_{\Omega'} w_1 \left\{ \rho \frac{\partial u}{\partial t} - \frac{\partial}{\partial x} \left( 2\mu \frac{\partial u}{\partial x} \right) - \frac{\partial}{\partial y} \left[ \mu \left( \frac{\partial u}{\partial y} + \frac{\partial v}{\partial x} \right) \right] + \frac{\partial P}{\partial x} - f_x \right\} dx dy \\
0 &= \int_{\Omega'} w_2 \left\{ \rho \frac{\partial v}{\partial t} - \frac{\partial}{\partial x} \left[ \mu \left( \frac{\partial u}{\partial y} + \frac{\partial v}{\partial x} \right) \right] - \frac{\partial}{\partial y} \left( 2\mu \frac{\partial v}{\partial y} \right) + \frac{\partial P}{\partial y} - f_y \right\} dx dy \\
0 &= \int_{\Omega'} w_3 \left( \frac{\partial u}{\partial x} + \frac{\partial v}{\partial y} \right) dx dy
\end{aligned} \tag{3.35}$$

A close examination of the weak form reveals that  $u$  and  $v$  are the primary variables and should be made continuous at interelement boundaries, while  $P$  is a nodal variable that is not to be made continuous across the interelement boundaries. The minimum continuity requirements on  $(u, v, P)$  are that  $u$  and  $v$  should be linear in  $x$  and  $y$ , and that  $P$  should be constant. The continuity requirements on the interpolation of the velocity field and pressure are

$$u = \sum_{j=1}^n u_j \psi_j^e, \quad v = \sum_{j=1}^n v_j \psi_j^e, \quad P = \sum_{j=1}^m P_j \phi_j^e \tag{3.36}$$

where  $\psi_j^e$  and  $\phi_j^e$  are the interpolation functions of different order ( $m < n$ ;  $m+1=n$ ).

The program FEM2DV2 uses the penalty function method, which is used to reformulate a problem with constraints as one without constraints. Consider a constrained algebraic problem:

$$\text{minimize the function } f(x, y) \text{ subject to the constraint } G(x, y)=0$$

The minimum of the modified function  $F_p$  must be found as

$$F_p(x, y) = f(x, y) + \frac{1}{2} \gamma [G(x, y)]^2 \tag{3.37}$$

where  $\gamma$  is a preassigned weight parameter, called the penalty parameter. The solution to this problem is given by the two partial differential equations

$$\frac{\partial F_p}{\partial x} = 0, \quad \frac{\partial F_p}{\partial y} = 0 \quad (3.38)$$

The solution  $(x_\gamma, y_\gamma)$  will be a function of the penalty parameter. As the value of  $\gamma$  is increased, the constraint is satisfied more accurately and the solution approaches the actual solution  $(x, y)$  as  $\gamma \rightarrow \infty$  (Reddy, p.488).

### 3.3.3 Computer Implementation of Two-Dimensional Problems

Section 3.2.2 discussed the computer implementation of 1-D problems; in this section, the focus will be on 2-D problems, specifically examining the analysis which was done to obtain the velocity distributions in a 90 degree duct bend. The imposition of the boundary conditions and the solution of the equations remain the same as in 1-D problems. The program FEM2DV2 was written by J.N. Reddy and it is used to analyze 2-D problems. Linear, quadratic triangular, and rectangular elements can be used for the finite element analysis of heat conduction and convection problems, laminar flows of viscous incompressible fluids using the penalty function formulation (one of the focuses of this thesis), plane elasticity problems, and plate bending problems using classical and shear deformation theories. A flow chart of the program FEM2DV2 is presented in figure 3.3 along with a brief explanation of what each of the subroutines does. The program solves eigenvalue problems with the subroutine DGVCSP, an IBM system-supplied subroutine, but this was edited out of the program and replaced with a subroutine to perform the same analysis, obtained from the program FEM1DV2, so that the program is self-sufficient, not depending on system-supplied subroutines for any of the analysis.



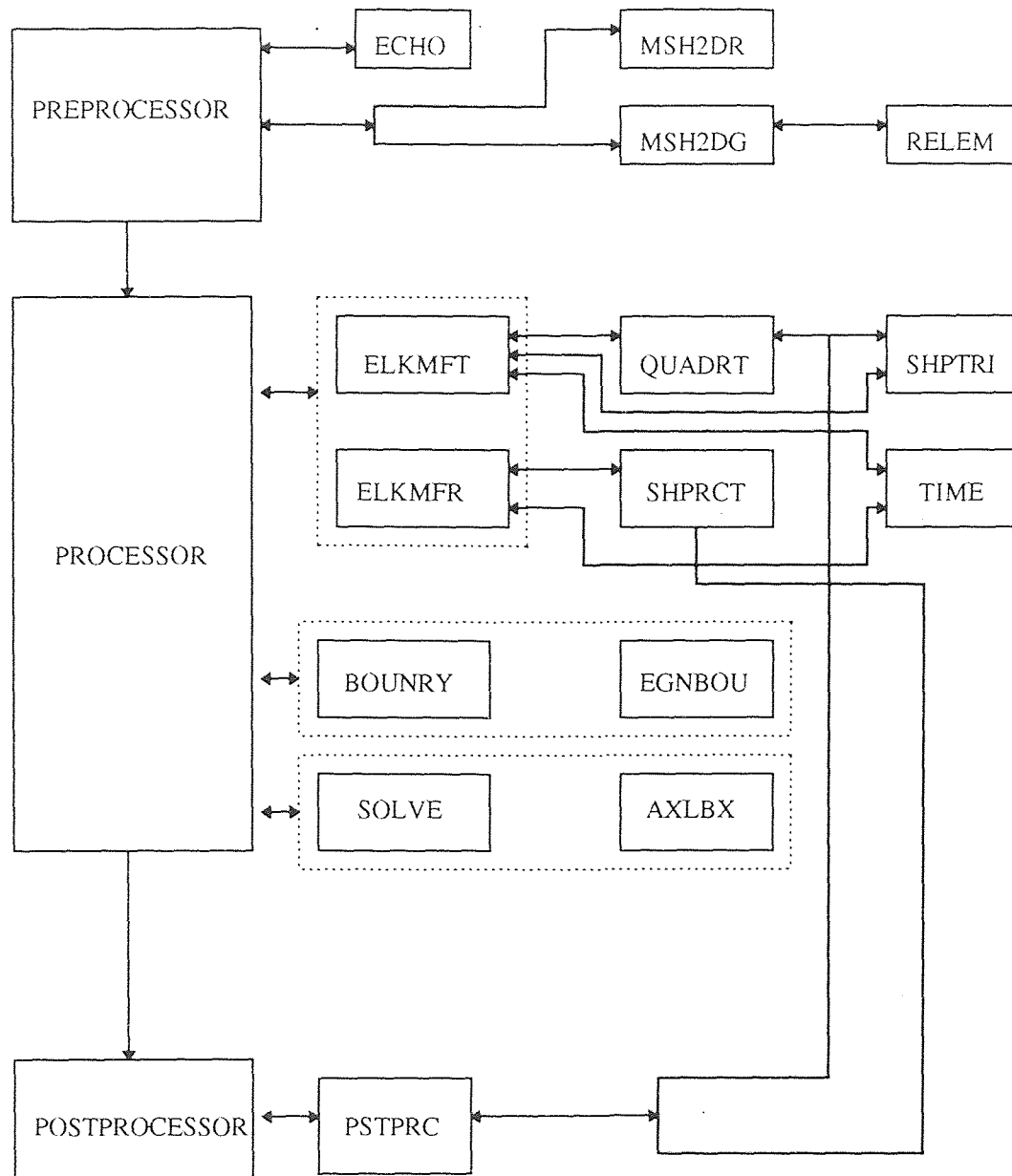


**Figure 3.3** Flow chart of the computer program FEM2DV2 along with the subroutines.

Figure 3.3 (Continued)

<b>AXLBX:</b>	Subroutine to solve an eigenvalue problem of the type $[K]\{U\}=L(M)\{U\}$ , where $[K]$ and $(M)$ are positive definite matrices.
<b>BOUNRY:</b>	Subroutine to impose specified boundary conditions on the primary and secondary variables when a steady-state or transient analysis is carried out.
<b>ECHO:</b>	Subroutine to echo the input data to the program.
<b>EGNBOU:</b>	Subroutine to impose specified boundary conditions on the primary variables when an eigenvalue problem is analyzed.
<b>ELKMFR:</b>	Subroutine to compute the element $[K]$ , $(M)$ , and $\{F\}$ matrices and vectors for the rectangular elements.
<b>ELKMFT:</b>	Subroutine to compute the element $[K]$ , $(M)$ , and $\{F\}$ matrices and vectors for the triangular elements.
<b>MSH2DG:</b>	Subroutine to generate mesh for general domains.
<b>MSH2DR:</b>	Subroutine to generate mesh for rectangular domains only.
<b>PSTPRC:</b>	Subroutine to post-complete the solution, gradient of solution, and stresses.
<b>QUADRT:</b>	Subroutine to generate the quadrature points and weights for the triangular elements.
<b>RELEM:</b>	Subroutine called in MSH2DG to generate element data.
<b>SHPRCT:</b>	Subroutine to compute the shape functions for linear and quadratic (eight- and nine-node) rectangular elements.
<b>SHPTRI:</b>	Subroutine to compute the shape functions for linear and quadratic triangular elements.
<b>SOLVE:</b>	Subroutine to solve a banded, symmetric system of algebraic equations.
<b>TIME:</b>	Subroutine to compute the equivalent coefficient matrices and column vectors for parabolic and hyperbolic equations when time-dependent analysis is carried out.

The element calculations in 2-D problems consider the following (Reddy, p.534):

- Various geometric shapes of the elements
- Single and multivariable problems
- Integrations performed along areas as opposed to along lines (as in 1-D analysis)
- Mixed-order integrations used in certain formulations (for shear-deformable plates and penalty function formulations of viscous incompressible fluids)

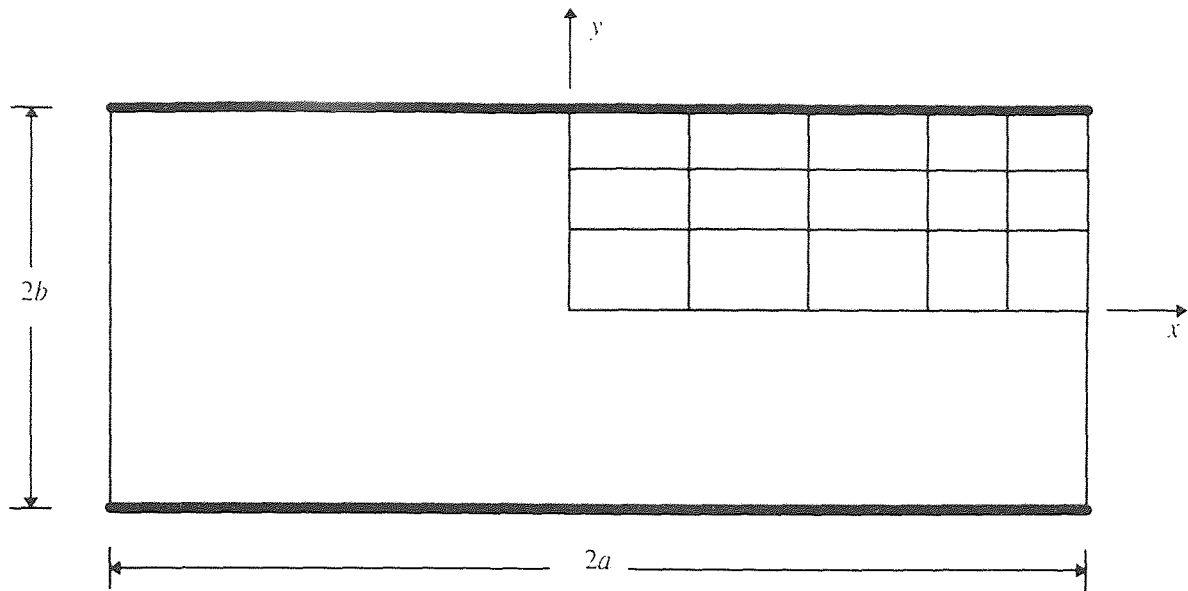
The preprocessor part of the program generates the triangular and rectangular element meshes, as well as nonrectangular meshes. The global coordinates of the nodes and the connectivity matrix are also generated in this section. If the mesh generators cannot be used, for example in a curved section, then the mesh information is read in from the input data file. A complete listing of the input variables to the program FEM2DV2 can be found on pages 542-547 of the book. The processor part of the program evaluates the interpolation functions and their derivatives with respect to the global coordinates, performs numerical integration of the coefficients of the element matrices using numerical quadrature formulas, and sets up the element matrices required for the class of problems being solved (e.g. static, transient, and eigenvalue problems). The post processor post-completes the solution, gradient of solution, and stresses, and prints out the data in a specified format.

Again, this program was scanned into the computer with a scanner, and then it was examined line-by-line for accuracy. After the adjustments were made, the program was ready to be executed. The program was not modified except for the fact that there were two subroutines added to compute the eigenvalues and eigenvectors because the program

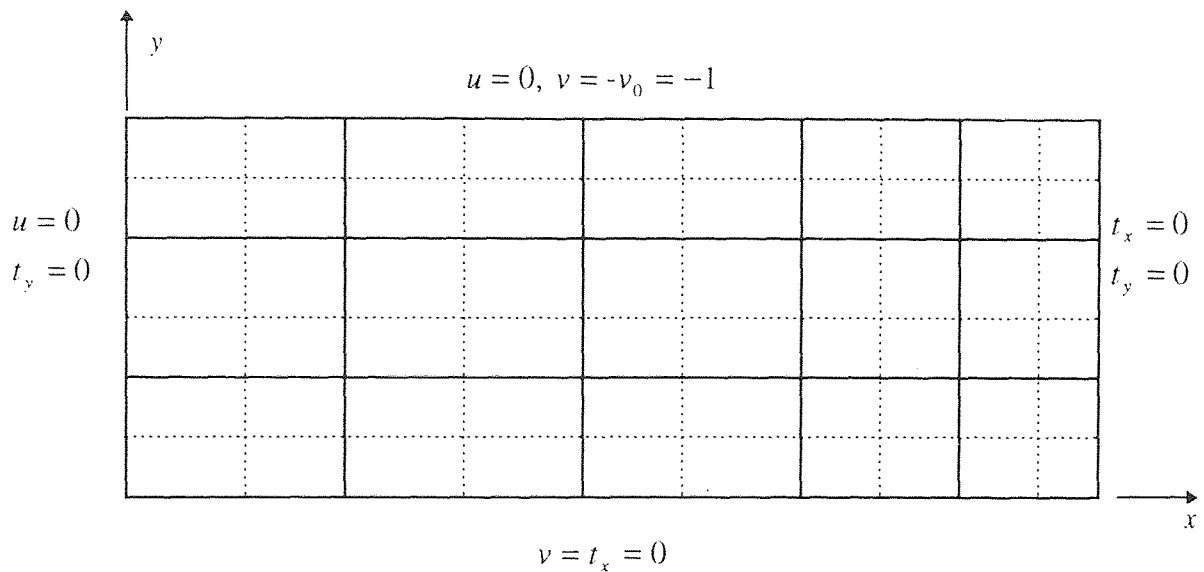
refers to system subroutines which the PC did not have. This was all done on a personal computer (PC) with a pentium processor. However, unlike FEM1DV2, the executable file for FEM2DV2 could not be created on a PC. The program was simply too large (consisting of over several thousand lines of code). Therefore, the program was transferred to a Sun System SPARC 20 workstation. The program was executed and tested successfully. It was found that the program ran much much quicker on the workstation than on the PC, facilitating the analysis. The actual compiler used to run the program was a SPARC compiler FORTRAN version 3.00.

### **3.3.4 Illustrative Example of FEM2DV2: Viscous Fluid Squeezed Between Plates**

In order to show how the program FEM2DV2 works, consider the time-dependent analysis of a viscous fluid squeezed between parallel plates, as shown in figure 3.4(a). The flow is induced by the uniform motion of the plates towards each other. The boundary conditions are shown in figure 3.4(b) and the initial boundary conditions are zero. Using a 12 X 8 uniform mesh of linear rectangular elements with nine nodes per element, the analysis can be done by looking at one section of the domain, as shown in figure 3.4(b). The program FEM2DV2 computes the values of the velocities  $u$  and  $v$  at each of the nodes, along with the stresses  $\sigma_x, \sigma_y, \sigma_{xy}$  and the pressure. This is done until the solution has reached a steady state. The output file of this analysis is shown in appendix B. Note that the first section of the output file reprints the input file, which was read by the program in the analysis of this problem. This analysis is consistent with the



(a)



(b)

**Figure 3.4** Boundary conditions and finite element meshes for the problem of an incompressible viscous fluid squeezed between plates: (a) geometry of the flow domain; (b) finite element mesh of a quadrant.

book's analysis of this same problem showing that the program FEM2DV2 works as it should (Reddy, p.560).

Other examples which were tested successfully were heat transfer with convection boundary conditions and a flow about a circular cylinder (Reddy, p. 552-554). Again, as mentioned for FEM1DV2, FEM2DV2 ran successfully for these examples and it compiled; however, there is no guarantee that it will yield the correct output for its other applications. Some minor debugging of the program may have to be done. This program consists of over 2000 lines, and some errors are certainly possible in the source code.

### **3.3.5 Use of FEM2DV2 to Obtain Velocity Distributions for a 90 Degree Duct Bend**

The problem at hand was to obtain the velocity distributions of a 90 degree duct bend (known as an "elbow"; this is a 2-D simulation of a pipe) so that a particle deposition analysis could later be performed. The elbow is shown in figure 3.5 along with the dimensions of the duct and the input and output velocity distributions. The analysis done in this thesis is a dimensionless one. The input velocity was parabolic and the fluid coming into the duct had a fully developed flow. The parabolic velocity distribution at the inlet was completely in the  $x$  direction, so that  $v$  at the inlet was equal to zero. In the  $x$  direction,

$$u = 1.5(1 - y^2) \quad (3.39)$$

at the inlet. The local value of  $y$  is zero at the center of the duct for this velocity distribution, so that the value of  $u$  is 1.5 at the center of the duct and zero at the outer walls (where  $y$  is equal to 1 and -1, making (3.39) equal to zero). The width of the duct is

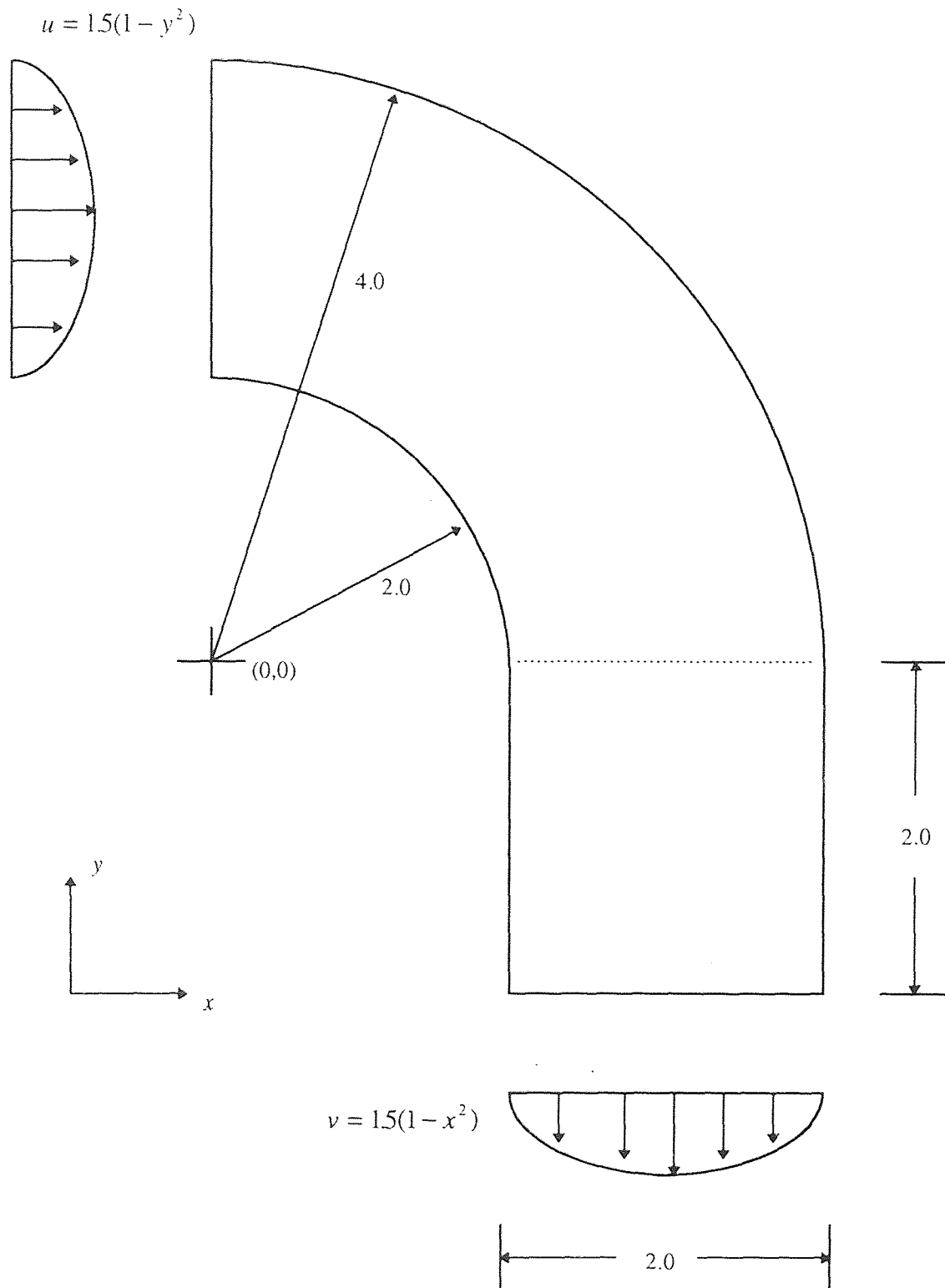


**Figure 3.5** The 90 degree duct bend with entrance and exit velocity distributions, dimensions, and global origin.

2 throughout. Also, the global coordinates are such that the origin is 2 units below the lower wall of the duct at the inlet section. The exit section of the duct has a fully developed flow as well, with a fully developed velocity distribution completely in the  $v$  direction, with  $u$  at the exit being equal to zero. The velocity at the exit section is described by

$$v = 1.5(1 - x^2) \quad (3.40)$$

For this velocity distribution, the local value of  $x$  is zero at the center of the exit section of the duct, again the width being 2. The value of  $v$  is 1.5 at the center in the negative  $y$  direction and zero at the inner and outer walls of the exit section. The velocity distributions were chosen such that the average velocities at the inlet and outlet sections were equal to 1.0 in the  $u$  and  $v$  directions, respectively.

The exit section of the elbow is vertical and equal to 2 units. It was determined that an exit section equal to 2 would allow the flow to become fully developed over that distance. This was done by analyzing a straight section of a duct, as shown in figure 3.6. The straight duct has a diameter of 2 and a length of 6. The flow coming in is uniform, with a value of  $u=1.0$ . At the exit, there is fully developed flow and  $u$  is described by (3.39), with  $y$  being zero at the center of the duct. The flow has a low Reynolds number, where the Reynolds number is defined as (Hesketh, p.16)

$$Re = \frac{Dv_g \rho_g}{\mu_g} \quad (3.41)$$

where  $D$  is the diameter of the duct,  $v_g$  is the velocity of the fluid,  $\rho_g$  is the density of the fluid, and  $\mu_g$  is the viscosity of the fluid. The flow is laminar and is moving at a



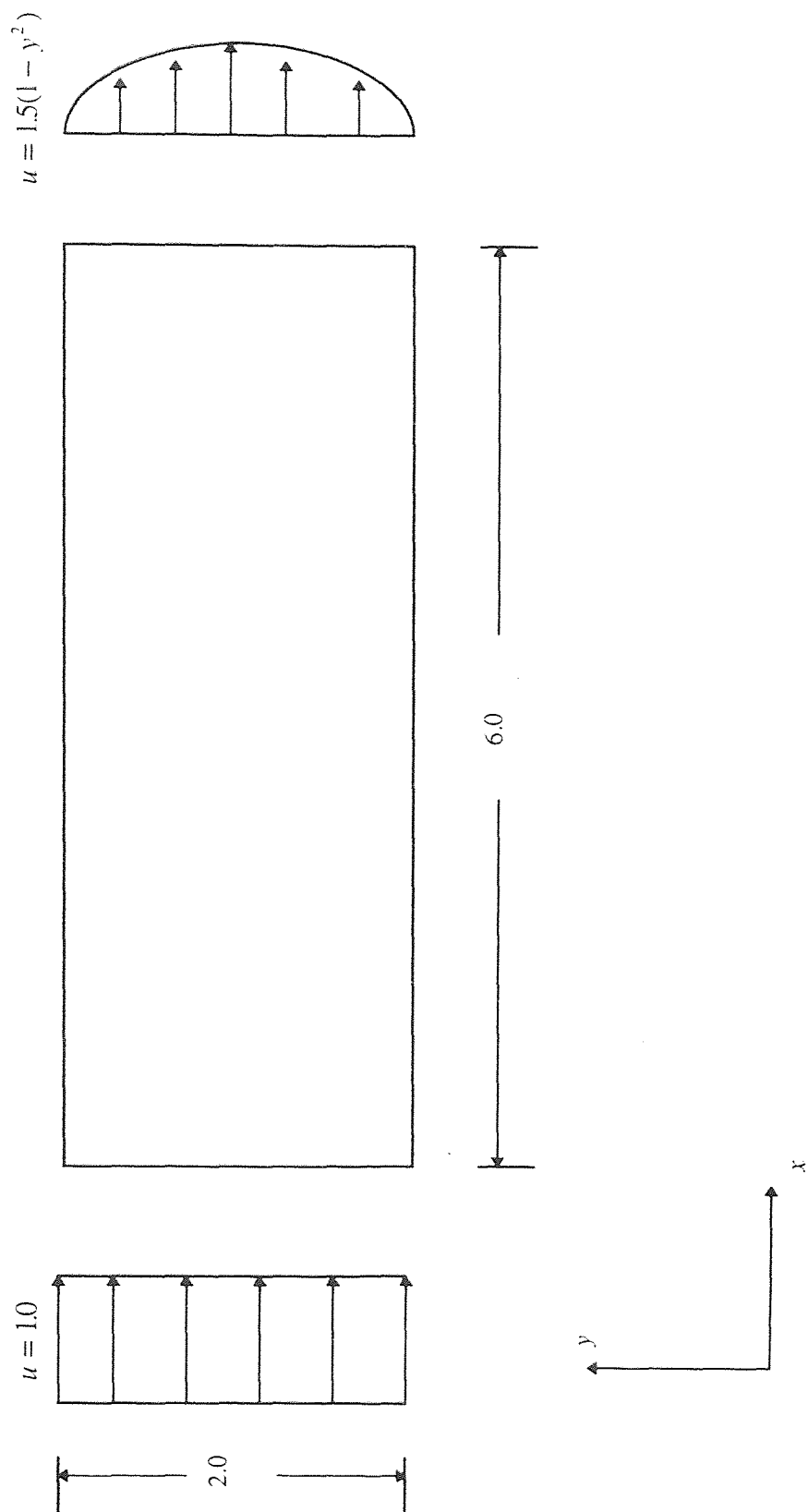


**Figure 3.6** Straight section of the duct used to determine the distance at which a uniform flow will become fully developed.

very low rate. This type of flow is referred to as “creeping flow”. Creeping flow is a type of flow where the flow rate is low so that the flow is laminar and the pressure gradient due to convective acceleration in the gap is negligible compared to the gradient due to viscous forces (Fox & McDonald, p.393).

The analysis of figure 3.6 was done using the program FEM2DV2. A 6 X 4 evenly spread element mesh with 9 nodes per element was used to examine this steady-state flow with the initial conditions being  $u=0$ ,  $v=0$  at the walls of the duct (top and bottom sections of figure 3.6),  $u=1$ ,  $v=0$  at the inlet section of the duct, and  $u = 1.5(1 - y^2)$ ,  $v=0$  at the exit section of the duct. The viscosity of the fluid was equal to 2.0 and the penalty parameter was set at  $1.0 \times 10^8$ , a value within the suggested limits established by Reddy (Reddy, p.494). The purpose of analyzing this straight section was to determine how much distance it would take for a uniform flow to become fully developed. With such a low flow rate, a flow through a duct will become fully developed quite rapidly. It turned out that at a distance of about 1.7 units, the flow was fully developed. Therefore, the exit section in figure 3.5 was set at 2.0, a distance in which the flow would become fully developed.

An important note in this type of analysis is that the duct is being modeled as a flow between two parallel plates of infinite distance in the  $z$  direction, simulating a two-dimensional pipe. There is nothing occurring in the  $z$  direction, and the flows in the  $x$  and  $y$  directions are independent of the  $z$  direction, hence yielding a two-dimensional flow.

The analysis of figure 3.6 was simple using FEM2DV2. The input file for the program is shown in appendix C. The program generates all of the mesh coordinates on

its own using rectangular nine node elements. Only one half of the domain has to be analyzed due to symmetry, so the analysis becomes even easier. However, when the analysis was performed on figure 3.5, all of the mesh data had to be input manually. This included describing the connectivity of the nodes in each element and inputting the coordinates of every node in the mesh. A sample input to the program FEM2DV2 using a 21 element mesh is given in appendix D. The mesh is shown in figure 3.7. This is an extremely simple mesh and it requires an input file which is three pages long, specifying the element connectivity of 21 elements and the coordinates of 105 nodes (nine nodes per element). It becomes evident that using a much larger mesh can become a formidable task due to the specification of all of the elements' connectivity information and the coordinates of every node in the mesh; but these types of problems can be dealt with. By examining the input file in appendix D, it becomes clear that the connectivity of the elements is in such a way (as defined by Reddy, see p. 550) that relationships exist among interconnected elements. For instance, the node numbers begin at the lowest left point of the domain, namely the lower wall at the entrance section of the duct. This is node number one. Nodes 2, 3, 4, ... are along the lower wall of the duct, until node number 15 is reached. Next, node number 16 is at the entrance section, just above node number 1 (at a distance of 0.333 units above it, determined by evenly spreading seven nodes at the entrance over a diameter of 2). From here, with the origin as shown in figure 3.5, the nodes along this constant radius are 16, 17, 18, ..., 30. This same procedure is followed until node number 105 is reached.

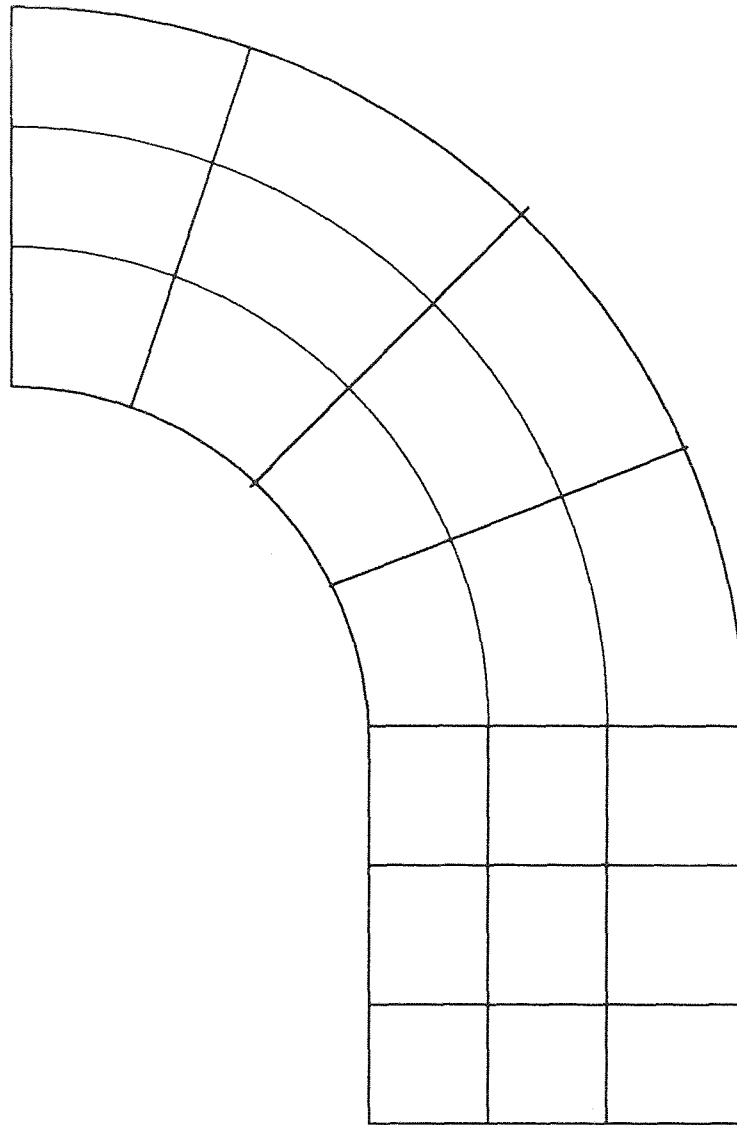


**Figure 3.7** A sample 21 element mesh used for the velocity distribution analysis; nine nodes per quadrilateral element.

Reddy's program is written in such a way that the connectivity of the elements must be described as follows. For a nine-node rectangular element, as in figure 3.7, the first element is the one with node number 1 at the lowest left corner. The connectivity of the elements goes: lowest left, lowest right, highest right, highest left, lowest center, right center, highest center, left center, center, as shown in figure 3.8. While this may sound a bit tricky, it is the same procedure for all 21 elements and a pattern develops along a fixed radius. For instance, at the lower wall, the first three elements have the connectivity (this is read from left to right; the first line is the first element, the second line is the second element, etc.)

1	3	33	31	2	18	32	16	17
3	5	35	33	4	20	34	18	19
5	7	37	35	6	22	36	20	21

This is the first three input lines in appendix D. By looking at the first column, the numbers are increasing by 2. This is true for the 2nd, 3rd, and the rest of the columns. For the seven elements in the lowest section of figure 3.7, only the connectivity of the first element (the left most) must be thought about in this case. The others can be computed by adding 2 to each of the node numbers in this case as shown. This same principle is true throughout these types of meshes, so that only the connectivity of the three elements at the entrance of the duct must be specified, with the others coming from a very simple program which adds 2 to each node. Those results are then put into the input file. This technique becomes very useful in the analysis of the mesh which was actually used to obtain the final velocity distributions, which had 16 elements along each

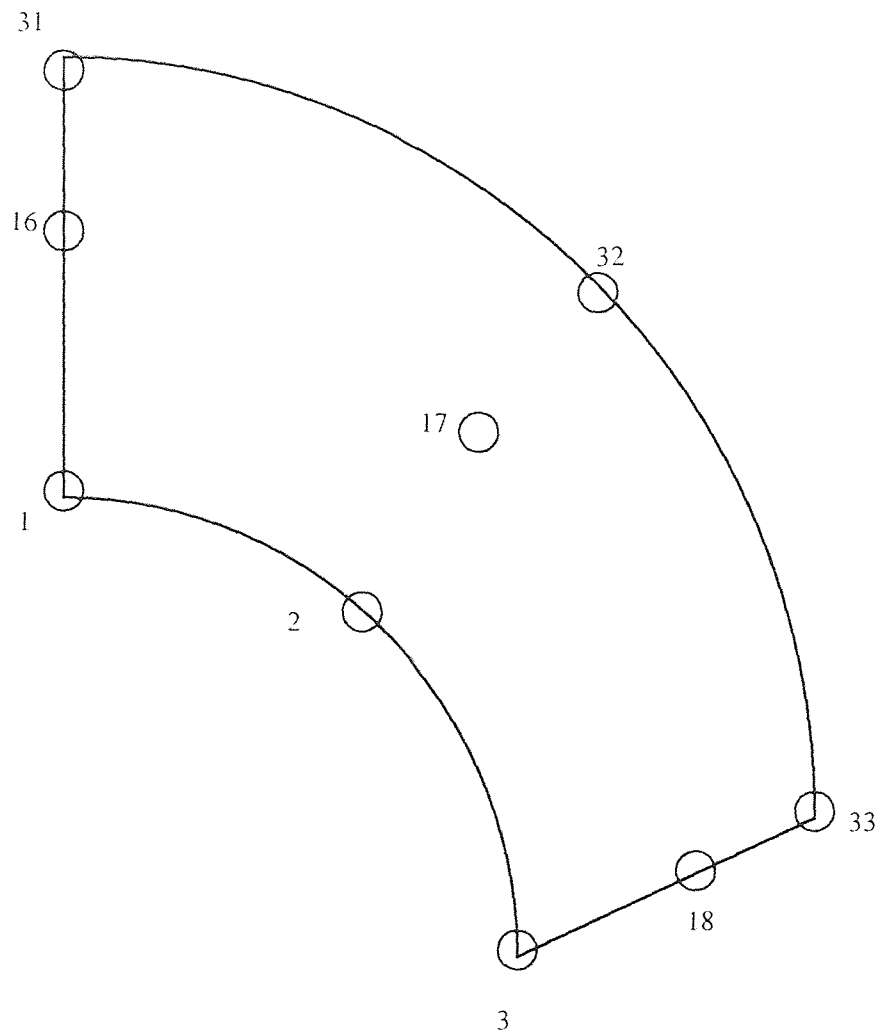


**Figure 3.8** The first element of the 21 element mesh showing the node numbers demonstrating the connectivity of an element for the input file of FEM2DV2.

fixed radius and 8 elements along the entrance; therefore, only 8 node connectivities were described, with the other 120 elements' connectivity being generated by a simple program. This simple program for this case is shown in appendix E.

The next problem becomes specifying the coordinates of every node in the mesh when the mesh is not generated by the program FEM2DV2, as was the case with figure 3.7. In figure 3.7, there are 21 elements and 105 nodes. 105 coordinates have to be specified, beginning with the  $x$  and  $y$  coordinates of node number 1 and continuing down to node number 105. That means that the user has to input 210 numbers for a simple 21 element mesh. This problem can be overcome by a simple program as well. By closely examining figure 3.7 and taking into account the number of nodes along each fixed radius and the dimensions of the duct, the coordinates of the nodes along each radius are obtained through evenly spreading the nodes over the domain. The next set of coordinates begin by increasing the radius, then going through the same procedure until the coordinates of all the nodes have been computed. The program which was used in this analysis is shown in appendix F.

Similar programs such as those found in appendices E and F in this case can be used when the program FEM2DV2 does not generate the mesh data for the user. An analysis of the domain must be performed by the user and patterns between node connectivities of the elements as well as the coordinates of the elements must be sought for maximum efficiency in creating the input data file.

The actual mesh which was used in this analysis is shown in figure 3.9. A 16 X 8 element mesh (for a total of 128 elements) was used with 561 nodes. There were 9 nodes

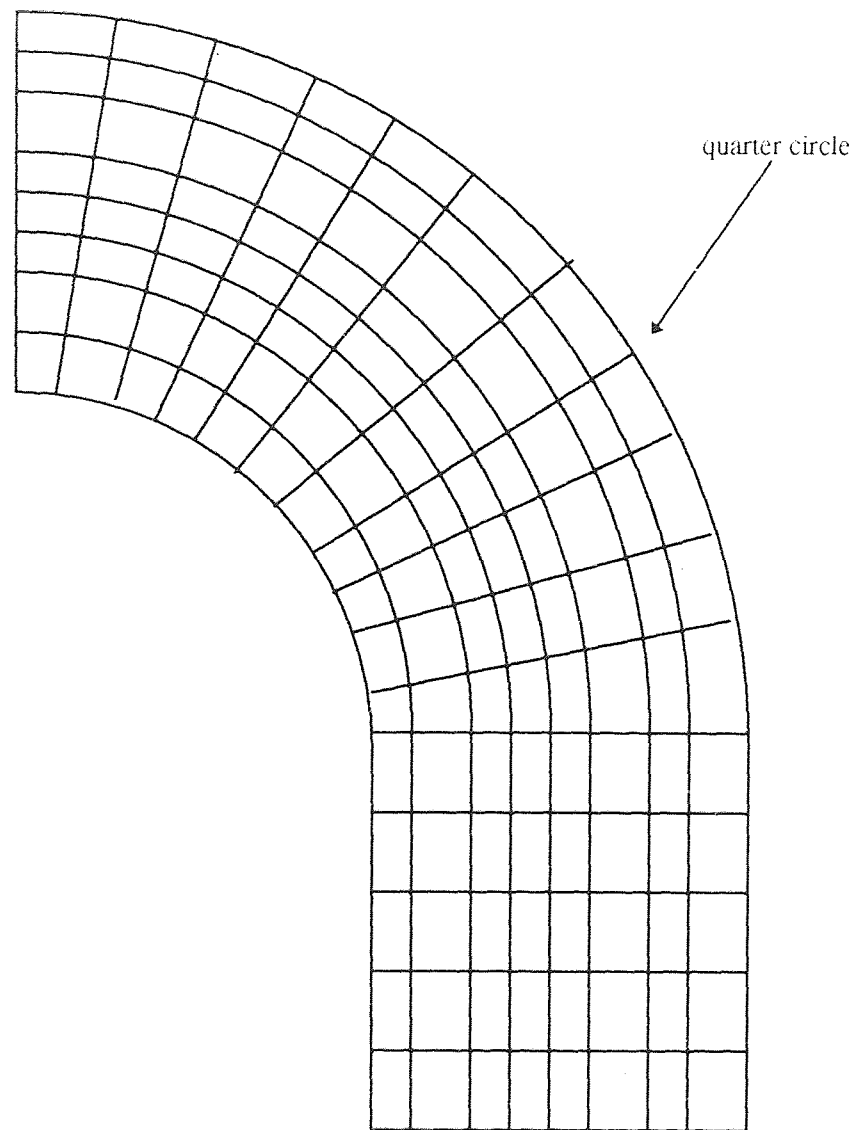


**Figure 3.9** 128 element mesh used to obtain the velocity distributions from the program FEM2DV2; nine nodes per quadrilateral element for a total of 561 nodes.



per quadrilateral element. The input file to the program FEM2DV2 is very similar to the one for the 21 element mesh. The 128 element mesh simply has more specifications for the connectivity of the nodes and the coordinates of all 561 nodes. The output of the program FEM2DV2 which was of interest in this case was the velocity distribution at each of the 561 nodes. The boundary conditions in this analysis were such that  $u = 1.5(1 - y^2)$ ,  $v=0$  at the entrance,  $u=0$ ,  $v=0$  at the lower and upper walls, and  $u=0$ ,  $v = 1.5(1 - x^2)$  at the exit. The velocity distributions which were obtained were used in the analysis of particle deposition in fluid-particle suspension through a 90 degree turn in a two-dimensional duct.

## CHAPTER 4

### PARTICLE DEPOSITION ANALYSIS

This section discusses particle deposition in a fluid-particle motion through a 90 degree bend in a parallel-plate channel. The parameter which was varied in the particle motion equations was the inertia parameter. The velocity distributions at each position were obtained through finite element analysis as discussed in section 3.3.5 and through interpolation.

Particle deposition analysis in a duct bend as shown in figure 3.5 is very useful in determining where the particles will impact against the wall with the most concentration. As the inertia parameter is varied, the deposition rates will change. The section in which there is the most deposition is the section which must be protected foremost in such applications where the particles can erode the wall. Uniformly coating a wall with protectants can be costly in some cases. It may be more economically sound to protect the wall with a supplement in the section in which there is the most impact. Extra supplements in the area of maximum particle deposition can reduce the wear on the duct in the section most likely to fail due to maximum erosion.

#### 4.1 Governing Equations

Particle motion in two dimensions is affected by the image charge, inertia force, viscous force, and gravity force. For this analysis, the following assumptions are made:

- incompressible, steady flow
- two-dimensional uniform flow

- fluid-particle interaction negligible
- particle to particle interaction negligible
- thickness of the layer of deposit is much smaller than the duct diameter
- negligible lift forces act on the particle
- no chemical reactions
- material density of the fluid is much smaller than the material density of the solid particles

For a solid particle suspension in an incompressible steady, laminar flow, the Lagrangian frame momentum balances are

$$\begin{aligned} m \frac{du_p}{dt} &= k(u - u_p) + f_x \\ m \frac{dv_p}{dt} &= k(v - v_p) - mg + f_y \end{aligned} \tag{4.1}$$

where  $u$  and  $v$  are the velocities of the fluid in the  $x$  and  $y$  direction, respectively,  $m$  is the mass of the particle,  $k$  is equal to  $6\pi\mu a$  (Stoke's drag law),  $\mu$  is the dynamic viscosity of the fluid,  $a$  is the radius of the spherical particle, and  $f_x, f_y$  denote the electrostatic force components in the  $x$  and  $y$  directions, respectively,  $g$  is the gravitational acceleration, and the subscript  $p$  denotes a particle.

The equations can be non-dimensionalized with the following nondimensionless terms:

$$\begin{aligned}
T &= \frac{tu_0}{h_0} \\
X &= \frac{x}{h_0} \\
Y &= \frac{y}{h_0} \\
U &= \frac{u}{u_0} \\
V &= \frac{v}{v_0}
\end{aligned} \tag{4.2}$$

where  $t$  is the time unit,  $h_0$  is the characteristic length, and  $u_0, v_0$  are the velocities in the  $x$  and  $y$  directions at the entrance. With the parameters  $S$ ,  $G$ , and  $Q$ , (4.1) becomes

$$\begin{aligned}
S \frac{d^2 X}{dT^2} &= U - \frac{dX}{dT} + QF_x \\
S \frac{d^2 Y}{dT^2} &= V - \frac{dY}{dT} - G + QF_y
\end{aligned} \tag{4.3}$$

where

$$\begin{aligned}
S &= \frac{\text{inertia force}}{\text{viscous force}} = \frac{mu_0}{h_0 k} \\
Q &= \frac{\text{charge force}}{\text{viscous force}} = \frac{q^2}{4\pi\epsilon_0 h_0^2 k u_0} \\
G &= \frac{\text{gravity force}}{\text{viscous force}} = \frac{mg}{k u_0}
\end{aligned} \tag{4.4}$$

Since the charge forces are not being considered in this case, (4.3) can be rewritten as

$$\begin{aligned}
S \frac{d^2 X}{dT^2} &= U - \frac{dX}{dT} \\
S \frac{d^2 Y}{dT^2} &= V - \frac{dY}{dT} - G
\end{aligned} \tag{4.5}$$

Finally, if

$$\begin{aligned}
 A &= \frac{dX}{dT} \\
 B &= \frac{dY}{dT}
 \end{aligned}
 \tag{4.6}$$

then (4.5) becomes

$$\begin{aligned}
 S \frac{dA}{dT} &= U - A \\
 S \frac{dB}{dT} &= V - B - G
 \end{aligned}
 \tag{4.7}$$

These are the equations which are used in the analysis of particle deposition through a 90 degree duct bend. The parameter  $S$  is referred to as the inertia force throughout this document.

## 4.2 Method of Solution

The equations of particle motion are defined in (4.7). These equations were used to compute the values of the nondimensionless terms  $A$  and  $B$  so that the positions  $x$  and  $y$  for the particle could be computed. This was done using the fourth order Runge-Kutta method. The equations for this application are as follows:

$$\begin{aligned}
 x_{i+1} &= x_i + \frac{K_1 + 2K_2 + 2K_3 + K_4}{6} \\
 A_{i+1} &= A_i + \frac{K'_1 + 2K'_2 + 2K'_3 + K'_4}{6}
 \end{aligned}
 \tag{4.8}$$

where

$$\begin{aligned}
K'_1 &= \frac{dT}{S} \cdot (U_i - A_i) \\
K'_2 &= \frac{dT}{S} \cdot \left( U_i - \left[ A_i + \frac{K'_1}{2} \right] \right) \\
K'_3 &= \frac{dT}{S} \cdot \left( U_i - \left[ A_i + \frac{K'_2}{2} \right] \right) \\
K'_4 &= \frac{dT}{S} \cdot (U_i - [A_i + K'_3]) \\
K_1 &= dT \cdot A_i \\
K_2 &= dT \cdot \left( A_i + \frac{K'_1}{2} \right) \\
K_3 &= dT \cdot \left( A_i + \frac{K'_2}{2} \right) \\
K_4 &= dT \cdot (A_i + K'_3)
\end{aligned} \tag{4.9}$$

and

$$\begin{aligned}
y_{i+1} &= y_i + \frac{K''_1 + 2K''_2 + 2K''_3 + K''_4}{6} \\
B_{i+1} &= B_i + \frac{K'''_1 + 2K'''_2 + 2K'''_3 + K'''_4}{6}
\end{aligned} \tag{4.10}$$

where

$$\begin{aligned}
K_1''' &= \frac{dT}{S} \cdot (V_i - B_i - G) \\
K_2''' &= \frac{dT}{S} \cdot \left( V_i - \left[ B_i + \frac{K_1'''}{2} \right] - G \right) \\
K_3''' &= \frac{dT}{S} \cdot \left( V_i - \left[ B_i + \frac{K_2'''}{2} \right] - G \right) \\
K_4''' &= \frac{dT}{S} \cdot (V_i - [B_i + K_3'''] - G) \\
K_1'' &= dT \cdot B_i \\
K_2'' &= dT \cdot \left( B_i + \frac{K_1'''}{2} \right) \\
K_3'' &= dT \cdot \left( B_i + \frac{K_2'''}{2} \right) \\
K_4'' &= dT \cdot (B_i + K_3''')
\end{aligned} \tag{4.11}$$

Equations (4.8)-(4.11) were used to compute the next position of a particle entering the duct shown in figure 3.5. The velocity terms in these equations ( $U$  and  $V$ ) come from the finite element analysis of this domain using the 128 element mesh from figure 3.9. A particle starting at a set position at the entrance of the duct had specified  $x$  and  $y$  initial values. This was the starting position. For example, if a particle were to start at the center of the duct, then, from figure 3.5,  $x=0.0$ ,  $y=3.0$ . This is the initial position. The initial velocity is computed using (3.39). The initial velocities in the  $x$  and  $y$  directions for this particle are  $U=1.5$  and  $V=0.0$ . The initial values of  $A$  and  $B$  are equal to the initial values of  $U$  and  $V$ , respectively. With this given information, (4.8)-(4.11) are used to compute the next values of  $x$ ,  $y$ ,  $A$ , and  $B$ . The values of  $U$  and  $V$  are constantly coming from the results of the finite element analysis as explained in chapter 3. This process continues until one of the following conditions are met (refer to figure 3.5):

1. The particle hits the top circular wall; this happens when the radius of the particle,  $Z$ , where  $Z = \sqrt{x^2 + y^2}$ , is greater than or equal to 4.0, the outer radius of the duct, and  $y$  is greater than 0.0. If this occurs, then the particle has been deposited on the upper wall of the duct.
2. The particle hits the lower circular wall; this happens when  $Z$  is less than or equal to 2.0, the inner radius of the circular portion of the duct, and  $y$  is greater than 0.0. If this occurs, then the particle has been deposited on the lower circular wall of the duct.
3. The particle hits the lower right wall of the duct; this is in the exit vertical section. This occurs when  $y$  is less than or equal to 0.0 and  $x$  is greater than or equal to 4.0.
4. The particle hits the lower left wall of the duct; this is in the exit vertical section. This occurs when  $y$  is less than or equal to 0.0 and  $x$  is less than or equal to 2.0.
5. The particle exits the duct through the vertical exit; this occurs when  $y$  is less than or equal to -2.0 and  $x$  is greater than 2.0 and less than 4.0.

The particle is considered to be deposited if (1)-(4) occurs. The particle exits the duct when (5) occurs. Equations (4.8)-(4.11) are used to compute the next position of the particle until one of these five situations occurs, and then the next particle coming in at the entrance is analyzed.



#### 4.2.1 Program “particles.f” Used to Analyze Particle Motion

Equations (4.8)-(4.11) are used to analyze the particle motion until the particle is either deposited on the wall or until it exits the duct. This is a systematic procedure and it was done using a FORTRAN program written for this thesis, called “particles.f”, given in appendix G. The program has comments in it describing exactly what it is doing, step by step. A flow chart of this program is shown in figure 4.1. The program reads in the node positions and the velocities  $U$  and  $V$  at each node; next it computes the initial position of each particle, based on the number of particles in the analysis. The user specifies the number of particles in the analysis and then the program distributes the particles throughout the entrance region’s diameter. In this case, for instance, there were 100 particles coming in at the entrance, which had a diameter of 2.0 (see figure 3.5). Because  $2.0/100=0.02$ , the particles were situated such that there were 0.02 units of distance between them. The particles were assumed to be entering the duct in an evenly distributed fashion. The initial velocity  $U$  was computed for each particle using equation (3.39) and the value of the initial velocity  $V$  was equal to 0.0 at the entrance. Next, using the fourth order Runge-Kutta equations, (4.8)-(4.11), the next position of the particle was computed (the user specifies  $S$  and  $G$ ). The analysis took place for one particle at a time. The particle was analyzed completely until it either was deposited or until it exited the duct. Having computed the particle’s next position, the program checked whether or not the particle had been deposited. If it had not, then the particle’s velocities  $U$  and  $V$  had to be determined using the finite element analysis velocity data and the value of the time

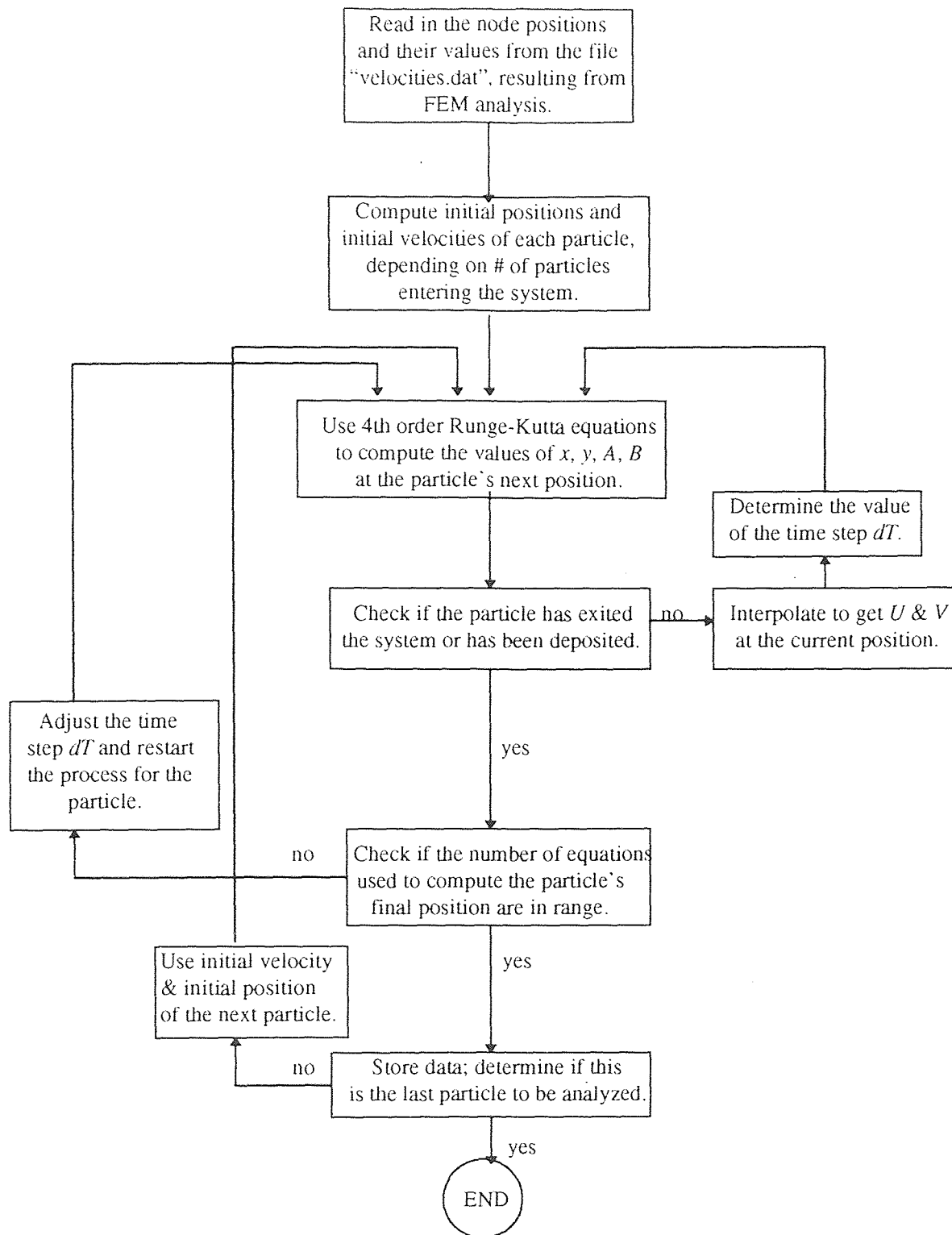


**Figure 4.1** Flowchart for the program "particles.f"; the program is listed completely in appendix G.

step  $dT$  had to be computed. Then the particle's next position was computed and a check was done again to see if the particle had either exited or been deposited.

If the particle had exited the duct, then the number of computations to exit the system was checked. The desired number of computations was set between 2000-3000. If this range of computations was not set, some particles would require 100 steps while others would go through 40,000 steps; this was not desirable, so a criterion was established. If the number of computations to exit the duct or deposit were less than 2000, then the program was run again for the same particle with a smaller time step,  $dT$ , so that the number of iterations would be increased. While running through the program, if the particle had not been deposited by 3000 iterations, then the program was terminated and the value of  $dT$  was increased to yield a lower number of iterations.

The value of the time step  $dT$  was computed using the equation

$$dT = \left| \frac{x_{i+1} - x_i}{U_{i+1}} \right| \quad (4.12)$$

If the value of  $dx$  was equal to 0.0, then  $dT$  would equal 0.0 from (4.12); however, the program checked for this and if  $dT$  was equal to 0.0 then

$$dT = \left| \frac{y_{i+1} - y_i}{V_{i+1}} \right| \quad (4.13)$$

If the particle exited the duct or was deposited and the number of equations was between 2000-3000, then the final positions of the particle were stored to a file. The next particle was then examined. This process was continued until all of the particles had been analyzed.

One of the most difficult things about using equations (4.8)-(4.11) was obtaining the values of  $U$  and  $V$ . Their values were read in at the nodes in the beginning of the program "particles.f". Their values came from the finite element analysis of figure 3.5. However, the problem was that a particle's position was virtually never at a node point; instead, it was located between nodes. Interpolation had to be done. The interpolation was a little tricky because the particle was in a curved section for a good portion of its journey. Theoretically, it is possible to compute the velocity components in an element using the interpolation functions for nine-node elements; however, for the sake of simplicity, the values of  $U$  and  $V$  were found as follows.

First the four closest node points to the particle had to be determined. Whether the particle was located in the curved section or the vertical exit section of the duct, it had four nodes next to it which were used to determine the values of the velocity. While in the curved section, the value of the particle's radius  $Z = \sqrt{x^2 + y^2}$  was computed. From this radius, the node numbers at the entrance were examined along with their distances from the origin (at the entrance, the nodes have positions  $x=0.0, 2.0 \leq y \leq 4.0$ ). Based on the  $y$  value of the nodes, there is a node which is immediately below  $Z$  and one which is immediately above  $Z$ . The lower node is known as MINNOD and the upper node is MAXNOD (see figure 4.2). With the value of MINNOD, the node numbers are ordered in such a way that the value of MINNOD's distance from the origin is constant as the node numbers are increased by 1. For example, suppose MINNOD were equal to 166, and MAXNOD were equal to 199. These node numbers were specified based on the value of  $Z$ . The value of  $Z$  falls between the  $y$  values of the node numbers 166 and 199,

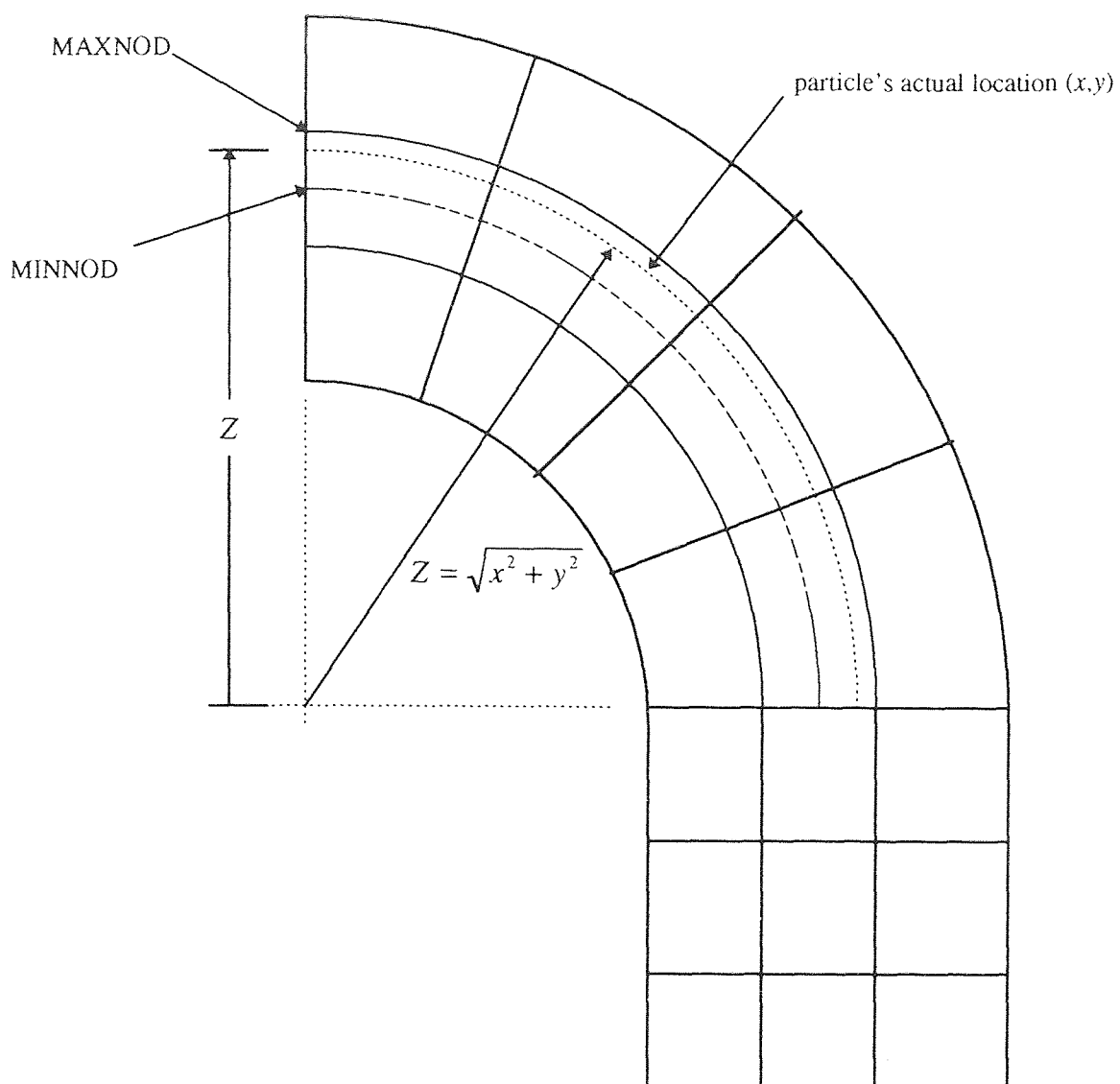
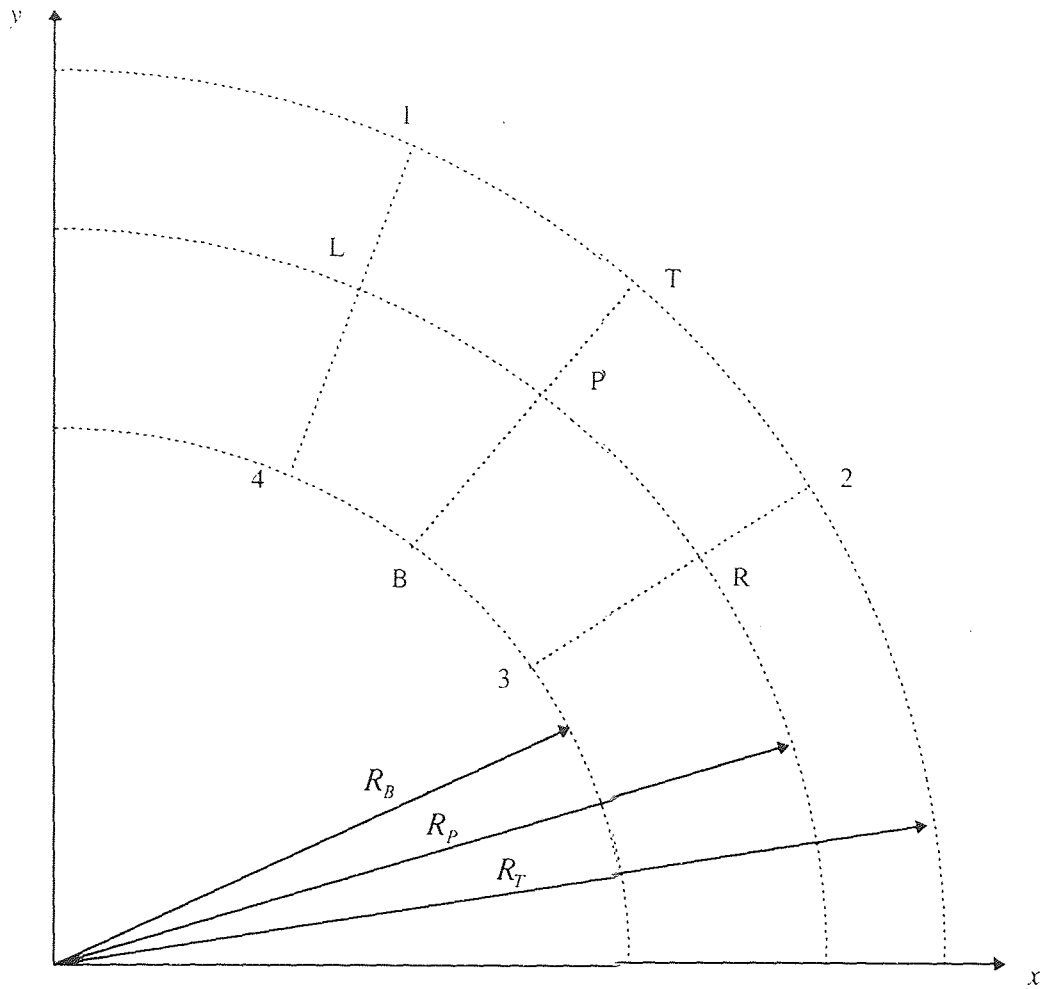


**Figure 4.2** Determining the four closest nodes to the particle based upon which nodes lie above and below it at the entrance when the particle is in the 90 degree turn.

located directly above the origin. Given MINNOD=166, the node number 166 is increased from 166, 167, 168, ... In doing so, the radius of these nodes from the origin is constant because they all lie along a constant radius line along the mesh, as shown in figure 3.9. As the node number is increased, the  $x$  and  $y$  values of the node's position are changing because this is a different node, but  $Z$  is constant, so the particle is just above this constant radius line. As the node numbers along MINNOD are increased, so are the values along MAXNOD, in the same way. So initially, the four closest nodes are considered to be 166, 167, 199, and 200. If the particle's position is between these nodes, then stop; if not, then look at nodes 167, 168, 200, 201; continue until the particle lies between these four nodes, as shown in figure 4.3.

Once the four closest nodes are determined, the next step is to interpolate to get the velocities. Supposing the particle is located such that it is between nodes 167, 168, 200, and 201. Then the lower left node (LL, or #4) is 167, the lower right node (RL, or #3) is 168, the upper left node (LU, or #1) is 200, and the upper right node (RU, or #2) is 201. The particle lies between these four nodes in the circular section of the duct and these four nodes have four different velocity values. Now interpolation must be performed to compute the particle's velocity at this current position. Referring to figure 4.3, the problem becomes finding  $x_L, y_L, x_R, y_R, x_T, y_T, x_B, y_B$  given  $x_1, y_1, x_2, y_2, x_3, y_3, x_4, y_4, x_p, y_p$  where  $p$  denotes the particle.

From figure 4.3,



- 1: Upper Left Node
- 2: Upper Right Node
- 3: Lower Right Node
- 4: Lower Left Node
- P: Particle's Actual Position
- L: Left Position of the Element
- R: Right Position of the Element
- T: Top Position of the Element
- B: Bottom Position of the Element
- R: Radius (subscripts indicate top, bottom, and particle)

**Figure 4.3:** Interpolating to get the velocity of the particle from the four closest nodes; this particle is in the 90 degree turn of the duct.

$$\begin{aligned}
R_T &= \sqrt{x_1^2 + y_1^2} \\
R_B &= \sqrt{x_4^2 + y_4^2} \\
R_p &= \sqrt{x_p^2 + y_p^2}
\end{aligned} \tag{4.14}$$

where  $R_T, R_B, R_p$  denote the radius of the top, bottom, and particle, respectively. The radius of the particle lies between the radius of the bottom and the radius of the top. Interpolating between the bottom and the top surfaces of figure 4.3, then

$$I = \frac{R_p - R_B}{R_T - R_B} \tag{4.15}$$

where  $I$  is the radial interpolation between the top and bottom surfaces. Also note that

$$I = \frac{x_L - x_4}{x_1 - x_4} \tag{4.16}$$

and therefore

$$\begin{aligned}
x_L &= (x_1 - x_4)I + x_4 \\
y_L &= (y_1 - y_4)I + y_4 \\
x_R &= (x_2 - x_3)I + x_3 \\
y_R &= (y_2 - y_3)I + y_3
\end{aligned} \tag{4.17}$$

From here, the values of the velocities on the left and right sides of figure 4.3 can be determined as

$$\begin{aligned}
u_L &= (u_1 - u_4)I + u_4 \\
v_L &= (v_1 - v_4)I + v_4 \\
u_R &= (u_2 - u_3)I + u_3 \\
v_R &= (v_2 - v_3)I + v_3
\end{aligned} \tag{4.18}$$



The next step is to determine the positions and velocities at the top and bottom of figure 4.3. This is done through interpolation again, as shown in figure 4.4. Referring to figure 4.4,

$$\begin{aligned}
 OA &= x_L \\
 LA &= y_L \\
 \theta_1 &= \tan^{-1} \left( \frac{y_L}{x_L} \right) \\
 \theta_2 &= \tan^{-1} \left( \frac{y_p}{x_p} \right) \\
 \theta_3 &= \tan^{-1} \left( \frac{y_R}{x_R} \right)
 \end{aligned} \tag{4.19}$$

the angles are related such that

$$\begin{aligned}
 \phi_1 &= \theta_1 - \theta_2 \\
 \phi_2 &= \theta_2 - \theta_3
 \end{aligned} \tag{4.20}$$

the interpolations become

$$\begin{aligned}
 I_T &= \frac{R_T \phi_1}{R_T \phi_1 + R_T \phi_2} \\
 I_B &= \frac{R_B \phi_1}{R_B \phi_1 + R_B \phi_2} \\
 I_p &= \frac{R_p \phi_1}{R_p \phi_1 + R_p \phi_2}
 \end{aligned} \tag{4.21}$$

and therefore

$$\begin{aligned}
 x_T &= (x_2 - x_1)I_T + x_1 \\
 y_T &= (y_2 - y_1)I_T + y_1 \\
 x_B &= (x_3 - x_4)I_B + x_4 \\
 y_B &= (y_3 - y_4)I_B + y_4
 \end{aligned} \tag{4.22}$$

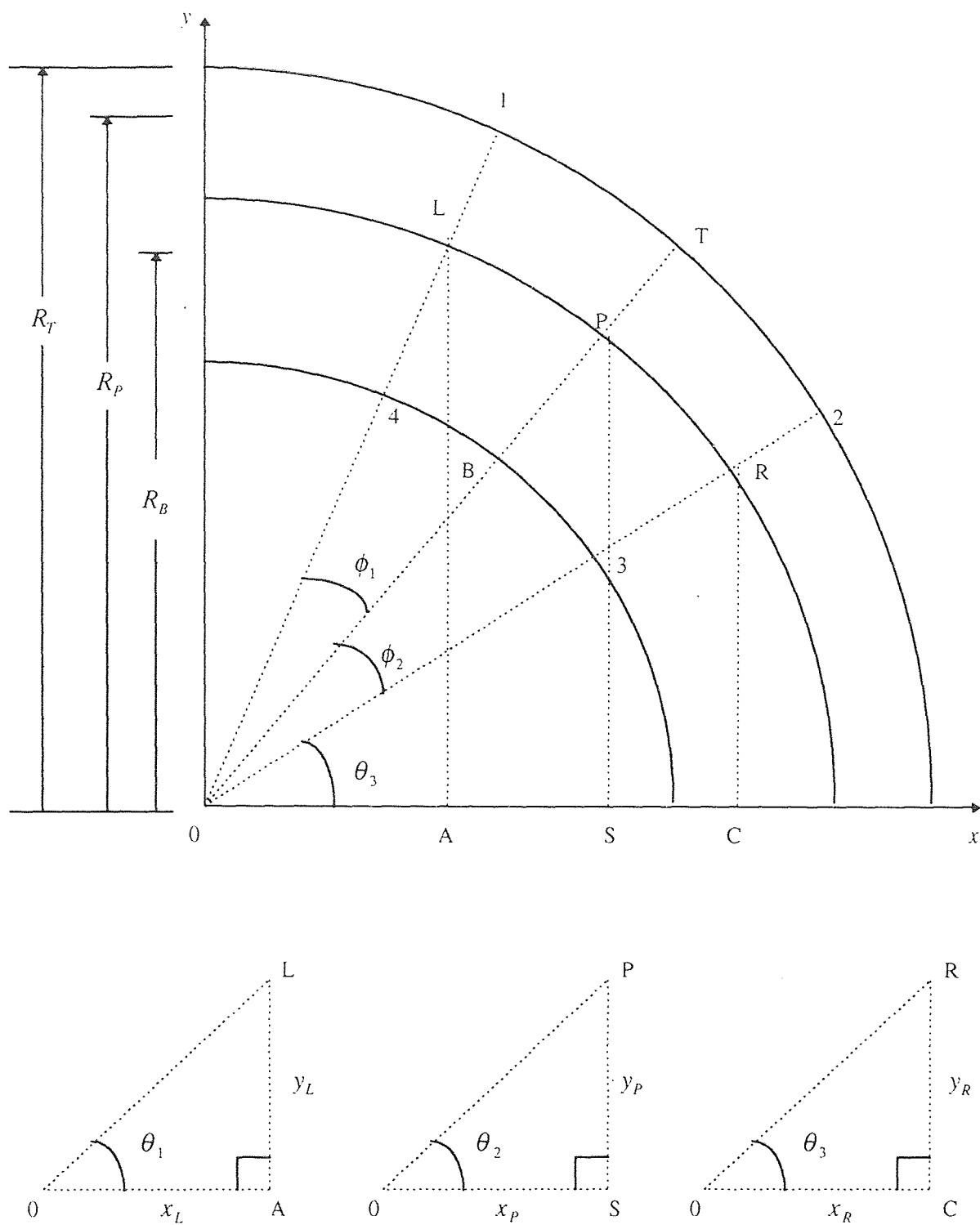


**Figure 4.4** Interpolating to get the velocity of the particle from the four closest nodes; computing the velocities at the top and bottom of the section enclosing the particle (the particle is in the 90 degree turn of the duct).

and

$$\begin{aligned}
 u_T &= (u_2 - u_1)I_T + u_1 \\
 v_T &= (v_2 - v_1)I_T + v_1 \\
 u_B &= (u_3 - u_4)I_B + u_4 \\
 v_B &= (v_3 - v_4)I_B + v_4
 \end{aligned} \tag{4.23}$$

Now that there are 4 values of  $u$  and 4 values of  $v$ , the horizontal and vertical components of these velocities can be computed as

$$\begin{aligned}
 u_{horiz} &= (u_R - u_L)I_p + u_L \\
 v_{horiz} &= (v_B - v_L)I_p + v_L \\
 u_{vert} &= (u_T - u_B)I + u_B \\
 v_{vert} &= (v_T - v_B)I + v_B
 \end{aligned} \tag{4.24}$$

and finally, the values of  $U$  and  $V$  for the particle's position are calculated as

$$\begin{aligned}
 U &= \frac{u_{horiz} + u_{vert}}{2} \\
 V &= \frac{v_{horiz} + v_{vert}}{2}
 \end{aligned} \tag{4.25}$$

When the particle is passed the 90 degree turn and is in the lower exit vertical section of the duct (see figure 3.5), the values of  $U$  and  $V$  are computed using figure 4.5.

In this case,

$$\begin{aligned}
 y_R &= y_L = y_p \\
 x_T &= x_B = x_p \\
 x_L &= x_1 \\
 x_R &= x_2 \\
 y_T &= y_1 \\
 y_B &= y_4
 \end{aligned} \tag{4.26}$$

The relevant interpolations are

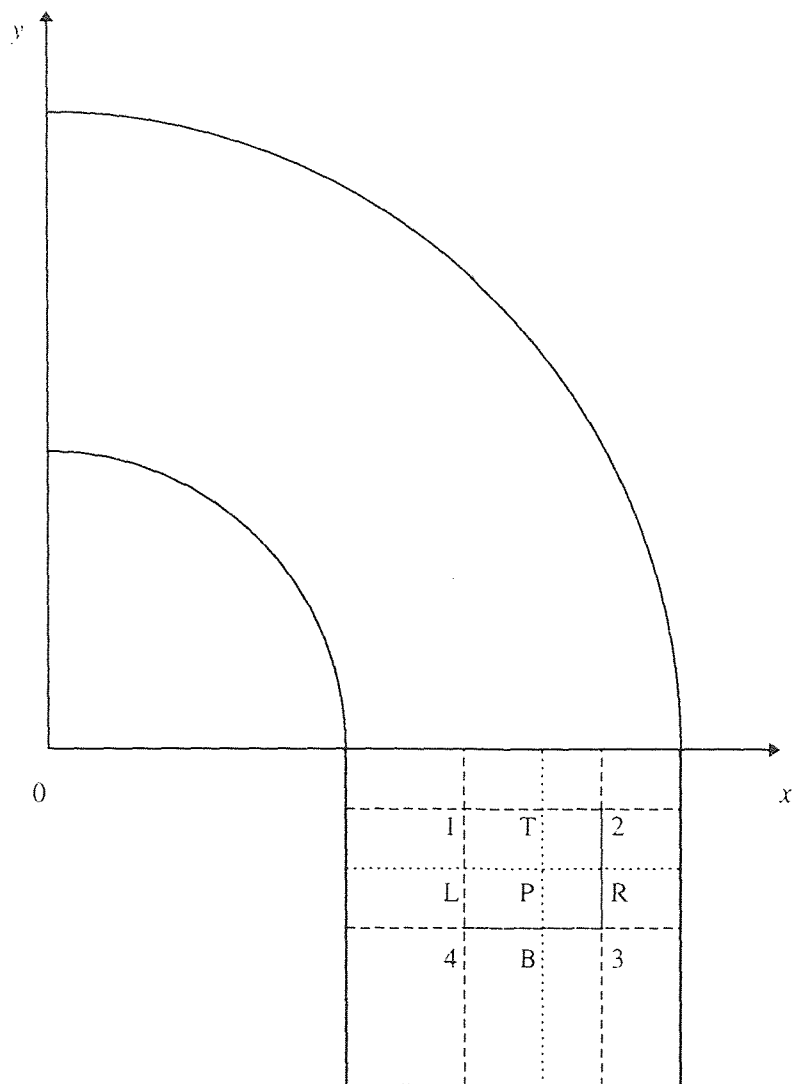


**Figure 4.5** Interpolating to get the velocity of the particle in the exit vertical section of the duct.

$$\begin{aligned}
I_{vert} &= \frac{y_L - y_4}{y_1 - y_4} \\
I_{horiz} &= \frac{x_T - x_1}{x_2 - x_1}
\end{aligned} \tag{4.27}$$

And the velocities are

$$\begin{aligned}
u_L &= (u_1 - u_4)I_{vert} + u_4 \\
u_R &= (u_2 - u_3)I_{vert} + u_3 \\
u_T &= (u_2 - u_1)I_{horiz} + u_1 \\
u_B &= (u_3 - u_4)I_{horiz} + u_4
\end{aligned} \tag{4.28}$$

and

$$\begin{aligned}
u_{horiz} &= (u_R - u_L)I_{horiz} + u_L \\
u_{vert} &= (u_T - u_B)I_{vert} + u_B
\end{aligned} \tag{4.29}$$

The values of  $v$  are computed just as in (4.28) and (4.29), but with  $u$  replaced by  $v$ . The values of  $U$  and  $V$  are computed using equations (4.25). With the values of  $U$  and  $V$  computed, the program “particles.f” was run until the particle either exited the duct or was deposited on one of its walls. The program ended when all of the particles were examined.

#### 4.2.2 Program “particlesout.f” Used to Analyze Particle Deposition

After the program “particles.f” was run (see section 4.2.1), the output was written to various data files. These data files were read by the program “particlesout.f” when it was run. This program’s purpose is to check the location of the particle deposition throughout the duct (figure 3.5). A flow chart of the program “particlesout.f” is shown in figure 4.6. The program is presented in its entirety in appendix H along with a typical output file from this program, known as “particles.output”.

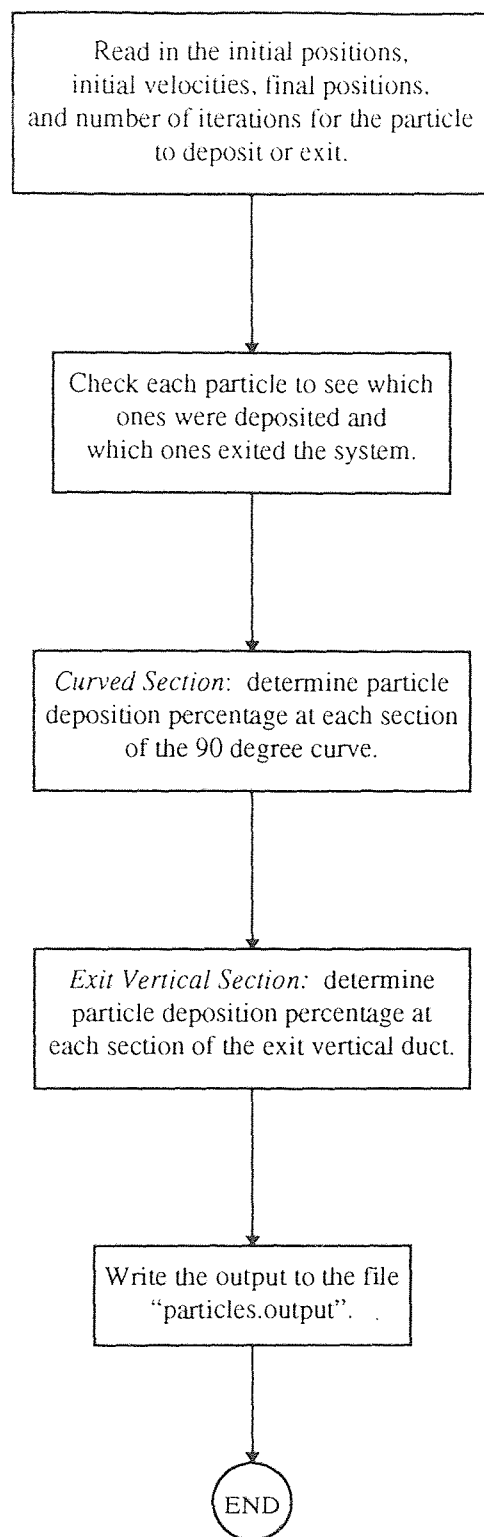


**Figure 4.6** Flowchart for the program "particlesout.f"; the program is listed completely in appendix H.

The program “particlesout.f” first reads in all of the relevant data, including the parameters  $S$ ,  $G$ , and the number of particles coming in at the entrance of the duct. It also reads the initial positions and velocities along with the final positions of all of the particles. Next, the program checks if the  $y$  value of the particle is greater than 0.0; if it is, then the particle has been deposited somewhere in the curved section of the duct. When this is the case, then a radius of 4.0 or more means that the particle has been deposited on the upper circular wall; a radius of 2.0 or less means that the particle has been deposited on the lower circular wall. When  $y$  is less than 0.0 but greater than -2.0, then the particle has been deposited on one of the exit vertical sections of the duct, depending on the value of  $x$ . Finally, if  $y$  is less than or equal to -2.0, then the particle has successfully exited the duct without hitting its walls.

The next step in the program is to check where the particles which have hit the walls of the duct actually landed. The 90 degree bend was split up into 16 pieces while the exit vertical section was split up into 5 pieces. This was done because most of the particles were deposited on the upper walls of the circular portion of the duct and the right exit vertical section of the duct (see figure 3.5). Since the data was later plotted in 21 sections (as will be shown in chapter 5), the distance each section occupied was made as equal as possible. For the 90 degree bend, the outer section of the duct has a radius of 4.0, making a  $1/16$  section distance equal to

$$\frac{2\pi \cdot 4.0}{4 \cdot 16} \approx 0.393 \quad (4.30)$$

The exit vertical section has a total length of 2.0 and it was split into 5 sections, so that  $2.0/5=0.4$ . The values 0.4 and 0.393 are very close, differing only by about 2%.

Examining the circular portion of the duct, the 90 degree turn was split up into 16 pieces. The first step was to set an angle at  $90-90/16$  degrees, or 84.38 degrees ( $\phi$ ; see figure 4.7). Next, the particles which were deposited in the circular portion were examined; if the angle

$$\theta = \tan^{-1} \left( \frac{y_{final}}{x_{final}} \right) \quad (4.31)$$

was greater than or equal to 84.38 degrees, then the particle was deposited in section 1. This is shown graphically in figure 4.7. All of the particles deposited in the 90 degree section were tested. Next, those same particles were tested again, but this time the angle they were checked against was set at  $90-90*2/16$  degrees, or 78.76 degrees. Particles with an angle greater than or equal to 78.76 degrees were deposited in section 2. This process was continued until the angle became 0 degrees, for section 16.

Section 17 was in the exit vertical section of the duct, between the y values of 0.0 and -0.4. If a particle was deposited in the exit vertical section and its y value was in this range, then it was deposited in section 17. The next step checked -0.4 to -0.8 for section 18, etc.

The output was sent to the data file “particles.output”. A sample of this output file is shown in appendix H.



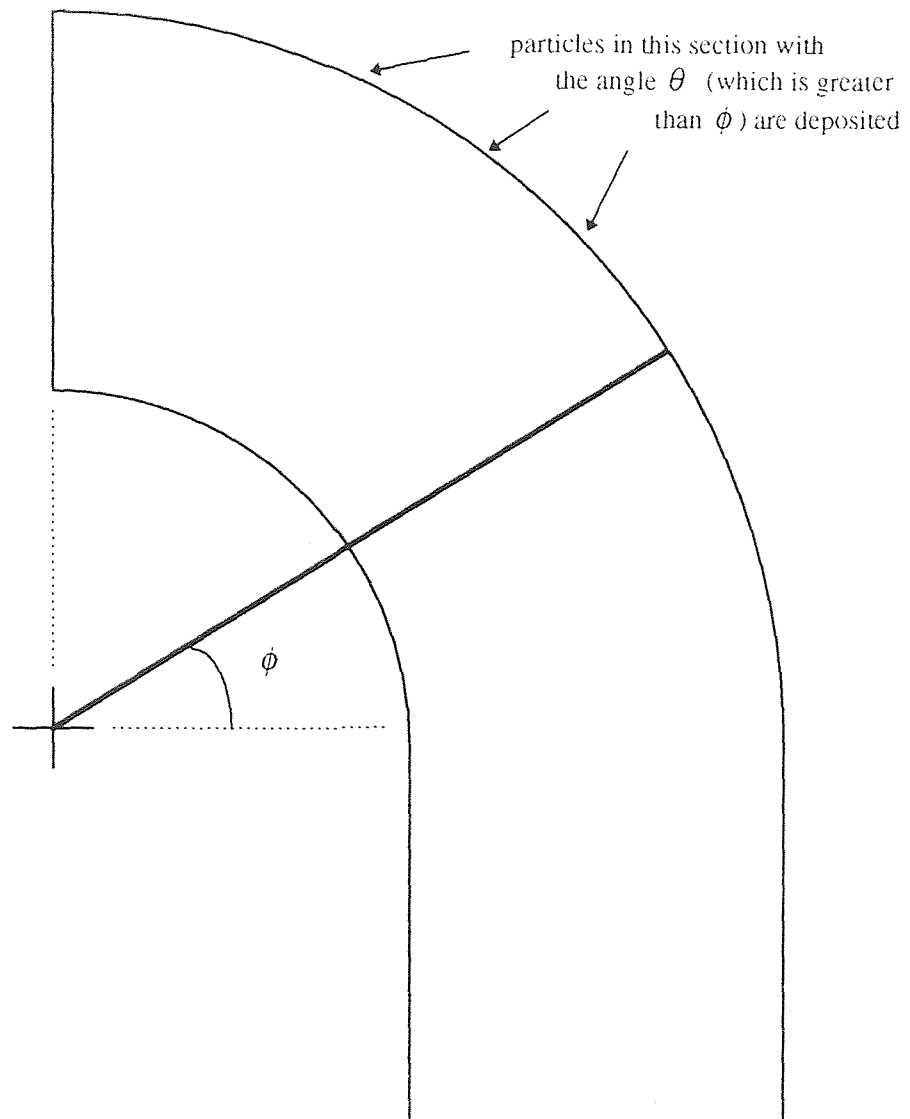


**Figure 4.7** Particle deposition in the 90 degree turn of the duct; particles are deposited in the current section when their location angle  $\theta$  is greater than the section angle  $\phi$ .

## CHAPTER 5

### RESULTS AND DISCUSSION OF PARTICLE DEPOSITION

After analyzing the fluid flow through the 90 degree duct bend of figure 3.5 using two-dimensional finite element analysis with the program FEM2DV2, particle deposition was studied in the duct using the program “particles.f”. Particle deposition was examined using the program “particlesout.f” (see chapter 4). This section shows the results of the analysis and discusses its significance.

#### 5.1 Results of Particle Deposition

The program “particles.f” (appendix G) was written in such a way that the particle deposition analysis is dependent upon the specification of the parameters  $S$  and  $G$  (these are the inertia and gravity parameters, as discussed in chapter 4). The program could also be modified to include the other dimensionless parameters for further analysis, but this study was to be kept simple due to the time constraint of this thesis. Therefore,  $G$  was set to zero and  $S$  was the only parameter varied.

The inertia parameter  $S$  of equation (4.4) took on the values of 0.5, 0.66, 1.0, 5.0, 10.0, and 100.0. The particle deposition in the duct of figure 3.5 was studied. Deposition is defined as

$$\text{Fraction of deposition} = \frac{\text{total number of particles deposited on wall}}{\text{total number of particles entering duct}}$$

The total number of particles entering the duct was fixed at 100. The total number of particles deposited on the wall varied with each section number, as defined in chapter 4

and shown in figure 5.1. Sections 1-16 represent curved sections of the duct, while sections 17-21 are the vertical exit sections of the duct. The outer radius of the curved sections have an arc length of 0.393, which is almost equal to the length of each vertical exit section which has a length of 0.4. A graph of particle deposition in each section of the duct is shown in figure 5.2 at varied  $S$ . Appendix I shows the exact values of the particle deposition percentages for each value of  $S$  at the corresponding section numbers.

Note that the program “particlesout.f” was written in such a way that a particle could be semi-deposited. For example, in section 1, if only 3 particles were deposited, and the next particle was deposited in section 2, then interpolation was done to check the distance between the last particle deposited in section 1 and the first particle deposited in section 2. From this interpolation, instead of 3% of the total incoming particles being deposited in section 1, 3.432% could be deposited in this section. This technique makes for smoother curves, like the ones shown in figure 5.2.

The actual velocity distributions for each node from the 128 element mesh (figure 3.9) generated using the program FEM2DV2 is shown in appendix J. The node number, position, and velocity is shown for each of the 561 nodes of this nine nodes per element mesh. The boundary conditions for this flow were such that a fully developed parabolic flow in the  $u$  direction was coming in at the entrance while a fully developed parabolic flow in the  $v$  direction was leaving at the exit. As the flow enters the duct,  $v$  is zero; however,  $v$  increases in the downward direction as the flow moves through the duct. At the same time,  $u$  is not equal to zero at the entrance, but it decreases to zero by the time the flow exits the duct. This is illustrated using figure 5.3. In figure 5.3, the velocities at

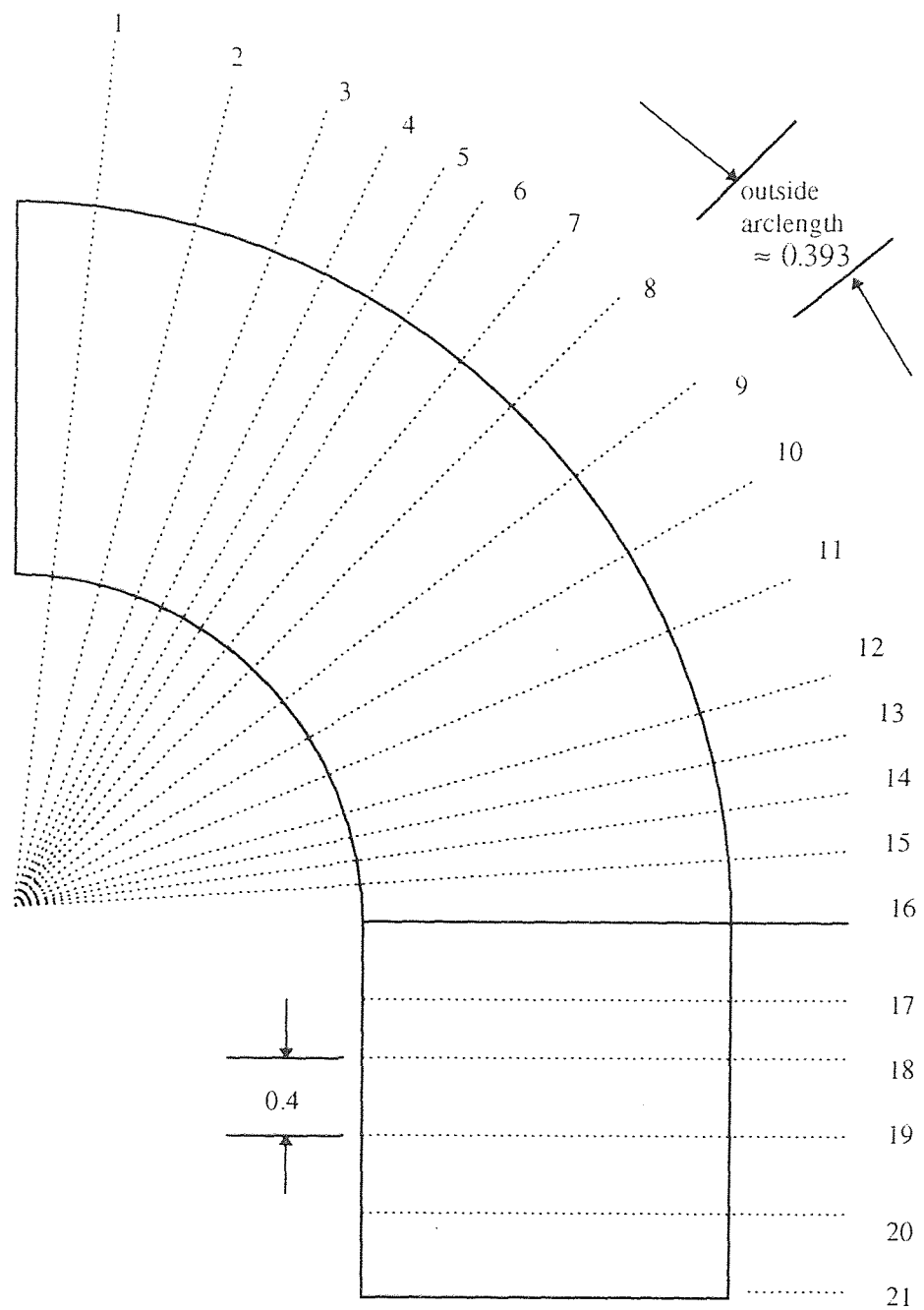


**Figure 5.1** Section numbers used for determining the particle deposition in the duct; these numbers correspond to the  $x$  axis of figure 5.2.

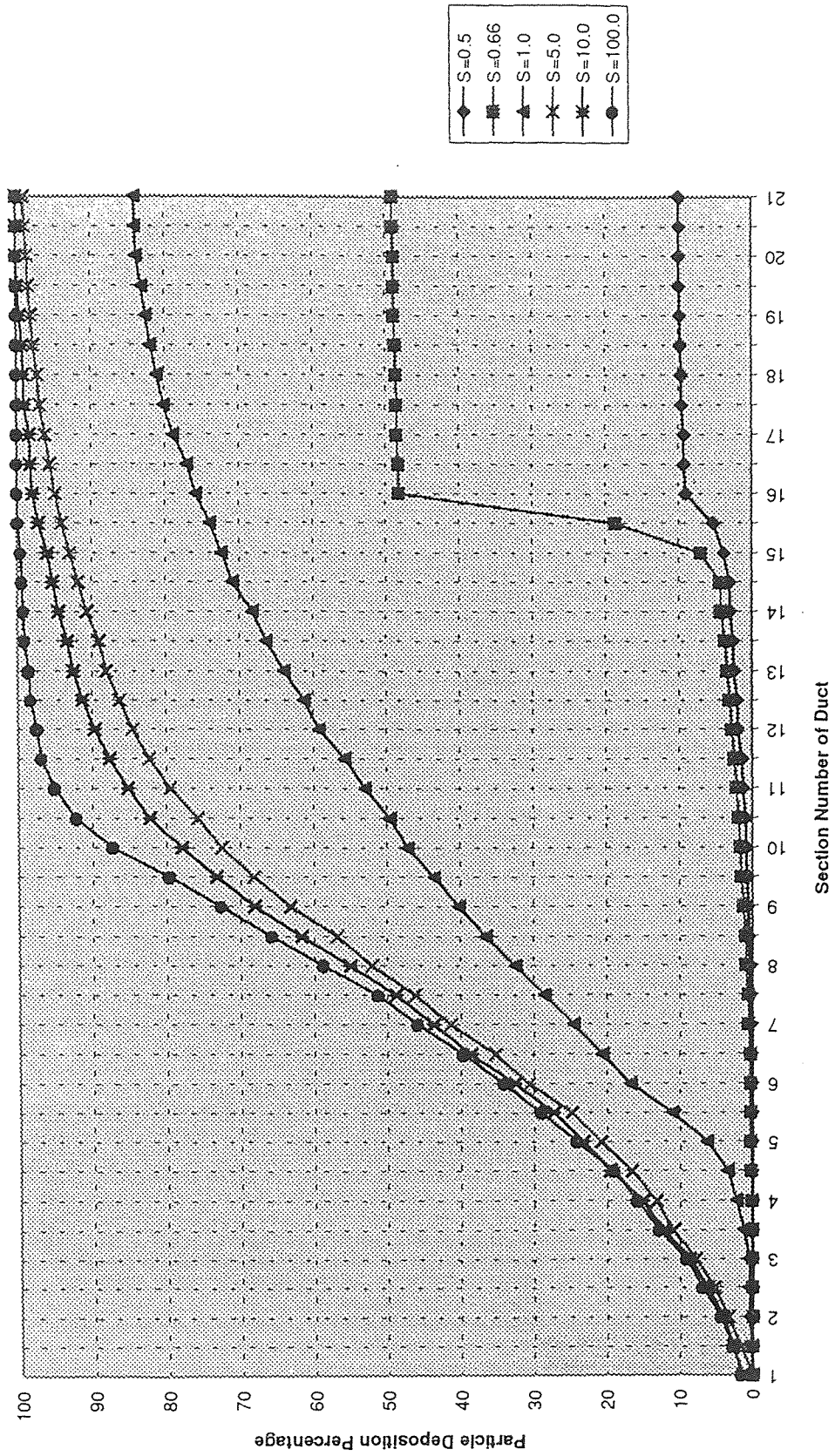


Figure 5.2 Particle deposition in the 90 degree duct bend as a function of the S parameter.



several nodes are examined. These nodes are at the entrance (90 degrees), at 57.3 degrees, 24.6 degrees, 0 degrees, 0.8 units above the exit, and at the exit. The velocity is examined along lines which are at a constant distance from the bottom wall of the duct, namely at 25%, 50%, and 75% away from the bottom wall of the duct, as shown in figure 5.3. The actual velocities at these nodes is shown in table 5.1.

**Table 5.1** Velocity Distributions at Selected Locations from Figure 5.3

<b>Node # (25%)</b>	$u$	$v$	<b>Node # (50%)</b>	$u$	$v$	<b>Node # (75%)</b>	$u$	$v$
<b>133</b>	1.125	0.000	<b>265</b>	1.500	0.000	<b>397</b>	1.125	0.000
<b>141</b>	1.043	-0.682	<b>273</b>	1.241	-0.812	<b>405</b>	0.848	-0.551
<b>149</b>	0.520	-1.144	<b>281</b>	0.615	-1.348	<b>413</b>	0.417	-0.912
<b>155</b>	0.089	-1.180	<b>287</b>	0.119	-1.489	<b>419</b>	0.066	-1.065
<b>161</b>	-0.002	-1.121	<b>293</b>	-0.001	-1.498	<b>425</b>	0.001	-1.125
<b>165</b>	0.000	-1.125	<b>297</b>	0.000	-1.500	<b>429</b>	0.000	-1.125

As can be seen in table 5.1, the velocity in the  $u$  direction is at its greatest value at the entrance nodes (133, 265, and 397). As the flow moves through the duct, this velocity decreases to zero, since the boundary conditions were set such that  $u$  was zero at the exit section of the duct. The values of  $v$ , on the other hand, are zero at the entrance (due to the boundary conditions) and they increase steadily in the downward direction until they are at a maximum value at the exit section (nodes 165, 297, and 429). At a distance 75% away from the bottom wall (nodes 397, 405, 413, 419, 425, and 429), the value of  $u$  decreases to zero more rapidly than for the distance 25% from the bottom wall (nodes 133, 141, 149, 155, 161, and 165). This is because the actual distance at the 75% position

from node to node is greater than the distance from node to node for the 25% position. The values of  $v$  at the 75% position increased in the downward direction a little more slowly than the values of  $v$  at the 25% position. The velocity distributions are shown graphically in figure 5.3 at A, B, C, and F. The velocity enters as parabolic, varies, and then exits as parabolic.

## 5.2 Discussion of Particle Deposition

To get some perspective of what the inertia parameter  $S$  physically represents, a magnitude analysis can be done. The inertia parameter was defined as

$$S = \frac{mu_0}{h_0(6\pi\mu a)} \quad (5.1)$$

in equation (4.4). Consider an air flow coming into the entrance of the duct (figure 3.5) which is fully developed; the pressure is 1 atm, the temperature is 80° F, and the position of one particle is at 0.2 ft from the bottom wall of the duct, with a specific gravity of 1.0.

The dynamic viscosity at these conditions is equal to  $3.85 \times 10^{-7} \frac{\text{lbf} \cdot \text{sec}}{\text{ft}^2}$  and the particle

is spherical in shape. Therefore,

$$S = \frac{\left(\frac{4}{3}\pi a^3 \cdot 62.4 \frac{\text{lbm}}{\text{ft}^3}\right) \left(2 \frac{\text{ft}}{\text{sec}}\right)}{(0.2 \text{ ft})(6\pi) \left(3.85 \times 10^{-7} \frac{\text{lbf} \cdot \text{sec}}{\text{ft}^2}\right) (a) \left(32.2 \frac{\text{lbm} \cdot \text{ft}}{\text{lbf} \cdot \text{sec}^2}\right)}$$

The radius  $a$  of the spherical particle is in ft. Canceling all of the units and solving for  $a$ ,

$$a = \sqrt{\frac{S}{11185501.87}}$$



The radius of the spherical particle can be computed using  $S$  values of 0.01, 0.1, 1.0, 10.0, and 100.0 ( $a \propto \sqrt{S}$ ). This is shown in table 5.2.

**Table 5.2** Typical Radius of a Spherical Particle at Varying Inertia Parameter Values

Inertia Parameter, $S$	Particle Radius, $a$ (ft)	Particle Radius, $a$ ( $\mu$ m)
0.01	$2.99 \times 10^{-5}$	9.11
0.1	$9.46 \times 10^{-5}$	28.83
1.0	$2.99 \times 10^{-4}$	91.14
10.0	$9.46 \times 10^{-4}$	288.34
100.0	$2.99 \times 10^{-3}$	911.35

This example shows how a typical particle's radius would affect the inertia parameter at a given set of conditions.

As can be seen in figure 5.2, particle deposition is very low when the inertia parameter is below 0.5. At  $S=0.5$ , there were only a total of 9.846% of the particles being deposited. Most of these particles were deposited after section 15, just above the area in which the circular duct meets the vertical exit section. Below  $S=0.5$ , almost no particles were deposited. As  $S$  was increased to 0.66, the curve was similar to 0.5, until section 15. At section 15, there were much more particles being deposited at this inertia parameter. A total of almost 49 particles were deposited at the same critical section, where the curved duct meets the straight vertical exit section. Half of the particles that entered the duct were deposited with  $S=0.66$ . For flows with an inertia parameter below 1.0, maximum deposition occurred at section 16, between the curved and straight parts of the duct. This is the part of the duct which would most likely be eroded if the particles were corrosive to the duct's material, as would be the case in a flow which carried contaminants, like in exhaust pipes (this 90 degree duct bend simulates a pipe in two dimensions).

As  $S$  was increased to 1.0, there was much more particle deposition between sections 5 and 15 than there was for the lower values of  $S$  which were examined. In fact, by section 16, about 76% of the particles had already been deposited for  $S=1.0$ . By the time the exit section was reached, 84% had been deposited.

The deposition became even greater when  $S$  took on the values of 5.0, 10.0, and 100.0. At these inertia parameters, the deposition was very intense even half way through the curved section of the duct. By the time the particles reached the 45 degree turn in the duct (section 8), more than half of all of the particles entering were deposited for each of these  $S$  values. At section 16, the point which was so critical for flows with inertia parameters below 1.0, more than 94% of the particles were deposited. This section had very little increased deposition and was not the critical section at  $S$  values greater than 1.0. For a flow through this type of duct with corrosive particulates, an inertia parameter of 5.0 or more would most likely erode the duct from sections 4-10 or so, or in the middle of the 90 degree turn. Anti-corrosive agents would most effectively be used in these sections, since they are the place in which the duct would most likely disintegrate first.

Particles with higher inertia parameters have the tendency to move straight, right into the circular wall of the duct. They are less affected by the changing direction of the fluid flow than the particles with smaller inertia parameters, which follow the flow more closely. The greater the inertia parameter, the more likely the particles will just flow straight through the duct and right into the top wall. Increased particle deposition is a direct result of increased  $S$  when the other parameters are not being considered.

## CHAPTER 6

### CONCLUSION

This thesis focused on the debugging and implementation of one-dimensional and two-dimensional finite element analysis FORTRAN programs by J.N. Reddy. The programs were shown to be executable and accurate, as demonstrated by examples in chapter 3. These programs are available for the use of the students studying finite element analysis or for other students who would like to implement the finite element method for their theses. Using the 2-D program FEM2DV2, a fluid flow through a 90 degree two-dimensional duct bend was examined. This was a steady viscous incompressible fluid. The program FEM2DV2 was used to obtain the velocity distributions for this duct (figure 3.5). Given these velocity distributions at each of the 561 nodes used in the mesh, particle deposition analysis was performed. A 128 element mesh was used with 9 nodes per element. The inertia parameter was varied from 0.5 to 100.0. It was found that with an increased inertia parameter, overall particle deposition was increased in the duct. With the inertia parameter  $S$  equal to 5.0 or higher, almost 100% of the particles entering the duct were deposited by the time the flow exited the system. When the flow carries corrosive particulates, this type of deposition can corrode the duct and cause it to wear out. Anti-corrosive agents should be spread throughout the duct in this type of flow, but extra protection should be applied at the point in which the 90 degree duct bend meets the exit vertical section when  $S$  is below 1.0; with  $S$  equal to 1.0, the duct should be evenly coated throughout, since particle deposition occurs uniformly throughout most of the duct; and

finally, extra protection should be placed throughout the 90 degree turn (especially in the middle of it) when  $S$  is above 1.0.

The particle deposition analysis of this thesis did not consider the other parameters such as the charge force  $Q$  and the gravitational force  $G$ . This analysis was not performed because this was a two-part thesis; the first part concentrated on the debugging and implementation of finite element FORTRAN programs, while the second part showed a specific example of the finite element implementation. As the inertia parameter is increased, the gravitational parameter  $G$  would probably affect the deposition of particles more, since heavier particles would tend to move downward. The variation of the parameter  $G$  along with  $S$  should be considered in further studies of this type of duct.

## CHAPTER 7

### RECOMMENDATIONS

The finite element analysis programs FEM1DV2 and FEM2DV2 can be used by other students who are doing theses and need a good finite element method source code. The programs can do more than fluid flow analysis as was done in this thesis: the applications of each program is discussed in chapter 3.

Particle deposition analysis on a 90 degree duct bend (as shown in figure 3.5) can also be further analyzed by considering the dimensionless parameters  $G$  and  $Q$ , varied separately or along with the parameter  $S$ . More trials could be run and further analysis done, since the source code for the finite element method is now readily available. Other types of ducts or walls could be studied as well, like converging planes or straight ducts, etc., using similar techniques developed in this thesis.

# APPENDIX A

## EXAMPLE INPUT FILE TO FEM1DV2

Example 7.1: Steady heat transfer in a fin (Set 1 boundary conditions)

```

1      0      0
1      4
1      1
      0.0      0.0625  0.0625  0.0625  0.0625
      1.0      0.0
      0.0      0.0
256.0      0.0
      0.0      0.0      0.0
      1
      1      1      100.0
      0
      0

```

\*\*\* ECHO OF THE INPUT DATA STARTS \*\*\*

Example 7.1: Steady heat transfer in a fin (Set 1 boundary conditions)

```

1      0      0
1      4
1      1
      0.0      0.0625  0.0625  0.0625  0.0625
      1.0      0.0
      0.0      0.0
256.0      0.0
      0.0      0.0      0.0
      1
      1      1      100.0
      0
      0

```

\*\*\*\* ECHO OF THE INPUT DATA ENDS \*\*\*\*

---

OUTPUT FROM PROGRAM FEM1DV2 BY J.N. REDDY  
 EDITED BY P. LOIACONO (SEPTEMBER 1995)

---

Example 7.1: Steady heat transfer in a fin (Set 1 boundary conditions)

\*\*\* ANALYSIS OF MODEL 1, AND TYPE 0 PROBLEM \*\*\*  
 (see the code below)

```

MODEL=1,NTYPE=0: A problem described by MODEL EQ. 1
MODEL=1,NTYPE=1: A circular DISK (PLANE STRESS)
MODEL=1,NTYPE>1: A circular DISK (PLANE STRAIN)
MODEL=2,NTYPE=0: A Timoshenko BEAM (RIE) problem
MODEL=2,NTYPE=1: A Timoshenko PLATE (RIE) problem
MODEL=2,NTYPE=2: A Timoshenko BEAM (CIE) problem
MODEL=2,NTYPE>2: A Timoshenko PLATE (CIE) problem
MODEL=3,NTYPE=0: A Euler-Bernoulli BEAM problem
MODEL=3,NTYPE>0: A Euler-Bernoulli Circular plate
MODEL=4,NTYPE=0: A plane TRUSS problem
MODEL=4,NTYPE=1: A Euler-Bernoulli FRAME problem
MODEL=4,NTYPE=2: A Timoshenko (CIE) FRAME problem

```

```

Element type (0, Hermite, >0, Lagrange ).. = 1
No. of deg. of freedom per node, NDF..... = 1
No. of elements in the mesh, NEM.....= 4
No. of total DOF in the model, NEQ.....= 5
No. of specified primary DOF, NSPV.....= 1
No. of specified secondary DOF, NSSV.....= 0
No. of specified Newton B. C. : NNBC.....= 0

```

Boundary information on primary variables:

1 1 .10000E+03

Global coordinates of the nodes, {GLX}:

.00000E+00 .62500E-01 .12500E+00 .18750E+00 .25000E+00

Coefficients of the differential equation:

AX0 = .1000E+01      AX1 = .0000E+00  
 BX0 = .0000E+00      BX1 = .0000E+00  
 CX0 = .2560E+03      CX1 = .0000E+00  
 FX0 = .0000E+00      FX1 = .0000E+00      FX2 = .0000E+00

Element coefficient matrix, [ELK]:

.21333E+02    -.13333E+02  
 -.13333E+02    .21333E+02

Element source vector, {ELF}:

.00000E+00    .00000E+00

SOLUTION (values of PVs) at the NODES:

.10000E+03    .35158E+02    .12504E+02    .48560E+01    .30350E+01

---

X	P. Variable	S. Variable
<hr/>		
.00000E+00	.10000E+03	-.10375E+04
.78125E-02	.91895E+02	-.10375E+04
.15625E-01	.83789E+02	-.10375E+04
.23438E-01	.75684E+02	-.10375E+04
.31250E-01	.67579E+02	-.10375E+04
.39063E-01	.59473E+02	-.10375E+04
.46875E-01	.51368E+02	-.10375E+04
.54688E-01	.43263E+02	-.10375E+04
.62500E-01	.35158E+02	-.10375E+04
.62500E-01	.35158E+02	-.36245E+03
.70313E-01	.32326E+02	-.36245E+03
.78125E-01	.29494E+02	-.36245E+03
.85938E-01	.26663E+02	-.36245E+03
.93750E-01	.23831E+02	-.36245E+03
.10156E+00	.20999E+02	-.36245E+03
.10938E+00	.18168E+02	-.36245E+03
.11719E+00	.15336E+02	-.36245E+03
.12500E+00	.12504E+02	-.36245E+03
.12500E+00	.12504E+02	-.12237E+03
.13281E+00	.11548E+02	-.12237E+03
.14063E+00	.10592E+02	-.12237E+03

---



.14844E+00	.96362E+01	-.12237E+03
.15625E+00	.86801E+01	-.12237E+03
.16406E+00	.77241E+01	-.12237E+03
.17188E+00	.67681E+01	-.12237E+03
.17969E+00	.58120E+01	-.12237E+03
.18750E+00	.48560E+01	-.12237E+03
.18750E+00	.48560E+01	-.29136E+02
.19531E+00	.46284E+01	-.29136E+02
.20313E+00	.44008E+01	-.29136E+02
.21094E+00	.41731E+01	-.29136E+02
.21875E+00	.39455E+01	-.29136E+02
.22656E+00	.37179E+01	-.29136E+02
.23438E+00	.34903E+01	-.29136E+02
.24219E+00	.32626E+01	-.29136E+02
.25000E+00	.30350E+01	-.29136E+02

---

# APPENDIX B

## EXAMPLE OUTPUT FILE FROM FEM2DV2

\*\*\* ECHO OF THE INPUT DATA STARTS \*\*\*

Example 11.5: Transient analysis of fluid squeezed between plates

```

1      1      1      0
1      9      1      0

6      4
0.0    1.0    1.0    1.0    1.0    1.0    1.0
0.0    0.5    0.5    0.5    0.5

47
  1 1    1 2    2 2    3 2    4 2    5 2    6 2    7 2    8 2    9 2
 10 2   11 2   12 2   13 2   14 1   27 1   40 1   53 1   66 1   79 1
 92 1  105 1  105 2  106 1  106 2  107 1  107 2  108 1  108 2  109 1
109 2  110 1  110 2  111 1  111 2  112 1  112 2  113 1  113 2  114 1
114 2  115 1  115 2  116 1  116 2  117 1  117 2

  0.0    0.0    0.0    0.0    0.0    0.0    0.0    0.0    0.0    0.0
  0.0    0.0    0.0    0.0    0.0    0.0    0.0    0.0    0.0    0.0
  0.0    0.0   -1.0    0.0   -1.0    0.0   -1.0    0.0   -1.0    0.0
 -1.0    0.0   -1.0    0.0   -1.0    0.0   -1.0    0.0   -1.0    0.0
 -1.0    0.0   -1.0    0.0   -1.0    0.0   -1.0

0

1.0      1.0E8

0.0      0.0      0.0
1.0      0.0      0.0
20      50      1      0
0.1      0.5      0.25    1.0D-3

```

\*\*\*\* ECHO OF THE INPUT DATA ENDS \*\*\*\*

Example 11.5: Transient analysis of fluid squeezed between plates

---

OUTPUT FROM PROGRAM \*FEM2DV2\* BY J. N. REDDY  
 Edited by Pantaleo Loiacono.....14 September 1995

---

A VISCOUS INCOMPRESSIBLE FLOW IS ANALYZED

PARAMETERS OF THE FLUID FLOW PROBLEM:

Viscosity of the fluid, AMU.....= 0.1000E+1

Penalty parameter, PENLTY.....= 0.1000E+9

CONTINUOUS SOURCE COEFFICIENTS:

Coefficient, F0 .....= 0.0000E+0  
 Coefficient, FX .....= 0.0000E+0  
 Coefficient, FY .....= 0.0000E+0

\*\*\*\*\* A TRANSIENT PROBLEM is analyzed \*\*\*\*\*

PARAMETERS OF THE DYNAMIC ANALYSIS:

Coefficient, C0 .....= 0.1000E+1  
 Coefficient, CX .....= 0.0000E+0  
 Coefficient, CY .....= 0.0000E+0  
 Time increment used, DT .....= 0.1000E+0  
 Parameter, ALFA .....= 0.5000E+0  
 Parameter, GAMA .....= 0.2500E+0  
 Number of time steps used, NTIME ....= 20  
 Time step at which load is removed, NSTP= 50  
 Time interval at which soln. is printed= 1

\*\*\* A mesh of QUADRILATERALS is chosen by user \*\*\*

FINITE ELEMENT MESH INFORMATION:

Element type: (0 = Triangle; >0 = Quad.)= 1  
 Number of nodes per element, NPE .....= 9  
 No. of primary deg. of freedom/node, NDF= 2  
 Number of elements in the mesh, NEM ....= 24  
 Number of nodes in the mesh, NNM .....= 117  
 Number of equations to be solved, NEQ ..= 234  
 Half bandwidth of the matrix GLK, NHBW ..= 58  
 Mesh subdivisions, NX and NY .....= 6 4

No. of specified PRIMARY variables, NSPV = 47

---

Node	x-coord.	y-coord.	Speci. primary & secondary variables (0, unspecified; >0, specified)			
			Primary DOF		Secondary DOF	
1	0.0000E+0	0.0000E+0	1	2	0	0
2	0.5000E+0	0.0000E+0	0	2	0	0
3	0.1000E+1	0.0000E+0	0	2	0	0
4	0.1500E+1	0.0000E+0	0	2	0	0
5	0.2000E+1	0.0000E+0	0	2	0	0
6	0.2500E+1	0.0000E+0	0	2	0	0
7	0.3000E+1	0.0000E+0	0	2	0	0

---

8	0.3500E+1	0.0000E+0	0	2	0	0
9	0.4000E+1	0.0000E+0	0	2	0	0
10	0.4500E+1	0.0000E+0	0	2	0	0
11	0.5000E+1	0.0000E+0	0	2	0	0
12	0.5500E+1	0.0000E+0	0	2	0	0
13	0.6000E+1	0.0000E+0	0	2	0	0
14	0.0000E+0	0.2500E+0	1	0	0	0
15	0.5000E+0	0.2500E+0	0	0	0	0
16	0.1000E+1	0.2500E+0	0	0	0	0
17	0.1500E+1	0.2500E+0	0	0	0	0
18	0.2000E+1	0.2500E+0	0	0	0	0
19	0.2500E+1	0.2500E+0	0	0	0	0
20	0.3000E+1	0.2500E+0	0	0	0	0
21	0.3500E+1	0.2500E+0	0	0	0	0
22	0.4000E+1	0.2500E+0	0	0	0	0
23	0.4500E+1	0.2500E+0	0	0	0	0
24	0.5000E+1	0.2500E+0	0	0	0	0
25	0.5500E+1	0.2500E+0	0	0	0	0
26	0.6000E+1	0.2500E+0	0	0	0	0
27	0.0000E+0	0.5000E+0	1	0	0	0
28	0.5000E+0	0.5000E+0	0	0	0	0
29	0.1000E+1	0.5000E+0	0	0	0	0
30	0.1500E+1	0.5000E+0	0	0	0	0
31	0.2000E+1	0.5000E+0	0	0	0	0
32	0.2500E+1	0.5000E+0	0	0	0	0
33	0.3000E+1	0.5000E+0	0	0	0	0
34	0.3500E+1	0.5000E+0	0	0	0	0
35	0.4000E+1	0.5000E+0	0	0	0	0
36	0.4500E+1	0.5000E+0	0	0	0	0
37	0.5000E+1	0.5000E+0	0	0	0	0
38	0.5500E+1	0.5000E+0	0	0	0	0
39	0.6000E+1	0.5000E+0	0	0	0	0
40	0.0000E+0	0.7500E+0	1	0	0	0
41	0.5000E+0	0.7500E+0	0	0	0	0
42	0.1000E+1	0.7500E+0	0	0	0	0
43	0.1500E+1	0.7500E+0	0	0	0	0
44	0.2000E+1	0.7500E+0	0	0	0	0
45	0.2500E+1	0.7500E+0	0	0	0	0
46	0.3000E+1	0.7500E+0	0	0	0	0
47	0.3500E+1	0.7500E+0	0	0	0	0
48	0.4000E+1	0.7500E+0	0	0	0	0
49	0.4500E+1	0.7500E+0	0	0	0	0
50	0.5000E+1	0.7500E+0	0	0	0	0
51	0.5500E+1	0.7500E+0	0	0	0	0
52	0.6000E+1	0.7500E+0	0	0	0	0
53	0.0000E+0	0.1000E+1	1	0	0	0
54	0.5000E+0	0.1000E+1	0	0	0	0
55	0.1000E+1	0.1000E+1	0	0	0	0
56	0.1500E+1	0.1000E+1	0	0	0	0
57	0.2000E+1	0.1000E+1	0	0	0	0
58	0.2500E+1	0.1000E+1	0	0	0	0
59	0.3000E+1	0.1000E+1	0	0	0	0
60	0.3500E+1	0.1000E+1	0	0	0	0

61	0.4000E+1	0.1000E+1	0	0	0	0
62	0.4500E+1	0.1000E+1	0	0	0	0
63	0.5000E+1	0.1000E+1	0	0	0	0
64	0.5500E+1	0.1000E+1	0	0	0	0
65	0.6000E+1	0.1000E+1	0	0	0	0
66	0.0000E+0	0.1250E+1	1	0	0	0
67	0.5000E+0	0.1250E+1	0	0	0	0
68	0.1000E+1	0.1250E+1	0	0	0	0
69	0.1500E+1	0.1250E+1	0	0	0	0
70	0.2000E+1	0.1250E+1	0	0	0	0
71	0.2500E+1	0.1250E+1	0	0	0	0
72	0.3000E+1	0.1250E+1	0	0	0	0
73	0.3500E+1	0.1250E+1	0	0	0	0
74	0.4000E+1	0.1250E+1	0	0	0	0
75	0.4500E+1	0.1250E+1	0	0	0	0
76	0.5000E+1	0.1250E+1	0	0	0	0
77	0.5500E+1	0.1250E+1	0	0	0	0
78	0.6000E+1	0.1250E+1	0	0	0	0
79	0.0000E+0	0.1500E+1	1	0	0	0
80	0.5000E+0	0.1500E+1	0	0	0	0
81	0.1000E+1	0.1500E+1	0	0	0	0
82	0.1500E+1	0.1500E+1	0	0	0	0
83	0.2000E+1	0.1500E+1	0	0	0	0
84	0.2500E+1	0.1500E+1	0	0	0	0
85	0.3000E+1	0.1500E+1	0	0	0	0
86	0.3500E+1	0.1500E+1	0	0	0	0
87	0.4000E+1	0.1500E+1	0	0	0	0
88	0.4500E+1	0.1500E+1	0	0	0	0
89	0.5000E+1	0.1500E+1	0	0	0	0
90	0.5500E+1	0.1500E+1	0	0	0	0
91	0.6000E+1	0.1500E+1	0	0	0	0
92	0.0000E+0	0.1750E+1	1	0	0	0
93	0.5000E+0	0.1750E+1	0	0	0	0
94	0.1000E+1	0.1750E+1	0	0	0	0
95	0.1500E+1	0.1750E+1	0	0	0	0
96	0.2000E+1	0.1750E+1	0	0	0	0
97	0.2500E+1	0.1750E+1	0	0	0	0
98	0.3000E+1	0.1750E+1	0	0	0	0
99	0.3500E+1	0.1750E+1	0	0	0	0
100	0.4000E+1	0.1750E+1	0	0	0	0
101	0.4500E+1	0.1750E+1	0	0	0	0
102	0.5000E+1	0.1750E+1	0	0	0	0
103	0.5500E+1	0.1750E+1	0	0	0	0
104	0.6000E+1	0.1750E+1	0	0	0	0
105	0.0000E+0	0.2000E+1	1	2	0	0
106	0.5000E+0	0.2000E+1	1	2	0	0
107	0.1000E+1	0.2000E+1	1	2	0	0
108	0.1500E+1	0.2000E+1	1	2	0	0
109	0.2000E+1	0.2000E+1	1	2	0	0
110	0.2500E+1	0.2000E+1	1	2	0	0
111	0.3000E+1	0.2000E+1	1	2	0	0
112	0.3500E+1	0.2000E+1	1	2	0	0
113	0.4000E+1	0.2000E+1	1	2	0	0

114	0.4500E+1	0.2000E+1	1	2	0	0
115	0.5000E+1	0.2000E+1	1	2	0	0
116	0.5500E+1	0.2000E+1	1	2	0	0
117	0.6000E+1	0.2000E+1	1	2	0	0

---

# NUMERICAL INTEGRATION DATA:

Full quadrature (IPDF x IPDF) rule, IPDF= 3  
 Reduced quadrature (IPDR x IPDR), IPDR= 2  
 Quadrature rule used in postproc., ISTR= 2

\*TIME\* = 0.14000E+1 Time Step Number = 14

# S O L U T I O N :

---

Node	x-coord.	y-coord.	Value of u	Value of v
1	0.00000E+0	0.00000E+0	0.00000E+0	0.00000E+0
2	0.50000E+0	0.00000E+0	0.37519E+0	0.00000E+0
3	0.10000E+1	0.00000E+0	0.74860E+0	0.00000E+0
4	0.15000E+1	0.00000E+0	0.11257E+1	0.00000E+0
5	0.20000E+1	0.00000E+0	0.14979E+1	0.00000E+0
6	0.25000E+1	0.00000E+0	0.18774E+1	0.00000E+0
7	0.30000E+1	0.00000E+0	0.22512E+1	0.00000E+0
8	0.35000E+1	0.00000E+0	0.26375E+1	0.00000E+0
9	0.40000E+1	0.00000E+0	0.30221E+1	0.00000E+0
10	0.45000E+1	0.00000E+0	0.34251E+1	0.00000E+0
11	0.50000E+1	0.00000E+0	0.38103E+1	0.00000E+0
12	0.55000E+1	0.00000E+0	0.41330E+1	0.00000E+0
13	0.60000E+1	0.00000E+0	0.42203E+1	0.00000E+0
14	0.00000E+0	0.25000E+0	0.00000E+0	-0.18605E+0
15	0.50000E+0	0.25000E+0	0.36887E+0	-0.18667E+0
16	0.10000E+1	0.25000E+0	0.73868E+0	-0.18611E+0
17	0.15000E+1	0.25000E+0	0.11068E+1	-0.18674E+0
18	0.20000E+1	0.25000E+0	0.14777E+1	-0.18649E+0
19	0.25000E+1	0.25000E+0	0.18460E+1	-0.18746E+0
20	0.30000E+1	0.25000E+0	0.22197E+1	-0.18851E+0
21	0.35000E+1	0.25000E+0	0.25929E+1	-0.19132E+0
22	0.40000E+1	0.25000E+0	0.29766E+1	-0.19546E+0
23	0.45000E+1	0.25000E+0	0.33658E+1	-0.19827E+0
24	0.50000E+1	0.25000E+0	0.37507E+1	-0.18623E+0
25	0.55000E+1	0.25000E+0	0.40709E+1	-0.11874E+0
26	0.60000E+1	0.25000E+0	0.41706E+1	0.40836E-1
27	0.00000E+0	0.50000E+0	0.00000E+0	-0.36881E+0
28	0.50000E+0	0.50000E+0	0.35190E+0	-0.36623E+0
29	0.10000E+1	0.50000E+0	0.70170E+0	-0.36876E+0
30	0.15000E+1	0.50000E+0	0.10558E+1	-0.36650E+0

31	0.20000E+1	0.50000E+0	0.14038E+1	-0.36893E+0
32	0.25000E+1	0.50000E+0	0.17603E+1	-0.36813E+0
33	0.30000E+1	0.50000E+0	0.21082E+1	-0.37150E+0
34	0.35000E+1	0.50000E+0	0.24696E+1	-0.37574E+0
35	0.40000E+1	0.50000E+0	0.28236E+1	-0.38251E+0
36	0.45000E+1	0.50000E+0	0.31979E+1	-0.39025E+0
37	0.50000E+1	0.50000E+0	0.35592E+1	-0.36653E+0
38	0.55000E+1	0.50000E+0	0.38904E+1	-0.24484E+0
39	0.60000E+1	0.50000E+0	0.40057E+1	0.77788E-1
40	0.00000E+0	0.75000E+0	0.00000E+0	-0.53464E+0
41	0.50000E+0	0.75000E+0	0.32200E+0	-0.53669E+0
42	0.10000E+1	0.75000E+0	0.64523E+0	-0.53474E+0
43	0.15000E+1	0.75000E+0	0.96600E+0	-0.53684E+0
44	0.20000E+1	0.75000E+0	0.12905E+1	-0.53556E+0
45	0.25000E+1	0.75000E+0	0.16101E+1	-0.53833E+0
46	0.30000E+1	0.75000E+0	0.19361E+1	-0.54004E+0
47	0.35000E+1	0.75000E+0	0.22558E+1	-0.54681E+0
48	0.40000E+1	0.75000E+0	0.25848E+1	-0.55614E+0
49	0.45000E+1	0.75000E+0	0.29101E+1	-0.56561E+0
50	0.50000E+1	0.75000E+0	0.32491E+1	-0.54544E+0
51	0.55000E+1	0.75000E+0	0.35756E+1	-0.37743E+0
52	0.60000E+1	0.75000E+0	0.37397E+1	0.85478E-1
53	0.00000E+0	0.10000E+1	0.00000E+0	-0.69118E+0
54	0.50000E+0	0.10000E+1	0.28189E+0	-0.68550E+0
55	0.10000E+1	0.10000E+1	0.56121E+0	-0.69121E+0
56	0.15000E+1	0.10000E+1	0.84570E+0	-0.68570E+0
57	0.20000E+1	0.10000E+1	0.11219E+1	-0.69155E+0
58	0.25000E+1	0.10000E+1	0.14093E+1	-0.68747E+0
59	0.30000E+1	0.10000E+1	0.16809E+1	-0.69438E+0
60	0.35000E+1	0.10000E+1	0.19707E+1	-0.69705E+0
61	0.40000E+1	0.10000E+1	0.22361E+1	-0.70709E+0
62	0.45000E+1	0.10000E+1	0.25263E+1	-0.72037E+0
63	0.50000E+1	0.10000E+1	0.27972E+1	-0.69857E+0
64	0.55000E+1	0.10000E+1	0.31387E+1	-0.53162E+0
65	0.60000E+1	0.10000E+1	0.33420E+1	0.80067E-1
66	0.00000E+0	0.12500E+1	0.00000E+0	-0.81275E+0
67	0.50000E+0	0.12500E+1	0.22827E+0	-0.81665E+0
68	0.10000E+1	0.12500E+1	0.45783E+0	-0.81271E+0
69	0.15000E+1	0.12500E+1	0.68465E+0	-0.81685E+0
70	0.20000E+1	0.12500E+1	0.91570E+0	-0.81296E+0
71	0.25000E+1	0.12500E+1	0.11399E+1	-0.81813E+0
72	0.30000E+1	0.12500E+1	0.13722E+1	-0.81594E+0
73	0.35000E+1	0.12500E+1	0.15892E+1	-0.82484E+0
74	0.40000E+1	0.12500E+1	0.18191E+1	-0.83050E+0
75	0.45000E+1	0.12500E+1	0.20212E+1	-0.84115E+0
76	0.50000E+1	0.12500E+1	0.22443E+1	-0.83655E+0
77	0.55000E+1	0.12500E+1	0.25342E+1	-0.69077E+0
78	0.60000E+1	0.12500E+1	0.28490E+1	-0.13515E-1
79	0.00000E+0	0.15000E+1	0.00000E+0	-0.91938E+0
80	0.50000E+0	0.15000E+1	0.16466E+0	-0.91134E+0
81	0.10000E+1	0.15000E+1	0.32752E+0	-0.91967E+0
82	0.15000E+1	0.15000E+1	0.49401E+0	-0.91113E+0
83	0.20000E+1	0.15000E+1	0.65415E+0	-0.92079E+0

84	0.25000E+1	0.15000E+1	0.82296E+0	-0.91112E+0
85	0.30000E+1	0.15000E+1	0.97627E+0	-0.92406E+0
86	0.35000E+1	0.15000E+1	0.11476E+1	-0.91389E+0
87	0.40000E+1	0.15000E+1	0.12781E+1	-0.93227E+0
88	0.45000E+1	0.15000E+1	0.14550E+1	-0.92510E+0
89	0.50000E+1	0.15000E+1	0.15295E+1	-0.91125E+0
90	0.55000E+1	0.15000E+1	0.18167E+1	-0.87243E+0
91	0.60000E+1	0.15000E+1	0.21455E+1	-0.13368E+0
92	0.00000E+0	0.17500E+1	0.00000E+0	-0.97286E+0
93	0.50000E+0	0.17500E+1	0.87841E-1	-0.97990E+0
94	0.10000E+1	0.17500E+1	0.17591E+0	-0.97256E+0
95	0.15000E+1	0.17500E+1	0.26346E+0	-0.98022E+0
96	0.20000E+1	0.17500E+1	0.35176E+0	-0.97153E+0
97	0.25000E+1	0.17500E+1	0.43845E+0	-0.98116E+0
98	0.30000E+1	0.17500E+1	0.52657E+0	-0.96929E+0
99	0.35000E+1	0.17500E+1	0.60885E+0	-0.98416E+0
100	0.40000E+1	0.17500E+1	0.69517E+0	-0.96320E+0
101	0.45000E+1	0.17500E+1	0.75708E+0	-0.99399E+0
102	0.50000E+1	0.17500E+1	0.86035E+0	-0.92708E+0
103	0.55000E+1	0.17500E+1	0.86332E+0	-0.10056E+1
104	0.60000E+1	0.17500E+1	0.14390E+1	-0.54872E+0
105	0.00000E+0	0.20000E+1	0.00000E+0	-0.10000E+1
106	0.50000E+0	0.20000E+1	0.00000E+0	-0.10000E+1
107	0.10000E+1	0.20000E+1	0.00000E+0	-0.10000E+1
108	0.15000E+1	0.20000E+1	0.00000E+0	-0.10000E+1
109	0.20000E+1	0.20000E+1	0.00000E+0	-0.10000E+1
110	0.25000E+1	0.20000E+1	0.00000E+0	-0.10000E+1
111	0.30000E+1	0.20000E+1	0.00000E+0	-0.10000E+1
112	0.35000E+1	0.20000E+1	0.00000E+0	-0.10000E+1
113	0.40000E+1	0.20000E+1	0.00000E+0	-0.10000E+1
114	0.45000E+1	0.20000E+1	0.00000E+0	-0.10000E+1
115	0.50000E+1	0.20000E+1	0.00000E+0	-0.10000E+1
116	0.55000E+1	0.20000E+1	0.00000E+0	-0.10000E+1
117	0.60000E+1	0.20000E+1	0.00000E+0	-0.10000E+1

---

x-coord.	y-coord.	sigma-x	sigma-y	sigma-xy	pressure
0.211E+0	0.105E+0	0.173E+3	0.170E+3	-0.124E-1	-0.171E+3
0.211E+0	0.394E+0	0.173E+3	0.170E+3	-0.266E-1	-0.172E+3
0.788E+0	0.105E+0	0.170E+3	0.167E+3	-0.273E-1	-0.168E+3
0.788E+0	0.394E+0	0.170E+3	0.167E+3	-0.120E+0	-0.169E+3
0.121E+1	0.105E+0	0.165E+3	0.162E+3	-0.518E-1	-0.164E+3
0.121E+1	0.394E+0	0.166E+3	0.163E+3	-0.174E+0	-0.165E+3
0.178E+1	0.105E+0	0.157E+3	0.154E+3	-0.680E-1	-0.155E+3
0.178E+1	0.394E+0	0.157E+3	0.155E+3	-0.268E+0	-0.156E+3
0.221E+1	0.105E+0	0.148E+3	0.145E+3	-0.911E-1	-0.147E+3
0.221E+1	0.394E+0	0.149E+3	0.146E+3	-0.324E+0	-0.148E+3
0.278E+1	0.105E+0	0.134E+3	0.131E+3	-0.111E+0	-0.133E+3
0.278E+1	0.394E+0	0.135E+3	0.132E+3	-0.420E+0	-0.133E+3



0.321E+1	0.105E+0	0.122E+3	0.119E+3	-0.133E+0	-0.120E+3
0.321E+1	0.394E+0	0.122E+3	0.119E+3	-0.488E+0	-0.121E+3
0.378E+1	0.105E+0	0.102E+3	0.991E+2	-0.161E+0	-0.100E+3
0.378E+1	0.394E+0	0.102E+3	0.998E+2	-0.593E+0	-0.101E+3
0.421E+1	0.105E+0	0.856E+2	0.824E+2	-0.182E+0	-0.840E+2
0.421E+1	0.394E+0	0.862E+2	0.832E+2	-0.680E+0	-0.847E+2
0.478E+1	0.105E+0	0.605E+2	0.574E+2	-0.196E+0	-0.590E+2
0.478E+1	0.394E+0	0.610E+2	0.580E+2	-0.717E+0	-0.595E+2
0.521E+1	0.105E+0	0.404E+2	0.377E+2	-0.156E+0	-0.391E+2
0.521E+1	0.394E+0	0.408E+2	0.381E+2	-0.611E+0	-0.395E+2
0.578E+1	0.105E+0	0.111E+2	0.105E+2	-0.515E-1	-0.108E+2
0.578E+1	0.394E+0	0.112E+2	0.105E+2	-0.193E+0	-0.108E+2
0.211E+0	0.605E+0	0.174E+3	0.171E+3	-0.531E-1	-0.173E+3
0.211E+0	0.894E+0	0.176E+3	0.174E+3	-0.649E-1	-0.175E+3
0.788E+0	0.605E+0	0.171E+3	0.169E+3	-0.174E+0	-0.170E+3
0.788E+0	0.894E+0	0.173E+3	0.171E+3	-0.268E+0	-0.172E+3
0.121E+1	0.605E+0	0.167E+3	0.164E+3	-0.281E+0	-0.166E+3
0.121E+1	0.894E+0	0.169E+3	0.167E+3	-0.397E+0	-0.168E+3
0.178E+1	0.605E+0	0.159E+3	0.156E+3	-0.403E+0	-0.157E+3
0.178E+1	0.894E+0	0.160E+3	0.158E+3	-0.603E+0	-0.159E+3
0.221E+1	0.605E+0	0.150E+3	0.147E+3	-0.511E+0	-0.149E+3
0.221E+1	0.894E+0	0.152E+3	0.150E+3	-0.732E+0	-0.151E+3
0.278E+1	0.605E+0	0.136E+3	0.133E+3	-0.642E+0	-0.134E+3
0.278E+1	0.894E+0	0.138E+3	0.135E+3	-0.946E+0	-0.136E+3
0.321E+1	0.605E+0	0.123E+3	0.120E+3	-0.756E+0	-0.122E+3
0.321E+1	0.894E+0	0.125E+3	0.123E+3	-0.108E+1	-0.124E+3
0.378E+1	0.605E+0	0.103E+3	0.101E+3	-0.910E+0	-0.102E+3
0.378E+1	0.894E+0	0.105E+3	0.103E+3	-0.131E+1	-0.104E+3
0.421E+1	0.605E+0	0.869E+2	0.841E+2	-0.104E+1	-0.855E+2
0.421E+1	0.894E+0	0.889E+2	0.864E+2	-0.149E+1	-0.876E+2
0.478E+1	0.605E+0	0.617E+2	0.589E+2	-0.113E+1	-0.603E+2
0.478E+1	0.894E+0	0.630E+2	0.605E+2	-0.166E+1	-0.618E+2
0.521E+1	0.605E+0	0.413E+2	0.385E+2	-0.976E+0	-0.399E+2
0.521E+1	0.894E+0	0.425E+2	0.398E+2	-0.154E+1	-0.411E+2
0.578E+1	0.605E+0	0.114E+2	0.104E+2	-0.336E+0	-0.109E+2
0.578E+1	0.894E+0	0.117E+2	0.103E+2	-0.553E+0	-0.110E+2
0.211E+0	0.110E+1	0.178E+3	0.176E+3	-0.937E-1	-0.177E+3
0.211E+0	0.139E+1	0.181E+3	0.180E+3	-0.106E+0	-0.181E+3
0.788E+0	0.110E+1	0.175E+3	0.173E+3	-0.323E+0	-0.174E+3
0.788E+0	0.139E+1	0.178E+3	0.177E+3	-0.413E+0	-0.178E+3
0.121E+1	0.110E+1	0.171E+3	0.169E+3	-0.512E+0	-0.170E+3
0.121E+1	0.139E+1	0.174E+3	0.173E+3	-0.624E+0	-0.174E+3
0.178E+1	0.110E+1	0.162E+3	0.160E+3	-0.739E+0	-0.161E+3
0.178E+1	0.139E+1	0.166E+3	0.164E+3	-0.936E+0	-0.165E+3
0.221E+1	0.110E+1	0.154E+3	0.152E+3	-0.935E+0	-0.153E+3
0.221E+1	0.139E+1	0.157E+3	0.156E+3	-0.114E+1	-0.157E+3
0.278E+1	0.110E+1	0.140E+3	0.138E+3	-0.116E+1	-0.139E+3
0.278E+1	0.139E+1	0.143E+3	0.141E+3	-0.146E+1	-0.142E+3
0.321E+1	0.110E+1	0.127E+3	0.125E+3	-0.137E+1	-0.126E+3
0.321E+1	0.139E+1	0.131E+3	0.129E+3	-0.165E+1	-0.130E+3
0.378E+1	0.110E+1	0.107E+3	0.105E+3	-0.161E+1	-0.106E+3
0.378E+1	0.139E+1	0.110E+3	0.108E+3	-0.202E+1	-0.109E+3
0.421E+1	0.110E+1	0.903E+2	0.883E+2	-0.184E+1	-0.893E+2

0.421E+1	0.139E+1	0.939E+2	0.924E+2	-0.217E+1	-0.931E+2
0.478E+1	0.110E+1	0.647E+2	0.626E+2	-0.209E+1	-0.636E+2
0.478E+1	0.139E+1	0.668E+2	0.657E+2	-0.256E+1	-0.662E+2
0.521E+1	0.110E+1	0.434E+2	0.408E+2	-0.207E+1	-0.421E+2
0.521E+1	0.139E+1	0.459E+2	0.437E+2	-0.281E+1	-0.448E+2
0.578E+1	0.110E+1	0.122E+2	0.102E+2	-0.840E+0	-0.112E+2
0.578E+1	0.139E+1	0.126E+2	0.991E+1	-0.137E+1	-0.112E+2
0.211E+0	0.160E+1	0.184E+3	0.183E+3	-0.131E+0	-0.184E+3
0.211E+0	0.189E+1	0.189E+3	0.189E+3	-0.162E+0	-0.189E+3
0.788E+0	0.160E+1	0.181E+3	0.180E+3	-0.472E+0	-0.181E+3
0.788E+0	0.189E+1	0.186E+3	0.186E+3	-0.546E+0	-0.186E+3
0.121E+1	0.160E+1	0.177E+3	0.176E+3	-0.737E+0	-0.177E+3
0.121E+1	0.189E+1	0.182E+3	0.182E+3	-0.874E+0	-0.182E+3
0.178E+1	0.160E+1	0.169E+3	0.168E+3	-0.107E+1	-0.168E+3
0.178E+1	0.189E+1	0.173E+3	0.173E+3	-0.125E+1	-0.173E+3
0.221E+1	0.160E+1	0.160E+3	0.159E+3	-0.134E+1	-0.160E+3
0.221E+1	0.189E+1	0.165E+3	0.165E+3	-0.158E+1	-0.165E+3
0.278E+1	0.160E+1	0.146E+3	0.145E+3	-0.167E+1	-0.146E+3
0.278E+1	0.189E+1	0.150E+3	0.150E+3	-0.195E+1	-0.150E+3
0.321E+1	0.160E+1	0.133E+3	0.132E+3	-0.196E+1	-0.132E+3
0.321E+1	0.189E+1	0.138E+3	0.138E+3	-0.229E+1	-0.138E+3
0.378E+1	0.160E+1	0.113E+3	0.112E+3	-0.223E+1	-0.113E+3
0.378E+1	0.189E+1	0.117E+3	0.117E+3	-0.262E+1	-0.117E+3
0.421E+1	0.160E+1	0.960E+2	0.950E+2	-0.262E+1	-0.955E+2
0.421E+1	0.189E+1	0.101E+3	0.101E+3	-0.293E+1	-0.101E+3
0.478E+1	0.160E+1	0.703E+2	0.694E+2	-0.264E+1	-0.699E+2
0.478E+1	0.189E+1	0.736E+2	0.731E+2	-0.318E+1	-0.734E+2
0.521E+1	0.160E+1	0.469E+2	0.460E+2	-0.361E+1	-0.465E+2
0.521E+1	0.189E+1	0.526E+2	0.531E+2	-0.330E+1	-0.529E+2
0.578E+1	0.160E+1	0.142E+2	0.974E+1	-0.203E+1	-0.120E+2
0.578E+1	0.189E+1	0.131E+2	0.101E+2	-0.411E+1	-0.116E+2

---

\*\*\* THE SOLUTION HAS REACHED A STEADY STATE \*\*\*

# APPENDIX C

## OUTPUT FILE FROM FEM2DV2 FOR FIGURE 3.6 ANALYSIS

\*\*\* ECHO OF THE INPUT DATA STARTS \*\*\*

STEADY-STATE ANALYSIS OF A FLUID PASSING THROUGH A PIPE  
(24 ELEMENTS)

1	1	0	0
1	9	1	0

6	4					
0.0	1.0	1.0	1.0	1.0	1.0	1.0
0.0	0.25	0.25	0.25	0.25		

69

1 1	1 2	2 2	3 2	4 2	5 2	6 2	7 2	8 2	9 2
10 2	11 2	12 2	13 1	13 2	14 1	14 2	26 1	26 2	27 1
27 2	39 1	39 2	40 1	40 2	52 1	52 2	53 1	53 2	65 1
65 2	66 1	66 2	78 1	78 2	79 1	79 2	91 1	91 2	92 1
92 2	104 1	104 2	105 1	105 2	106 1	106 2	107 1	107 2	108 1
108 2	109 1	109 2	110 1	110 2	111 1	111 2	112 1	112 2	113 1
113 2	114 1	114 2	115 1	115 2	116 1	116 2	117 1	117 2	

1.0	0.0	0.0	0.0	0.0	0.0	0.0	0.0	0.0	0.0
0.0	0.0	0.0	1.5	0.0	1.0	0.0	1.477	0.0	1.0
0.0	1.406	0.0	1.0	0.0	1.289	0.0	1.0	0.0	1.125
0.0	1.0	0.0	0.914	0.0	1.0	0.0	0.656	0.0	1.0
0.0	0.352	0.0	1.0	0.0	0.0	0.0	0.0	0.0	0.0
0.0	0.0	0.0	0.0	0.0	0.0	0.0	0.0	0.0	0.0
0.0	0.0	0.0	0.0	0.0	0.0	0.0	0.0	0.0	

0

2.0      1.0E8

0.0      0.0      0.0

\*\*\*\* ECHO OF THE INPUT DATA ENDS \*\*\*\*

STEADY-STATE ANALYSIS OF A FLUID PASSING THROUGH A PIPE  
(24 ELEMENTS)

---

OUTPUT FROM PROGRAM \*FEM2DV2\*    BY J. N. REDDY  
Edited by Pantaleo Loiacono.....14 September 1995

---

A VISCOUS INCOMPRESSIBLE FLOW IS ANALYZED

PARAMETERS OF THE FLUID FLOW PROBLEM:

Viscosity of the fluid, AMU.....= 0.2000E+1  
 Penalty parameter, PENLTY.....= 0.1000E+9

CONTINUOUS SOURCE COEFFICIENTS:

Coefficient, F0 .....= 0.0000E+0  
 Coefficient, FX .....= 0.0000E+0  
 Coefficient, FY .....= 0.0000E+0

\*\*\*\*\* A STEADY-STATE PROBLEM is analyzed \*\*\*\*\*

\*\*\* A mesh of QUADRILATERALS is chosen by user \*\*\*

FINITE ELEMENT MESH INFORMATION:

Element type: (0 = Triangle; >0 = Quad.)= 1  
 Number of nodes per element, NPE .....= 9  
 No. of primary deg. of freedom/node, NDF= 2  
 Number of elements in the mesh, NEM ....= 24  
 Number of nodes in the mesh, NNM .....= 117  
 Number of equations to be solved, NEQ ..= 234  
 Half bandwidth of the matrix GLK, NHBW .= 58  
 Mesh subdivisions, NX and NY .....= 6 4

No. of specified PRIMARY variables, NSPV = 69

---

Node	x-coord.	y-coord.	Speci. primary & secondary variables (0, unspecified; >0, specified)			
			Primary DOF		Secondary DOF	
1	0.0000E+0	0.0000E+0	1	2	0	0
2	0.5000E+0	0.0000E+0	0	2	0	0
3	0.1000E+1	0.0000E+0	0	2	0	0
4	0.1500E+1	0.0000E+0	0	2	0	0
5	0.2000E+1	0.0000E+0	0	2	0	0
6	0.2500E+1	0.0000E+0	0	2	0	0
7	0.3000E+1	0.0000E+0	0	2	0	0
8	0.3500E+1	0.0000E+0	0	2	0	0
9	0.4000E+1	0.0000E+0	0	2	0	0
10	0.4500E+1	0.0000E+0	0	2	0	0
11	0.5000E+1	0.0000E+0	0	2	0	0
12	0.5500E+1	0.0000E+0	0	2	0	0
13	0.6000E+1	0.0000E+0	1	2	0	0

---

14	0.0000E+0	0.1250E+0	1	2	0	0
15	0.5000E+0	0.1250E+0	0	0	0	0
16	0.1000E+1	0.1250E+0	0	0	0	0
17	0.1500E+1	0.1250E+0	0	0	0	0
18	0.2000E+1	0.1250E+0	0	0	0	0
19	0.2500E+1	0.1250E+0	0	0	0	0
20	0.3000E+1	0.1250E+0	0	0	0	0
21	0.3500E+1	0.1250E+0	0	0	0	0
22	0.4000E+1	0.1250E+0	0	0	0	0
23	0.4500E+1	0.1250E+0	0	0	0	0
24	0.5000E+1	0.1250E+0	0	0	0	0
25	0.5500E+1	0.1250E+0	0	0	0	0
26	0.6000E+1	0.1250E+0	1	2	0	0
27	0.0000E+0	0.2500E+0	1	2	0	0
28	0.5000E+0	0.2500E+0	0	0	0	0
29	0.1000E+1	0.2500E+0	0	0	0	0
30	0.1500E+1	0.2500E+0	0	0	0	0
31	0.2000E+1	0.2500E+0	0	0	0	0
32	0.2500E+1	0.2500E+0	0	0	0	0
33	0.3000E+1	0.2500E+0	0	0	0	0
34	0.3500E+1	0.2500E+0	0	0	0	0
35	0.4000E+1	0.2500E+0	0	0	0	0
36	0.4500E+1	0.2500E+0	0	0	0	0
37	0.5000E+1	0.2500E+0	0	0	0	0
38	0.5500E+1	0.2500E+0	0	0	0	0
39	0.6000E+1	0.2500E+0	1	2	0	0
40	0.0000E+0	0.3750E+0	1	2	0	0
41	0.5000E+0	0.3750E+0	0	0	0	0
42	0.1000E+1	0.3750E+0	0	0	0	0
43	0.1500E+1	0.3750E+0	0	0	0	0
44	0.2000E+1	0.3750E+0	0	0	0	0
45	0.2500E+1	0.3750E+0	0	0	0	0
46	0.3000E+1	0.3750E+0	0	0	0	0
47	0.3500E+1	0.3750E+0	0	0	0	0
48	0.4000E+1	0.3750E+0	0	0	0	0
49	0.4500E+1	0.3750E+0	0	0	0	0
50	0.5000E+1	0.3750E+0	0	0	0	0
51	0.5500E+1	0.3750E+0	0	0	0	0
52	0.6000E+1	0.3750E+0	1	2	0	0
53	0.0000E+0	0.5000E+0	1	2	0	0
54	0.5000E+0	0.5000E+0	0	0	0	0
55	0.1000E+1	0.5000E+0	0	0	0	0
56	0.1500E+1	0.5000E+0	0	0	0	0
57	0.2000E+1	0.5000E+0	0	0	0	0
58	0.2500E+1	0.5000E+0	0	0	0	0
59	0.3000E+1	0.5000E+0	0	0	0	0
60	0.3500E+1	0.5000E+0	0	0	0	0
61	0.4000E+1	0.5000E+0	0	0	0	0
62	0.4500E+1	0.5000E+0	0	0	0	0
63	0.5000E+1	0.5000E+0	0	0	0	0
64	0.5500E+1	0.5000E+0	0	0	0	0
65	0.6000E+1	0.5000E+0	1	2	0	0
66	0.0000E+0	0.6250E+0	1	2	0	0

67	0.5000E+0	0.6250E+0	0	0	0	0
68	0.1000E+1	0.6250E+0	0	0	0	0
69	0.1500E+1	0.6250E+0	0	0	0	0
70	0.2000E+1	0.6250E+0	0	0	0	0
71	0.2500E+1	0.6250E+0	0	0	0	0
72	0.3000E+1	0.6250E+0	0	0	0	0
73	0.3500E+1	0.6250E+0	0	0	0	0
74	0.4000E+1	0.6250E+0	0	0	0	0
75	0.4500E+1	0.6250E+0	0	0	0	0
76	0.5000E+1	0.6250E+0	0	0	0	0
77	0.5500E+1	0.6250E+0	0	0	0	0
78	0.6000E+1	0.6250E+0	1	2	0	0
79	0.0000E+0	0.7500E+0	1	2	0	0
80	0.5000E+0	0.7500E+0	0	0	0	0
81	0.1000E+1	0.7500E+0	0	0	0	0
82	0.1500E+1	0.7500E+0	0	0	0	0
83	0.2000E+1	0.7500E+0	0	0	0	0
84	0.2500E+1	0.7500E+0	0	0	0	0
85	0.3000E+1	0.7500E+0	0	0	0	0
86	0.3500E+1	0.7500E+0	0	0	0	0
87	0.4000E+1	0.7500E+0	0	0	0	0
88	0.4500E+1	0.7500E+0	0	0	0	0
89	0.5000E+1	0.7500E+0	0	0	0	0
90	0.5500E+1	0.7500E+0	0	0	0	0
91	0.6000E+1	0.7500E+0	1	2	0	0
92	0.0000E+0	0.8750E+0	1	2	0	0
93	0.5000E+0	0.8750E+0	0	0	0	0
94	0.1000E+1	0.8750E+0	0	0	0	0
95	0.1500E+1	0.8750E+0	0	0	0	0
96	0.2000E+1	0.8750E+0	0	0	0	0
97	0.2500E+1	0.8750E+0	0	0	0	0
98	0.3000E+1	0.8750E+0	0	0	0	0
99	0.3500E+1	0.8750E+0	0	0	0	0
100	0.4000E+1	0.8750E+0	0	0	0	0
101	0.4500E+1	0.8750E+0	0	0	0	0
102	0.5000E+1	0.8750E+0	0	0	0	0
103	0.5500E+1	0.8750E+0	0	0	0	0
104	0.6000E+1	0.8750E+0	1	2	0	0
105	0.0000E+0	0.1000E+1	1	2	0	0
106	0.5000E+0	0.1000E+1	1	2	0	0
107	0.1000E+1	0.1000E+1	1	2	0	0
108	0.1500E+1	0.1000E+1	1	2	0	0
109	0.2000E+1	0.1000E+1	1	2	0	0
110	0.2500E+1	0.1000E+1	1	2	0	0
111	0.3000E+1	0.1000E+1	1	2	0	0
112	0.3500E+1	0.1000E+1	1	2	0	0
113	0.4000E+1	0.1000E+1	1	2	0	0
114	0.4500E+1	0.1000E+1	1	2	0	0
115	0.5000E+1	0.1000E+1	1	2	0	0
116	0.5500E+1	0.1000E+1	1	2	0	0
117	0.6000E+1	0.1000E+1	1	2	0	0

---

## NUMERICAL INTEGRATION DATA:

Full quadrature (IPDF x IPDF) rule, IPDF= 3  
 Reduced quadrature (IPDR x IPDR), IPDR= 2  
 Quadrature rule used in postproc., ISTR= 2

## S O L U T I O N :

Node	x-coord.	y-coord.	Value of u	Value of v
1	0.00000E+0	0.00000E+0	0.10000E+1	0.00000E+0
2	0.50000E+0	0.00000E+0	0.12004E+1	0.00000E+0
3	0.10000E+1	0.00000E+0	0.15414E+1	0.00000E+0
4	0.15000E+1	0.00000E+0	0.14732E+1	0.00000E+0
5	0.20000E+1	0.00000E+0	0.15642E+1	0.00000E+0
6	0.25000E+1	0.00000E+0	0.14658E+1	0.00000E+0
7	0.30000E+1	0.00000E+0	0.15679E+1	0.00000E+0
8	0.35000E+1	0.00000E+0	0.14661E+1	0.00000E+0
9	0.40000E+1	0.00000E+0	0.15667E+1	0.00000E+0
10	0.45000E+1	0.00000E+0	0.14674E+1	0.00000E+0
11	0.50000E+1	0.00000E+0	0.15577E+1	0.00000E+0
12	0.55000E+1	0.00000E+0	0.14750E+1	0.00000E+0
13	0.60000E+1	0.00000E+0	0.15000E+1	0.00000E+0
14	0.00000E+0	0.12500E+0	0.10000E+1	0.00000E+0
15	0.50000E+0	0.12500E+0	0.12341E+1	-0.86002E-1
16	0.10000E+1	0.12500E+0	0.14379E+1	-0.14560E-1
17	0.15000E+1	0.12500E+0	0.14984E+1	0.15727E-2
18	0.20000E+1	0.12500E+0	0.14410E+1	-0.47990E-3
19	0.25000E+1	0.12500E+0	0.14934E+1	-0.47030E-3
20	0.30000E+1	0.12500E+0	0.14428E+1	0.43855E-3
21	0.35000E+1	0.12500E+0	0.14934E+1	-0.15736E-3
22	0.40000E+1	0.12500E+0	0.14435E+1	0.19217E-3
23	0.45000E+1	0.12500E+0	0.14930E+1	-0.63317E-4
24	0.50000E+1	0.12500E+0	0.14480E+1	0.61027E-4
25	0.55000E+1	0.12500E+0	0.14893E+1	-0.33713E-4
26	0.60000E+1	0.12500E+0	0.14770E+1	0.00000E+0
27	0.00000E+0	0.25000E+0	0.10000E+1	0.00000E+0
28	0.50000E+0	0.25000E+0	0.11813E+1	-0.16747E+0
29	0.10000E+1	0.25000E+0	0.14727E+1	-0.21500E-1
30	0.15000E+1	0.25000E+0	0.13767E+1	0.35494E-2
31	0.20000E+1	0.25000E+0	0.14718E+1	-0.13147E-2
32	0.25000E+1	0.25000E+0	0.13725E+1	-0.59937E-3
33	0.30000E+1	0.25000E+0	0.14740E+1	0.46204E-3
34	0.35000E+1	0.25000E+0	0.13724E+1	-0.14802E-3
35	0.40000E+1	0.25000E+0	0.14727E+1	0.11147E-3
36	0.45000E+1	0.25000E+0	0.13737E+1	-0.20179E-4
37	0.50000E+1	0.25000E+0	0.14638E+1	-0.98815E-5
38	0.55000E+1	0.25000E+0	0.13813E+1	-0.31728E-4
39	0.60000E+1	0.25000E+0	0.14060E+1	0.00000E+0

40	0.00000E+0	0.37500E+0	0.10000E+1	0.00000E+0
41	0.50000E+0	0.37500E+0	0.11917E+1	-0.23941E+0
42	0.10000E+1	0.37500E+0	0.12920E+1	-0.12581E-1
43	0.15000E+1	0.37500E+0	0.13046E+1	0.50589E-2
44	0.20000E+1	0.37500E+0	0.12568E+1	-0.76586E-3
45	0.25000E+1	0.37500E+0	0.13066E+1	-0.11065E-2
46	0.30000E+1	0.37500E+0	0.12551E+1	0.17087E-2
47	0.35000E+1	0.37500E+0	0.13059E+1	-0.79862E-3
48	0.40000E+1	0.37500E+0	0.12563E+1	0.10787E-2
49	0.45000E+1	0.37500E+0	0.13052E+1	-0.34939E-3
50	0.50000E+1	0.37500E+0	0.12609E+1	0.27192E-3
51	0.55000E+1	0.37500E+0	0.13015E+1	0.34855E-4
52	0.60000E+1	0.37500E+0	0.12890E+1	0.00000E+0
53	0.00000E+0	0.50000E+0	0.10000E+1	0.00000E+0
54	0.50000E+0	0.50000E+0	0.11021E+1	-0.29411E+0
55	0.10000E+1	0.50000E+0	0.12375E+1	0.15528E-1
56	0.15000E+1	0.50000E+0	0.10830E+1	0.54450E-2
57	0.20000E+1	0.50000E+0	0.11996E+1	-0.99998E-3
58	0.25000E+1	0.50000E+0	0.10908E+1	0.23720E-3
59	0.30000E+1	0.50000E+0	0.11927E+1	-0.30013E-3
60	0.35000E+1	0.50000E+0	0.10919E+1	0.14845E-3
61	0.40000E+1	0.50000E+0	0.11898E+1	-0.43616E-3
62	0.45000E+1	0.50000E+0	0.10936E+1	0.22447E-3
63	0.50000E+1	0.50000E+0	0.11803E+1	-0.40217E-3
64	0.55000E+1	0.50000E+0	0.11010E+1	0.11055E-3
65	0.60000E+1	0.50000E+0	0.11250E+1	0.00000E+0
66	0.00000E+0	0.62500E+0	0.10000E+1	0.00000E+0
67	0.50000E+0	0.62500E+0	0.10578E+1	-0.32211E+0
68	0.10000E+1	0.62500E+0	0.93428E+0	0.70441E-1
69	0.15000E+1	0.62500E+0	0.91591E+0	-0.32743E-2
70	0.20000E+1	0.62500E+0	0.89323E+0	0.11633E-1
71	0.25000E+1	0.62500E+0	0.92942E+0	-0.31529E-2
72	0.30000E+1	0.62500E+0	0.88247E+0	0.65700E-2
73	0.35000E+1	0.62500E+0	0.93035E+0	-0.28988E-2
74	0.40000E+1	0.62500E+0	0.88299E+0	0.45535E-2
75	0.45000E+1	0.62500E+0	0.92912E+0	-0.16223E-2
76	0.50000E+1	0.62500E+0	0.88802E+0	0.16360E-2
77	0.55000E+1	0.62500E+0	0.92541E+0	0.17996E-4
78	0.60000E+1	0.62500E+0	0.91400E+0	0.00000E+0
79	0.00000E+0	0.75000E+0	0.10000E+1	0.00000E+0
80	0.50000E+0	0.75000E+0	0.85692E+0	-0.30418E+0
81	0.10000E+1	0.75000E+0	0.74819E+0	0.12511E+0
82	0.15000E+1	0.75000E+0	0.59747E+0	-0.13662E-1
83	0.20000E+1	0.75000E+0	0.75257E+0	0.15316E-1
84	0.25000E+1	0.75000E+0	0.61503E+0	0.21109E-2
85	0.30000E+1	0.75000E+0	0.72723E+0	-0.52893E-2
86	0.35000E+1	0.75000E+0	0.62574E+0	0.39087E-2
87	0.40000E+1	0.75000E+0	0.71107E+0	-0.62007E-2
88	0.45000E+1	0.75000E+0	0.63162E+0	0.24181E-2
89	0.50000E+1	0.75000E+0	0.69818E+0	-0.28381E-2
90	0.55000E+1	0.75000E+0	0.63846E+0	0.32282E-3
91	0.60000E+1	0.75000E+0	0.65600E+0	0.00000E+0
92	0.00000E+0	0.87500E+0	0.10000E+1	0.00000E+0



93	0.50000E+0	0.87500E+0	0.64615E+0	-0.21734E+0
94	0.10000E+1	0.87500E+0	0.22137E+0	0.18326E+0
95	0.15000E+1	0.87500E+0	0.38429E+0	-0.57833E-1
96	0.20000E+1	0.87500E+0	0.30607E+0	0.90138E-1
97	0.25000E+1	0.87500E+0	0.36516E+0	-0.31192E-1
98	0.30000E+1	0.87500E+0	0.33090E+0	0.48618E-1
99	0.35000E+1	0.87500E+0	0.35904E+0	-0.17081E-1
100	0.40000E+1	0.87500E+0	0.33910E+0	0.24808E-1
101	0.45000E+1	0.87500E+0	0.35677E+0	-0.75779E-2
102	0.50000E+1	0.87500E+0	0.34298E+0	0.82378E-2
103	0.55000E+1	0.87500E+0	0.35502E+0	-0.27563E-3
104	0.60000E+1	0.87500E+0	0.35200E+0	0.00000E+0
105	0.00000E+0	0.10000E+1	0.10000E+1	0.00000E+0
106	0.50000E+0	0.10000E+1	0.00000E+0	0.00000E+0
107	0.10000E+1	0.10000E+1	0.00000E+0	0.00000E+0
108	0.15000E+1	0.10000E+1	0.00000E+0	0.00000E+0
109	0.20000E+1	0.10000E+1	0.00000E+0	0.00000E+0
110	0.25000E+1	0.10000E+1	0.00000E+0	0.00000E+0
111	0.30000E+1	0.10000E+1	0.00000E+0	0.00000E+0
112	0.35000E+1	0.10000E+1	0.00000E+0	0.00000E+0
113	0.40000E+1	0.10000E+1	0.00000E+0	0.00000E+0
114	0.45000E+1	0.10000E+1	0.00000E+0	0.00000E+0
115	0.50000E+1	0.10000E+1	0.00000E+0	0.00000E+0
116	0.55000E+1	0.10000E+1	0.00000E+0	0.00000E+0
117	0.60000E+1	0.10000E+1	0.00000E+0	0.00000E+0

---

x-coord.	y-coord.	sigma-x	sigma-y	sigma-xy	pressure
0.211E+0	0.528E-1	0.137E+4	0.137E+4	0.486E+0	-0.137E+4
0.211E+0	0.197E+0	0.137E+4	0.136E+4	-0.133E+1	-0.137E+4
0.788E+0	0.528E-1	0.137E+4	0.137E+4	-0.260E+0	-0.137E+4
0.788E+0	0.197E+0	0.138E+4	0.137E+4	0.229E+0	-0.138E+4
0.121E+1	0.528E-1	0.138E+4	0.137E+4	-0.145E+0	-0.138E+4
0.121E+1	0.197E+0	0.137E+4	0.137E+4	-0.107E+1	-0.137E+4
0.178E+1	0.528E-1	0.138E+4	0.138E+4	-0.377E+0	-0.138E+4
0.178E+1	0.197E+0	0.138E+4	0.138E+4	-0.121E+1	-0.138E+4
0.221E+1	0.528E-1	0.138E+4	0.138E+4	-0.300E+0	-0.138E+4
0.221E+1	0.197E+0	0.138E+4	0.138E+4	-0.118E+1	-0.138E+4
0.278E+1	0.528E-1	0.138E+4	0.138E+4	-0.317E+0	-0.138E+4
0.278E+1	0.197E+0	0.139E+4	0.139E+4	-0.117E+1	-0.139E+4
0.321E+1	0.528E-1	0.139E+4	0.139E+4	-0.323E+0	-0.139E+4
0.321E+1	0.197E+0	0.138E+4	0.138E+4	-0.118E+1	-0.138E+4
0.378E+1	0.528E-1	0.139E+4	0.139E+4	-0.300E+0	-0.139E+4
0.378E+1	0.197E+0	0.139E+4	0.139E+4	-0.119E+1	-0.139E+4
0.421E+1	0.528E-1	0.139E+4	0.139E+4	-0.358E+0	-0.139E+4
0.421E+1	0.197E+0	0.139E+4	0.139E+4	-0.114E+1	-0.139E+4
0.478E+1	0.528E-1	0.139E+4	0.139E+4	-0.214E+0	-0.139E+4
0.478E+1	0.197E+0	0.140E+4	0.140E+4	-0.128E+1	-0.140E+4
0.521E+1	0.528E-1	0.140E+4	0.140E+4	-0.579E+0	-0.140E+4

0.521E+1	0.197E+0	0.139E+4	0.139E+4	-0.921E+0	-0.139E+4
0.578E+1	0.528E-1	0.140E+4	0.140E+4	0.346E+0	-0.140E+4
0.578E+1	0.197E+0	0.141E+4	0.141E+4	-0.184E+1	-0.141E+4
0.211E+0	0.302E+0	0.138E+4	0.138E+4	-0.352E+0	-0.138E+4
0.211E+0	0.447E+0	0.136E+4	0.136E+4	-0.221E+1	-0.136E+4
0.788E+0	0.302E+0	0.137E+4	0.136E+4	-0.356E+0	-0.136E+4
0.788E+0	0.447E+0	0.138E+4	0.138E+4	-0.974E-1	-0.138E+4
0.121E+1	0.302E+0	0.138E+4	0.138E+4	-0.148E+1	-0.138E+4
0.121E+1	0.447E+0	0.136E+4	0.136E+4	-0.270E+1	-0.136E+4
0.178E+1	0.302E+0	0.137E+4	0.137E+4	-0.196E+1	-0.137E+4
0.178E+1	0.447E+0	0.139E+4	0.139E+4	-0.275E+1	-0.139E+4
0.221E+1	0.302E+0	0.139E+4	0.139E+4	-0.178E+1	-0.139E+4
0.221E+1	0.447E+0	0.137E+4	0.137E+4	-0.265E+1	-0.137E+4
0.278E+1	0.302E+0	0.138E+4	0.138E+4	-0.180E+1	-0.138E+4
0.278E+1	0.447E+0	0.139E+4	0.139E+4	-0.269E+1	-0.139E+4
0.321E+1	0.302E+0	0.139E+4	0.139E+4	-0.183E+1	-0.139E+4
0.321E+1	0.447E+0	0.138E+4	0.138E+4	-0.267E+1	-0.138E+4
0.378E+1	0.302E+0	0.138E+4	0.138E+4	-0.179E+1	-0.138E+4
0.378E+1	0.447E+0	0.140E+4	0.140E+4	-0.270E+1	-0.140E+4
0.421E+1	0.302E+0	0.140E+4	0.140E+4	-0.186E+1	-0.140E+4
0.421E+1	0.447E+0	0.138E+4	0.138E+4	-0.264E+1	-0.138E+4
0.478E+1	0.302E+0	0.139E+4	0.139E+4	-0.171E+1	-0.139E+4
0.478E+1	0.447E+0	0.141E+4	0.141E+4	-0.278E+1	-0.141E+4
0.521E+1	0.302E+0	0.141E+4	0.141E+4	-0.207E+1	-0.141E+4
0.521E+1	0.447E+0	0.139E+4	0.139E+4	-0.242E+1	-0.139E+4
0.578E+1	0.302E+0	0.139E+4	0.139E+4	-0.116E+1	-0.139E+4
0.578E+1	0.447E+0	0.141E+4	0.141E+4	-0.332E+1	-0.141E+4
0.211E+0	0.552E+0	0.138E+4	0.138E+4	-0.118E+1	-0.138E+4
0.211E+0	0.697E+0	0.135E+4	0.135E+4	-0.342E+1	-0.135E+4
0.788E+0	0.552E+0	0.136E+4	0.136E+4	-0.101E+1	-0.136E+4
0.788E+0	0.697E+0	0.139E+4	0.139E+4	-0.165E+1	-0.139E+4
0.121E+1	0.552E+0	0.139E+4	0.139E+4	-0.347E+1	-0.139E+4
0.121E+1	0.697E+0	0.136E+4	0.136E+4	-0.504E+1	-0.136E+4
0.178E+1	0.552E+0	0.136E+4	0.136E+4	-0.334E+1	-0.136E+4
0.178E+1	0.697E+0	0.139E+4	0.139E+4	-0.397E+1	-0.139E+4
0.221E+1	0.552E+0	0.139E+4	0.139E+4	-0.332E+1	-0.139E+4
0.221E+1	0.697E+0	0.136E+4	0.136E+4	-0.420E+1	-0.136E+4
0.278E+1	0.552E+0	0.137E+4	0.137E+4	-0.328E+1	-0.137E+4
0.278E+1	0.697E+0	0.140E+4	0.140E+4	-0.425E+1	-0.140E+4
0.321E+1	0.552E+0	0.140E+4	0.140E+4	-0.336E+1	-0.140E+4
0.321E+1	0.697E+0	0.137E+4	0.137E+4	-0.410E+1	-0.137E+4
0.378E+1	0.552E+0	0.138E+4	0.138E+4	-0.325E+1	-0.138E+4
0.378E+1	0.697E+0	0.141E+4	0.141E+4	-0.426E+1	-0.141E+4
0.421E+1	0.552E+0	0.140E+4	0.140E+4	-0.339E+1	-0.140E+4
0.421E+1	0.697E+0	0.138E+4	0.138E+4	-0.410E+1	-0.138E+4
0.478E+1	0.552E+0	0.138E+4	0.138E+4	-0.320E+1	-0.138E+4
0.478E+1	0.697E+0	0.141E+4	0.141E+4	-0.429E+1	-0.141E+4
0.521E+1	0.552E+0	0.141E+4	0.141E+4	-0.356E+1	-0.141E+4
0.521E+1	0.697E+0	0.138E+4	0.138E+4	-0.396E+1	-0.138E+4
0.578E+1	0.552E+0	0.139E+4	0.139E+4	-0.270E+1	-0.139E+4
0.578E+1	0.697E+0	0.142E+4	0.142E+4	-0.470E+1	-0.142E+4
0.211E+0	0.802E+0	0.138E+4	0.138E+4	-0.217E+1	-0.138E+4
0.211E+0	0.947E+0	0.132E+4	0.133E+4	-0.739E+1	-0.132E+4

0.788E+0	0.802E+0	0.135E+4	0.135E+4	-0.381E+1	-0.135E+4
0.788E+0	0.947E+0	0.140E+4	0.140E+4	-0.773E+1	-0.140E+4
0.121E+1	0.802E+0	0.140E+4	0.140E+4	-0.625E+1	-0.140E+4
0.121E+1	0.947E+0	0.135E+4	0.135E+4	-0.575E+1	-0.135E+4
0.178E+1	0.802E+0	0.136E+4	0.136E+4	-0.383E+1	-0.136E+4
0.178E+1	0.947E+0	0.140E+4	0.140E+4	-0.555E+1	-0.140E+4
0.221E+1	0.802E+0	0.140E+4	0.140E+4	-0.550E+1	-0.140E+4
0.221E+1	0.947E+0	0.136E+4	0.136E+4	-0.586E+1	-0.136E+4
0.278E+1	0.802E+0	0.136E+4	0.136E+4	-0.436E+1	-0.136E+4
0.278E+1	0.947E+0	0.140E+4	0.140E+4	-0.553E+1	-0.140E+4
0.321E+1	0.802E+0	0.140E+4	0.140E+4	-0.514E+1	-0.140E+4
0.321E+1	0.947E+0	0.137E+4	0.137E+4	-0.582E+1	-0.137E+4
0.378E+1	0.802E+0	0.137E+4	0.137E+4	-0.460E+1	-0.137E+4
0.378E+1	0.947E+0	0.141E+4	0.141E+4	-0.558E+1	-0.141E+4
0.421E+1	0.802E+0	0.141E+4	0.141E+4	-0.497E+1	-0.141E+4
0.421E+1	0.947E+0	0.137E+4	0.137E+4	-0.575E+1	-0.137E+4
0.478E+1	0.802E+0	0.138E+4	0.138E+4	-0.468E+1	-0.138E+4
0.478E+1	0.947E+0	0.141E+4	0.141E+4	-0.565E+1	-0.141E+4
0.521E+1	0.802E+0	0.142E+4	0.142E+4	-0.499E+1	-0.142E+4
0.521E+1	0.947E+0	0.138E+4	0.138E+4	-0.567E+1	-0.138E+4
0.578E+1	0.802E+0	0.138E+4	0.138E+4	-0.445E+1	-0.138E+4
0.578E+1	0.947E+0	0.142E+4	0.142E+4	-0.576E+1	-0.142E+4

---

# APPENDIX D

INPUT FILE TO FEM2DV2 FOR MESH OF FIGURE 3.7

\*\*\* ECHO OF THE INPUT DATA STARTS \*\*\*

90 degree curve, 21 elements in the mesh  
(12 curved, 9 rectangular)

1	1	0	0
1	9	0	0

21	105
----	-----

1	3	33	31	2	18	32	16	17
3	5	35	33	4	20	34	18	19
5	7	37	35	6	22	36	20	21
7	9	39	37	8	24	38	22	23
9	11	41	39	10	26	40	24	25
11	13	43	41	12	28	42	26	27
13	15	45	43	14	30	44	28	29
31	33	63	61	32	48	62	46	47
33	35	65	63	34	50	64	48	49
35	37	67	65	36	52	66	50	51
37	39	69	67	38	54	68	52	53
39	41	71	69	40	56	70	54	55
41	43	73	71	42	58	72	56	57
43	45	75	73	44	60	74	58	59
61	63	93	91	62	78	92	76	77
63	65	95	93	64	80	94	78	79
65	67	97	95	66	82	96	80	81
67	69	99	97	68	84	98	82	83
69	71	101	99	70	86	100	84	85
71	73	103	101	72	88	102	86	87
73	75	105	103	74	90	104	88	89

0.0000E+0	0.2000E+1
0.3902E+0	0.1962E+1
0.7654E+0	0.1848E+1
0.1111E+1	0.1663E+1
0.1414E+1	0.1414E+1
0.1663E+1	0.1111E+1
0.1848E+1	0.7654E+0
0.1962E+1	0.3902E+0
0.2000E+1	0.0000E+0
0.2000E+1	-0.3333E+0
0.2000E+1	-0.6667E+0
0.2000E+1	-0.1000E+1
0.2000E+1	-0.1333E+1
0.2000E+1	-0.1667E+1
0.2000E+1	-0.2000E+1

0.0000E+0	0.2333E+1
0.4552E+0	0.2288E+1
0.8929E+0	0.2156E+1
0.1296E+1	0.1940E+1
0.1650E+1	0.1650E+1
0.1940E+1	0.1296E+1
0.2156E+1	0.8929E+0
0.2288E+1	0.4552E+0
0.2333E+1	0.0000E+0
0.2333E+1	-0.3333E+0
0.2333E+1	-0.6667E+0
0.2333E+1	-0.1000E+1
0.2333E+1	-0.1333E+1
0.2333E+1	-0.1667E+1
0.2333E+1	-0.2000E+1
0.0000E+0	0.2667E+1
0.5202E+0	0.2615E+1
0.1020E+1	0.2464E+1
0.1482E+1	0.2217E+1
0.1886E+1	0.1886E+1
0.2217E+1	0.1482E+1
0.2464E+1	0.1020E+1
0.2615E+1	0.5202E+0
0.2667E+1	0.0000E+0
0.2667E+1	-0.3333E+0
0.2667E+1	-0.6667E+0
0.2667E+1	-0.1000E+1
0.2667E+1	-0.1333E+1
0.2667E+1	-0.1667E+1
0.2667E+1	-0.2000E+1
0.0000E+0	0.3000E+1
0.5853E+0	0.2942E+1
0.1148E+1	0.2772E+1
0.1667E+1	0.2494E+1
0.2121E+1	0.2121E+1
0.2494E+1	0.1667E+1
0.2772E+1	0.1148E+1
0.2942E+1	0.5853E+0
0.3000E+1	0.0000E+0
0.3000E+1	-0.3333E+0
0.3000E+1	-0.6667E+0
0.3000E+1	-0.1000E+1
0.3000E+1	-0.1333E+1
0.3000E+1	-0.1667E+1
0.3000E+1	-0.2000E+1
0.0000E+0	0.3333E+1
0.6503E+0	0.3269E+1
0.1276E+1	0.3080E+1
0.1852E+1	0.2772E+1
0.2357E+1	0.2357E+1
0.2772E+1	0.1852E+1
0.3080E+1	0.1276E+1
0.3269E+1	0.6503E+0

0.3333E+1	0.0000E+0
0.3333E+1	-0.3333E+0
0.3333E+1	-0.6667E+0
0.3333E+1	-0.1000E+1
0.3333E+1	-0.1333E+1
0.3333E+1	-0.1667E+1
0.3333E+1	-0.2000E+1
0.0000E+0	0.3667E+1
0.7153E+0	0.3596E+1
0.1403E+1	0.3388E+1
0.2037E+1	0.3049E+1
0.2593E+1	0.2593E+1
0.3049E+1	0.2037E+1
0.3388E+1	0.1403E+1
0.3596E+1	0.7153E+0
0.3667E+1	0.0000E+0
0.3667E+1	-0.3333E+0
0.3667E+1	-0.6667E+0
0.3667E+1	-0.1000E+1
0.3667E+1	-0.1333E+1
0.3667E+1	-0.1667E+1
0.3667E+1	-0.2000E+1
0.0000E+0	0.4000E+1
0.7804E+0	0.3923E+1
0.1531E+1	0.3696E+1
0.2222E+1	0.3326E+1
0.2828E+1	0.2828E+1
0.3326E+1	0.2222E+1
0.3696E+1	0.1531E+1
0.3923E+1	0.7804E+0
0.4000E+1	0.0000E+0
0.4000E+1	-0.3333E+0
0.4000E+1	-0.6667E+0
0.4000E+1	-0.1000E+1
0.4000E+1	-0.1333E+1
0.4000E+1	-0.1667E+1
0.4000E+1	-0.2000E+1

80

1 1	1 2	2 1	2 2	3 1	3 2	4 1	4 2	5 1	5 2
6 1	6 2	7 1	7 2	8 1	8 2	9 1	9 2	10 1	10 2
11 1	11 2	12 1	12 2	13 1	13 2	14 1	14 2	15 1	15 2
16 1	16 2	30 1	30 2	31 1	31 2	45 1	45 2	46 1	46 2
60 1	60 2	61 1	61 2	75 1	75 2	76 1	76 2	90 1	90 2
91 1	91 2	92 1	92 2	93 1	93 2	94 1	94 2	95 1	95 2
96 1	96 2	97 1	97 2	98 1	98 2	99 1	99 2	100 1	100 2
101 1	101 2	102 1	102 2	103 1	103 2	104 1	104 2	105 1	105 2
0.0	0.0	0.0	0.0	0.0	0.0	0.0	0.0	0.0	0.0
0.0	0.0	0.0	0.0	0.0	0.0	0.0	0.0	0.0	0.0
0.0	0.0	0.0	0.0	0.0	0.0	0.0	0.0	0.0	0.0
0.833	0.0	0.0	-0.833	1.333	0.0	0.0	-1.333	1.5	0.0

```

0.0  -1.5   1.333  0.0   0.0  -1.333  0.833  0.0   0.0  -0.833
0.0   0.0   0.0   0.0   0.0   0.0   0.0   0.0   0.0   0.0
0.0   0.0   0.0   0.0   0.0   0.0   0.0   0.0   0.0   0.0
0.0   0.0   0.0   0.0   0.0   0.0   0.0   0.0   0.0   0.0

```

0

2.0        1.0E8

0.0        0.0        0.0

\*\*\*\* ECHO OF THE INPUT DATA ENDS \*\*\*\*

90 degree curve, 21 elements in the mesh  
                   (12 curved, 9 rectangular)

---

OUTPUT FROM PROGRAM \*FEM2DV2\*    BY J. N. REDDY  
 Edited by Pantaleo Loiacono.....14 September 1995

---

A VISCOUS INCOMPRESSIBLE FLOW IS ANALYZED

PARAMETERS OF THE FLUID FLOW PROBLEM:

Viscosity of the fluid, AMU.....= 0.2000E+1  
 Penalty parameter, PENLTY.....= 0.1000E+09

CONTINUOUS SOURCE COEFFICIENTS:

Coefficient, F0 .....= 0.0000E+0  
 Coefficient, FX .....= 0.0000E+0  
 Coefficient, FY .....= 0.0000E+0

\*\*\*\*\* A STEADY-STATE PROBLEM is analyzed \*\*\*\*\*

\*\*\* A mesh of QUADRILATERALS is chosen by user \*\*\*

FINITE ELEMENT MESH INFORMATION:

Element type: (0 = Triangle; >0 = Quad.)= 1  
 Number of nodes per element, NPE .....= 9  
 No. of primary deg. of freedom/node, NDF= 2  
 Number of elements in the mesh, NEM ....= 21  
 Number of nodes in the mesh, NNM .....= 105  
 Number of equations to be solved, NEQ ..= 210  
 Half bandwidth of the matrix GLK, NHBW .= 66  
 No. of specified PRIMARY variables, NSPV = 80

Node	x-coord.	y-coord.	Speci. primary & secondary variables (0, unspecified; >0, specified)				
			Primary DOF		Secondary DOF		
1	0.0000E+0	0.2000E+1	1	2	0	0	
2	0.3902E+0	0.1962E+1	1	2	0	0	
3	0.7654E+0	0.1848E+1	1	2	0	0	
4	0.1111E+1	0.1663E+1	1	2	0	0	
5	0.1414E+1	0.1414E+1	1	2	0	0	
6	0.1663E+1	0.1111E+1	1	2	0	0	
7	0.1848E+1	0.7654E+0	1	2	0	0	
8	0.1962E+1	0.3902E+0	1	2	0	0	
9	0.2000E+1	0.0000E+0	1	2	0	0	
10	0.2000E+1	-0.3333E+0	1	2	0	0	
11	0.2000E+1	-0.6667E+0	1	2	0	0	
12	0.2000E+1	-0.1000E+1	1	2	0	0	
13	0.2000E+1	-0.1333E+1	1	2	0	0	
14	0.2000E+1	-0.1667E+1	1	2	0	0	
15	0.2000E+1	-0.2000E+1	1	2	0	0	
16	0.0000E+0	0.2333E+1	1	2	0	0	
17	0.4552E+0	0.2288E+1	0	0	0	0	
18	0.8929E+0	0.2156E+1	0	0	0	0	
19	0.1296E+1	0.1940E+1	0	0	0	0	
20	0.1650E+1	0.1650E+1	0	0	0	0	
21	0.1940E+1	0.1296E+1	0	0	0	0	
22	0.2156E+1	0.8929E+0	0	0	0	0	
23	0.2288E+1	0.4552E+0	0	0	0	0	
24	0.2333E+1	0.0000E+0	0	0	0	0	
25	0.2333E+1	-0.3333E+0	0	0	0	0	
26	0.2333E+1	-0.6667E+0	0	0	0	0	
27	0.2333E+1	-0.1000E+1	0	0	0	0	
28	0.2333E+1	-0.1333E+1	0	0	0	0	
29	0.2333E+1	-0.1667E+1	0	0	0	0	
30	0.2333E+1	-0.2000E+1	1	2	0	0	
31	0.0000E+0	0.2667E+1	1	2	0	0	
32	0.5202E+0	0.2615E+1	0	0	0	0	
33	0.1020E+1	0.2464E+1	0	0	0	0	
34	0.1482E+1	0.2217E+1	0	0	0	0	
35	0.1886E+1	0.1886E+1	0	0	0	0	
36	0.2217E+1	0.1482E+1	0	0	0	0	
37	0.2464E+1	0.1020E+1	0	0	0	0	
38	0.2615E+1	0.5202E+0	0	0	0	0	
39	0.2667E+1	0.0000E+0	0	0	0	0	
40	0.2667E+1	-0.3333E+0	0	0	0	0	
41	0.2667E+1	-0.6667E+0	0	0	0	0	
42	0.2667E+1	-0.1000E+1	0	0	0	0	
43	0.2667E+1	-0.1333E+1	0	0	0	0	
44	0.2667E+1	-0.1667E+1	0	0	0	0	



45	0.2667E+1	-0.2000E+1	1	2	0	0
46	0.0000E+0	0.3000E+1	1	2	0	0
47	0.5853E+0	0.2942E+1	0	0	0	0
48	0.1148E+1	0.2772E+1	0	0	0	0
49	0.1667E+1	0.2494E+1	0	0	0	0
50	0.2121E+1	0.2121E+1	0	0	0	0
51	0.2494E+1	0.1667E+1	0	0	0	0
52	0.2772E+1	0.1148E+1	0	0	0	0
53	0.2942E+1	0.5853E+0	0	0	0	0
54	0.3000E+1	0.0000E+0	0	0	0	0
55	0.3000E+1	-0.3333E+0	0	0	0	0
56	0.3000E+1	-0.6667E+0	0	0	0	0
57	0.3000E+1	-0.1000E+1	0	0	0	0
58	0.3000E+1	-0.1333E+1	0	0	0	0
59	0.3000E+1	-0.1667E+1	0	0	0	0
60	0.3000E+1	-0.2000E+1	1	2	0	0
61	0.0000E+0	0.3333E+1	1	2	0	0
62	0.6503E+0	0.3269E+1	0	0	0	0
63	0.1276E+1	0.3080E+1	0	0	0	0
64	0.1852E+1	0.2772E+1	0	0	0	0
65	0.2357E+1	0.2357E+1	0	0	0	0
66	0.2772E+1	0.1852E+1	0	0	0	0
67	0.3080E+1	0.1276E+1	0	0	0	0
68	0.3269E+1	0.6503E+0	0	0	0	0
69	0.3333E+1	0.0000E+0	0	0	0	0
70	0.3333E+1	-0.3333E+0	0	0	0	0
71	0.3333E+1	-0.6667E+0	0	0	0	0
72	0.3333E+1	-0.1000E+1	0	0	0	0
73	0.3333E+1	-0.1333E+1	0	0	0	0
74	0.3333E+1	-0.1667E+1	0	0	0	0
75	0.3333E+1	-0.2000E+1	1	2	0	0
76	0.0000E+0	0.3667E+1	1	2	0	0
77	0.7153E+0	0.3596E+1	0	0	0	0
78	0.1403E+1	0.3388E+1	0	0	0	0
79	0.2037E+1	0.3049E+1	0	0	0	0
80	0.2593E+1	0.2593E+1	0	0	0	0
81	0.3049E+1	0.2037E+1	0	0	0	0
82	0.3388E+1	0.1403E+1	0	0	0	0
83	0.3596E+1	0.7153E+0	0	0	0	0
84	0.3667E+1	0.0000E+0	0	0	0	0
85	0.3667E+1	-0.3333E+0	0	0	0	0
86	0.3667E+1	-0.6667E+0	0	0	0	0
87	0.3667E+1	-0.1000E+1	0	0	0	0
88	0.3667E+1	-0.1333E+1	0	0	0	0
89	0.3667E+1	-0.1667E+1	0	0	0	0
90	0.3667E+1	-0.2000E+1	1	2	0	0
91	0.0000E+0	0.4000E+1	1	2	0	0
92	0.7804E+0	0.3923E+1	1	2	0	0
93	0.1531E+1	0.3696E+1	1	2	0	0
94	0.2222E+1	0.3326E+1	1	2	0	0
95	0.2828E+1	0.2828E+1	1	2	0	0
96	0.3326E+1	0.2222E+1	1	2	0	0
97	0.3696E+1	0.1531E+1	1	2	0	0

---

98	0.3923E+1	0.7804E+0	1	2	0	0
99	0.4000E+1	0.0000E+0	1	2	0	0
100	0.4000E+1	-0.3333E+0	1	2	0	0
101	0.4000E+1	-0.6667E+0	1	2	0	0
102	0.4000E+1	-0.1000E+1	1	2	0	0
103	0.4000E+1	-0.1333E+1	1	2	0	0
104	0.4000E+1	-0.1667E+1	1	2	0	0
105	0.4000E+1	-0.2000E+1	1	2	0	0

---

# NUMERICAL INTEGRATION DATA:

Full quadrature (IPDF x IPDF) rule, IPDF= 3  
 Reduced quadrature (IPDR x IPDR), IPDR= 2  
 Quadrature rule used in postproc., ISTR= 2

# S O L U T I O N :

---

Node	x-coord.	y-coord.	Value of u	Value of v
------	----------	----------	------------	------------

---

1	0.00000E+0	0.20000E+1	0.00000E+0	0.00000E+0
2	0.39020E+0	0.19620E+1	0.00000E+0	0.00000E+0
3	0.76540E+0	0.18480E+1	0.00000E+0	0.00000E+0
4	0.11110E+1	0.16630E+1	0.00000E+0	0.00000E+0
5	0.14140E+1	0.14140E+1	0.00000E+0	0.00000E+0
6	0.16630E+1	0.11110E+1	0.00000E+0	0.00000E+0
7	0.18480E+1	0.76540E+0	0.00000E+0	0.00000E+0
8	0.19620E+1	0.39020E+0	0.00000E+0	0.00000E+0
9	0.20000E+1	0.00000E+0	0.00000E+0	0.00000E+0
10	0.20000E+1	-0.33330E+0	0.00000E+0	0.00000E+0
11	0.20000E+1	-0.66670E+0	0.00000E+0	0.00000E+0
12	0.20000E+1	-0.10000E+1	0.00000E+0	0.00000E+0
13	0.20000E+1	-0.13330E+1	0.00000E+0	0.00000E+0
14	0.20000E+1	-0.16670E+1	0.00000E+0	0.00000E+0
15	0.20000E+1	-0.20000E+1	0.00000E+0	0.00000E+0
16	0.00000E+0	0.23330E+1	0.83300E+0	0.00000E+0
17	0.45520E+0	0.22880E+1	0.85891E+0	-0.20638E+0
18	0.89290E+0	0.21560E+1	0.87158E+0	-0.37521E+0
19	0.12960E+1	0.19400E+1	0.80140E+0	-0.54028E+0
20	0.16500E+1	0.16500E+1	0.68539E+0	-0.68744E+0
21	0.19400E+1	0.12960E+1	0.54025E+0	-0.80873E+0
22	0.21560E+1	0.89290E+0	0.37374E+0	-0.89772E+0
23	0.22880E+1	0.45520E+0	0.19902E+0	-0.94433E+0
24	0.23330E+1	0.00000E+0	0.47271E-1	-0.90005E+0
25	0.23330E+1	-0.33330E+0	0.16777E-1	-0.85101E+0
26	0.23330E+1	-0.66670E+0	0.47924E-2	-0.83536E+0
27	0.23330E+1	-0.10000E+1	0.82459E-3	-0.83078E+0
28	0.23330E+1	-0.13330E+1	-0.58853E-3	-0.83091E+0

29	0.23330E+1	-0.16670E+1	-0.87572E-3	-0.83218E+0
30	0.23330E+1	-0.20000E+1	0.00000E+0	-0.83300E+0
31	0.00000E+0	0.26670E+1	0.13330E+1	0.00000E+0
32	0.52020E+0	0.26150E+1	0.13239E+1	-0.34243E+0
33	0.10200E+1	0.24640E+1	0.12883E+1	-0.56550E+0
34	0.14820E+1	0.22170E+1	0.11748E+1	-0.79621E+0
35	0.18860E+1	0.18860E+1	0.10051E+1	-0.10079E+1
36	0.22170E+1	0.14820E+1	0.79001E+0	-0.11841E+1
37	0.24640E+1	0.10200E+1	0.54812E+0	-0.13164E+1
38	0.26150E+1	0.52020E+0	0.29957E+0	-0.13846E+1
39	0.26670E+1	0.00000E+0	0.11223E+0	-0.13787E+1
40	0.26670E+1	-0.33330E+0	0.43066E-1	-0.13524E+1
41	0.26670E+1	-0.66670E+0	0.14990E-1	-0.13383E+1
42	0.26670E+1	-0.10000E+1	0.24276E-2	-0.13328E+1
43	0.26670E+1	-0.13330E+1	-0.12198E-2	-0.13327E+1
44	0.26670E+1	-0.16670E+1	-0.18744E-2	-0.13328E+1
45	0.26670E+1	-0.20000E+1	0.00000E+0	-0.13330E+1
46	0.00000E+0	0.30000E+1	0.15000E+1	0.00000E+0
47	0.58530E+0	0.29420E+1	0.14520E+1	-0.37135E+0
48	0.11480E+1	0.27720E+1	0.13631E+1	-0.59609E+0
49	0.16670E+1	0.24940E+1	0.12266E+1	-0.83111E+0
50	0.21210E+1	0.21210E+1	0.10465E+1	-0.10489E+1
51	0.24940E+1	0.16670E+1	0.82180E+0	-0.12312E+1
52	0.27720E+1	0.11480E+1	0.56678E+0	-0.13685E+1
53	0.29420E+1	0.58530E+0	0.31465E+0	-0.14505E+1
54	0.30000E+1	0.00000E+0	0.11517E+0	-0.14908E+1
55	0.30000E+1	-0.33330E+0	0.52972E-1	-0.14995E+1
56	0.30000E+1	-0.66670E+0	0.17796E-1	-0.14993E+1
57	0.30000E+1	-0.10000E+1	0.36049E-2	-0.15002E+1
58	0.30000E+1	-0.13330E+1	-0.14806E-2	-0.14997E+1
59	0.30000E+1	-0.16670E+1	-0.21883E-2	-0.14999E+1
60	0.30000E+1	-0.20000E+1	0.00000E+0	-0.15000E+1
61	0.00000E+0	0.33330E+1	0.13330E+1	0.00000E+0
62	0.65030E+0	0.32690E+1	0.12626E+1	-0.30866E+0
63	0.12760E+1	0.30800E+1	0.11467E+1	-0.49242E+0
64	0.18520E+1	0.27720E+1	0.10209E+1	-0.68942E+0
65	0.23570E+1	0.23570E+1	0.86920E+0	-0.86996E+0
66	0.27720E+1	0.18520E+1	0.68140E+0	-0.10206E+1
67	0.30800E+1	0.12760E+1	0.46874E+0	-0.11324E+1
68	0.32690E+1	0.65030E+0	0.25550E+0	-0.12102E+1
69	0.33330E+1	0.00000E+0	0.86573E-1	-0.12835E+1
70	0.33330E+1	-0.33330E+0	0.39833E-1	-0.13130E+1
71	0.33330E+1	-0.66670E+0	0.13114E-1	-0.13306E+1
72	0.33330E+1	-0.10000E+1	0.26730E-2	-0.13342E+1
73	0.33330E+1	-0.13330E+1	-0.12414E-2	-0.13352E+1
74	0.33330E+1	-0.16670E+1	-0.16565E-2	-0.13339E+1
75	0.33330E+1	-0.20000E+1	0.00000E+0	-0.13330E+1
76	0.00000E+0	0.36670E+1	0.83300E+0	0.00000E+0
77	0.71530E+0	0.35960E+1	0.76923E+0	-0.17267E+0
78	0.14030E+1	0.33880E+1	0.67859E+0	-0.28456E+0
79	0.20370E+1	0.30490E+1	0.60126E+0	-0.40480E+0
80	0.25930E+1	0.25930E+1	0.51026E+0	-0.50933E+0
81	0.30490E+1	0.20370E+1	0.39997E+0	-0.59891E+0

82	0.33880E+1	0.14030E+1	0.27598E+0	-0.66494E+0
83	0.35960E+1	0.71530E+0	0.14337E+0	-0.70962E+0
84	0.36670E+1	0.00000E+0	0.36189E-1	-0.77703E+0
85	0.36670E+1	-0.33330E+0	0.13070E-1	-0.81575E+0
86	0.36670E+1	-0.66670E+0	0.54888E-2	-0.82994E+0
87	0.36670E+1	-0.10000E+1	0.66583E-3	-0.83454E+0
88	0.36670E+1	-0.13330E+1	-0.38987E-3	-0.83440E+0
89	0.36670E+1	-0.16670E+1	-0.46366E-3	-0.83353E+0
90	0.36670E+1	-0.20000E+1	0.00000E+0	-0.83300E+0
91	0.00000E+0	0.40000E+1	0.00000E+0	0.00000E+0
92	0.78040E+0	0.39230E+1	0.00000E+0	0.00000E+0
93	0.15310E+1	0.36960E+1	0.00000E+0	0.00000E+0
94	0.22220E+1	0.33260E+1	0.00000E+0	0.00000E+0
95	0.28280E+1	0.28280E+1	0.00000E+0	0.00000E+0
96	0.33260E+1	0.22220E+1	0.00000E+0	0.00000E+0
97	0.36960E+1	0.15310E+1	0.00000E+0	0.00000E+0
98	0.39230E+1	0.78040E+0	0.00000E+0	0.00000E+0
99	0.40000E+1	0.00000E+0	0.00000E+0	0.00000E+0
100	0.40000E+1	-0.33330E+0	0.00000E+0	0.00000E+0
101	0.40000E+1	-0.66670E+0	0.00000E+0	0.00000E+0
102	0.40000E+1	-0.10000E+1	0.00000E+0	0.00000E+0
103	0.40000E+1	-0.13330E+1	0.00000E+0	0.00000E+0
104	0.40000E+1	-0.16670E+1	0.00000E+0	0.00000E+0
105	0.40000E+1	-0.20000E+1	0.00000E+0	0.00000E+0

---

x-coord.	y-coord.	sigma-x	sigma-y	sigma-xy	pressure
0.178E+0	0.213E+1	-0.170E+2	-0.190E+2	0.472E+1	0.180E+2
0.210E+0	0.251E+1	-0.168E+2	-0.180E+2	0.149E+1	0.174E+2
0.651E+0	0.203E+1	-0.108E+2	-0.176E+2	0.417E+1	0.142E+2
0.768E+0	0.240E+1	-0.136E+2	-0.164E+2	0.122E+1	0.150E+2
0.981E+0	0.190E+1	-0.767E+1	-0.168E+2	0.314E+1	0.122E+2
0.115E+1	0.224E+1	-0.993E+1	-0.126E+2	0.792E+0	0.112E+2
0.138E+1	0.163E+1	-0.151E+1	-0.126E+2	0.919E+0	0.706E+1
0.163E+1	0.192E+1	-0.653E+1	-0.941E+1	0.220E+0	0.797E+1
0.163E+1	0.138E+1	0.508E+0	-0.106E+2	-0.948E+0	0.504E+1
0.192E+1	0.163E+1	-0.269E+1	-0.553E+1	-0.251E+0	0.411E+1
0.190E+1	0.981E+0	0.477E+1	-0.443E+1	-0.326E+1	-0.172E+0
0.224E+1	0.115E+1	0.426E+0	-0.193E+1	-0.849E+0	0.755E+0
0.203E+1	0.651E+0	0.555E+1	-0.103E+1	-0.462E+1	-0.225E+1
0.240E+1	0.768E+0	0.398E+1	0.224E+1	-0.117E+1	-0.311E+1
0.213E+1	0.178E+0	0.893E+1	0.639E+1	-0.535E+1	-0.766E+1
0.251E+1	0.210E+0	0.722E+1	0.573E+1	-0.174E+1	-0.648E+1
0.214E+1	-0.140E+0	0.949E+1	0.874E+1	-0.536E+1	-0.911E+1
0.252E+1	-0.140E+0	0.101E+2	0.901E+1	-0.243E+1	-0.957E+1
0.214E+1	-0.525E+0	0.121E+2	0.119E+2	-0.516E+1	-0.120E+2
0.252E+1	-0.525E+0	0.113E+2	0.110E+2	-0.275E+1	-0.111E+2
0.214E+1	-0.807E+0	0.129E+2	0.128E+2	-0.515E+1	-0.129E+2
0.252E+1	-0.807E+0	0.136E+2	0.135E+2	-0.280E+1	-0.135E+2

0.214E+1	-0.119E+1	0.158E+2	0.158E+2	-0.513E+1	-0.158E+2
0.252E+1	-0.119E+1	0.151E+2	0.151E+2	-0.283E+1	-0.151E+2
0.214E+1	-0.147E+1	0.168E+2	0.168E+2	-0.514E+1	-0.168E+2
0.252E+1	-0.147E+1	0.175E+2	0.175E+2	-0.284E+1	-0.175E+2
0.214E+1	-0.185E+1	0.198E+2	0.198E+2	-0.515E+1	-0.198E+2
0.252E+1	-0.185E+1	0.191E+2	0.191E+2	-0.285E+1	-0.191E+2
0.234E+0	0.279E+1	-0.188E+2	-0.188E+2	-0.299E+0	0.188E+2
0.266E+0	0.318E+1	-0.198E+2	-0.186E+2	-0.230E+1	0.192E+2
0.854E+0	0.267E+1	-0.144E+2	-0.144E+2	-0.616E-1	0.144E+2
0.971E+0	0.304E+1	-0.165E+2	-0.135E+2	-0.160E+1	0.150E+2
0.128E+1	0.249E+1	-0.122E+2	-0.116E+2	-0.231E+0	0.119E+2
0.146E+1	0.283E+1	-0.135E+2	-0.941E+1	-0.132E+1	0.114E+2
0.181E+1	0.214E+1	-0.781E+1	-0.675E+1	-0.988E-1	0.728E+1
0.206E+1	0.243E+1	-0.102E+2	-0.531E+1	-0.402E+0	0.777E+1
0.214E+1	0.181E+1	-0.534E+1	-0.423E+1	0.101E+0	0.479E+1
0.243E+1	0.206E+1	-0.676E+1	-0.181E+1	0.428E+0	0.428E+1
0.249E+1	0.128E+1	-0.586E+0	0.359E+0	0.318E+0	0.113E+0
0.283E+1	0.146E+1	-0.267E+1	0.144E+1	0.146E+1	0.612E+0
0.267E+1	0.854E+0	0.214E+1	0.270E+1	0.416E+0	-0.242E+1
0.304E+1	0.971E+0	0.136E+1	0.431E+1	0.200E+1	-0.284E+1
0.279E+1	0.234E+0	0.704E+1	0.696E+1	0.267E-1	-0.700E+1
0.318E+1	0.266E+0	0.588E+1	0.714E+1	0.204E+1	-0.651E+1
0.280E+1	-0.140E+0	0.885E+1	0.861E+1	-0.510E+0	-0.873E+1
0.319E+1	-0.140E+0	0.916E+1	0.972E+1	0.167E+1	-0.944E+1
0.280E+1	-0.525E+0	0.119E+2	0.117E+2	-0.920E+0	-0.118E+2
0.319E+1	-0.525E+0	0.109E+2	0.111E+2	0.139E+1	-0.110E+2
0.280E+1	-0.807E+0	0.128E+2	0.127E+2	-0.105E+1	-0.128E+2
0.319E+1	-0.807E+0	0.134E+2	0.134E+2	0.124E+1	-0.134E+2
0.280E+1	-0.119E+1	0.158E+2	0.158E+2	-0.114E+1	-0.158E+2
0.319E+1	-0.119E+1	0.150E+2	0.150E+2	0.117E+1	-0.150E+2
0.280E+1	-0.147E+1	0.168E+2	0.168E+2	-0.115E+1	-0.168E+2
0.319E+1	-0.147E+1	0.174E+2	0.174E+2	0.115E+1	-0.174E+2
0.280E+1	-0.185E+1	0.198E+2	0.198E+2	-0.117E+1	-0.198E+2
0.319E+1	-0.185E+1	0.190E+2	0.190E+2	0.114E+1	-0.190E+2
0.289E+0	0.346E+1	-0.208E+2	-0.191E+2	-0.355E+1	0.199E+2
0.321E+0	0.384E+1	-0.208E+2	-0.188E+2	-0.514E+1	0.198E+2
0.105E+1	0.330E+1	-0.170E+2	-0.123E+2	-0.263E+1	0.147E+2
0.117E+1	0.367E+1	-0.177E+2	-0.119E+2	-0.385E+1	0.148E+2
0.159E+1	0.308E+1	-0.147E+2	-0.886E+1	-0.197E+1	0.118E+2
0.176E+1	0.343E+1	-0.154E+2	-0.777E+1	-0.267E+1	0.115E+2
0.224E+1	0.265E+1	-0.109E+2	-0.394E+1	-0.566E+0	0.743E+1
0.249E+1	0.294E+1	-0.121E+2	-0.310E+1	-0.751E+0	0.764E+1
0.265E+1	0.224E+1	-0.812E+1	-0.112E+1	0.597E+0	0.462E+1
0.294E+1	0.249E+1	-0.892E+1	0.153E+0	0.762E+0	0.438E+1
0.308E+1	0.159E+1	-0.314E+1	0.260E+1	0.205E+1	0.269E+0
0.343E+1	0.176E+1	-0.424E+1	0.323E+1	0.265E+1	0.508E+0
0.330E+1	0.105E+1	0.383E+0	0.452E+1	0.287E+1	-0.245E+1
0.367E+1	0.117E+1	0.420E-1	0.530E+1	0.371E+1	-0.267E+1
0.346E+1	0.289E+0	0.585E+1	0.776E+1	0.328E+1	-0.680E+1
0.384E+1	0.321E+0	0.541E+1	0.734E+1	0.465E+1	-0.637E+1
0.347E+1	-0.140E+0	0.828E+1	0.926E+1	0.309E+1	-0.877E+1
0.385E+1	-0.140E+0	0.885E+1	0.941E+1	0.498E+1	-0.913E+1
0.347E+1	-0.525E+0	0.114E+2	0.118E+2	0.292E+1	-0.116E+2

0.385E+1	-0.525E+0	0.108E+2	0.110E+2	0.512E+1	-0.109E+2
0.347E+1	-0.807E+0	0.126E+2	0.127E+2	0.288E+1	-0.127E+2
0.385E+1	-0.807E+0	0.133E+2	0.133E+2	0.516E+1	-0.133E+2
0.347E+1	-0.119E+1	0.157E+2	0.157E+2	0.285E+1	-0.157E+2
0.385E+1	-0.119E+1	0.150E+2	0.150E+2	0.517E+1	-0.150E+2
0.347E+1	-0.147E+1	0.167E+2	0.167E+2	0.284E+1	-0.167E+2
0.385E+1	-0.147E+1	0.174E+2	0.174E+2	0.516E+1	-0.174E+2
0.347E+1	-0.185E+1	0.197E+2	0.197E+2	0.283E+1	-0.197E+2
0.385E+1	-0.185E+1	0.190E+2	0.190E+2	0.515E+1	-0.190E+2

---

# APPENDIX E

PROGRAM "nodgen.f"

```
C
C      program "nodgen.f"
C
C                                     by Pantaleo Loiacono
C
C      This program computes the values of "NOD(N,I)",
C      data card 6, from page 543 (Reddy)
C
C                                     7 November 1995
```

```
INTEGER a,b,c,d,e,f,g,h,r,dx,K
```

```
C      K is the number of values to be computed
C                                     (including original)
```

```
K=16
```

```
a=463
```

```
b=465
```

```
c=531
```

```
d=529
```

```
e=464
```

```
f=498
```

```
g=530
```

```
h=496
```

```
r=497
```

```
dx=0
```

```
DO 20 I=1,K
```

```
a=a+dx
```

```
b=b+dx
```

```
c=c+dx
```

```
d=d+dx
```

```
e=e+dx
```

```
f=f+dx
```

```
g=g+dx
```

```
h=h+dx
```

```
r=r+dx
```

```
WRITE (*,10) a,b,c,d,e,f,g,h,r
```

```
20    dx=2
```

```
10    FORMAT (9(I3,5X))
```

```
END
```

# APPENDIX F

PROGRAM "meshgencurve.f"

```

C
C
C   program "meshgencurve.f"
C
C   This program generates the coordinates of the nodal
C   values for a 90 degree turn which will be used for
C   the input data for the program "FEM2DV2"
C
C   written by Pantaleo Loiacono
C           6 November 1995
C
C
C   REAL dtheta, theta, phi, RI, x, y, Pi, R, xx, w, dy
C   INTEGER M, N, I, J
C   OPEN (UNIT=11,FILE='altmesh.dat',STATUS='NEW')
C
C   M is the number of angular divisions over the 90
C       degree turn
C   RI is the value of the inner radius
C   N is the number of elements in the mesh along the
C       radial axis
C   L is the number of elements in the rectangular part
C       of the mesh (yaxis)
C   R is the value of the radius at each increment
C       (varying)
C   xx is the value of the length of the rectangular part
C       (yaxis)
C   w is the value of the width of the rectangular part
C       (xaxis)
C   RO is the value of the outer radius.....NOTE: w=RO-RI
C
C   M=11
C   L=5
C   RI=2.0
C   RO=4.0
C   N=8
C   xx=2.0
C   w=RO-RI
C
C   NOTE:  this program has the value of w & xx fixed at
C           2, along with the value of RO which is fixed
C           at 2; modifications need to be made if the
C           dimensions of the 90 degree turn are changed
C
C   Pi=3.14159265359
C   theta=0.0

```



C For each value of R, compute all the values of x and  
 C y at the different values of phi (big loop, "10",  
 C varies R)

```
DO 10 I=0, (2*N)
      R=RI+I*1.0/N
```

C This loop values the angle of phi and computes x,y at  
 C fixed R

```
DO 21 J=1, (2*M+1)

      dtheta=Pi/(4.0*M)
      phi=(Pi/2.0)-theta
      IF (phi.LT.0.0001) THEN
            phi=0.0
      ENDIF

      x=R*cos(phi)
      y=R*sin(phi)

      IF (x.LT.0.0001) THEN
            x=0.0
      ENDIF

      IF (y.LT.0.0001) THEN
            y=0.0
      ENDIF

      WRITE (11,22) x,y
      theta=theta+dtheta
```

21 CONTINUE

C Here the values of the coordinates of the rectangular  
 C portion of the loop are computed at the value of R  
 C computed in the big "10" loop above; these values are  
 C computed at each value of R

```
y=0.0
```

```
DO 37 II=1, (2*L)
      y=0.0
      x=R
      dy=II*1.0/L
      y=y-dy

      IF (x.LT.0.0001) THEN
            x=0.0
      ENDIF

      IF (y.GT.-0.0001) y=0.0
```

```
                WRITE (11,34) x,y
37      CONTINUE
C      Reset the value of theta for the next loop
      theta=0.0
10     CONTINUE
89     FORMAT (/)
22     FORMAT (3X,E12.4,3X,E12.4)
34     FORMAT (3X,E12.4,3X,E12.4)

      END
```

## APPENDIX G

### PROGRAM "particles.f"

```
C
C
C      PROGRAM "particles.f"
C
C      written by Pantaleo Loiacono
C                  January 1996
C
C
C      This program examines the motion of particles,
C      one at a time, through a 90 degree turn. The
C      velocity distribution is obtained through
C      finite element analysis, using the program
C      "FEM2DV2". The program computes the next
C      position of the particle and determines
C      whether or not the particle has hit the wall
C      of the duct. When the particle hits the wall,
C      it is assumed that it has been deposited on
C      that wall. A Runge-Kutta 4th order method is
C      used to determine the next position of the
C      particle according to the governing equations
C      of motion. The output of this program is
C      later analyzed by the program "particlesout.f"
C
C      NOTE:      LU.....left upper node
C                  LL.....left lower node
C                  RU.....right upper node
C                  RL.....right lower node
C
C
C      MIN.....Number of Particles coming in at the
C                  Entrance
C      MAX.....Number of Equations to be solved
C      MINA.....Number of Nodes in the Mesh
C
C
C      DIMENSION OF LU, LL, RU, RL, Z, ETC. MAY HAVE
C      TO BE ADJUSTED WITH FINER MESHES
C
C
C
C      PARAMETER (MAX=3100,MIN=100,MINA=1000)
C
C      DIMENSION NOD(MINA), POS(MINA,2), VEL(MINA,2)
C      DIMENSION y(MIN,MAX), U(MIN,MAX), V(MIN,MAX)
C      DIMENSION A(MIN,MAX), B(MIN,MAX), LU(MAX), LL(MAX)
C      DIMENSION RL(MAX), x(MIN,MAX), Z(MIN,MAX), RU(MAX)
C
C      REAL K1,K2,K3,K4,K11,K21,K31,K41,K12,K22,K32,K42
```

```
REAL K112,K212,K312,K412,S,G,SPLIT,dTavg,dT
```

```
INTEGER LU,LL,RU,RL,RIGHTN,LEFTN,NPART,DIVIDE,ST
INTEGER MU,SECTION,FILEA
```

```
C      Read the values from "velocities.dat" and save them
C      into the appropriate arrays
```

```
OPEN (UNIT=7,FILE='velocities.dat',STATUS='OLD')
OPEN (UNIT=457,FILE='particles1.out',STATUS='OLD')
OPEN (UNIT=458,FILE='particles2.out',STATUS='OLD')
OPEN (UNIT=459,FILE='particles3.out',STATUS='OLD')
OPEN (UNIT=460,FILE='particles4.out',STATUS='OLD')
OPEN (UNIT=461,FILE='particles5.out',STATUS='OLD')
OPEN (UNIT=462,FILE='particles6.out',STATUS='OLD')
OPEN (UNIT=463,FILE='particles7.out',STATUS='OLD')
OPEN (UNIT=464,FILE='particles8.out',STATUS='OLD')
OPEN (UNIT=465,FILE='particles9.out',STATUS='OLD')
OPEN (UNIT=466,FILE='particles10.out',STATUS='OLD')
OPEN (UNIT=467,FILE='particles11.out',STATUS='OLD')
OPEN (UNIT=468,FILE='particles12.out',STATUS='OLD')
OPEN (UNIT=469,FILE='particles13.out',STATUS='OLD')
OPEN (UNIT=470,FILE='particles14.out',STATUS='OLD')
OPEN (UNIT=471,FILE='particles15.out',STATUS='OLD')
OPEN (UNIT=472,FILE='particles16.out',STATUS='OLD')
OPEN (UNIT=473,FILE='particles17.out',STATUS='OLD')
OPEN (UNIT=474,FILE='particles18.out',STATUS='OLD')
OPEN (UNIT=475,FILE='particles19.out',STATUS='OLD')
OPEN (UNIT=476,FILE='particles20.out',STATUS='OLD')
OPEN (UNIT=477,FILE='particles21.out',STATUS='OLD')
OPEN (UNIT=478,FILE='particles22.out',STATUS='OLD')
OPEN (UNIT=479,FILE='particles23.out',STATUS='OLD')
OPEN (UNIT=480,FILE='particles24.out',STATUS='OLD')
OPEN (UNIT=481,FILE='particles25.out',STATUS='OLD')
OPEN (UNIT=45,FILE='particles.info',STATUS='OLD')
```

```
C      These are the INPUT VALUES which need to be changed
C      when the program interprets a different mesh,
C      starts at a different point, etc.
```

```
      dT.....time step
```

```
      N.....the left entrance number to add to
               the first node in the mesh to get
               to the node above it, dependent
               upon the mesh size
```

```
      NNM.....the number of nodes in the mesh
```

```

C      ELEMENTS...the total number of elements in the
C      mesh
C
C      LOOPNDS...the number of nodes around the
C      circular loop only (include the
C      last horizontal one)
C
C      NPART.....the number of entrance particles
C      which will be analyzed as they move
C      through the duct system.  Specify
C      an odd number if a particle starting
C      at the center of the duct is desired
C      (x=0.0, y=3.0, U=1.5, V=0.0)
C
C      ENTRSZ....the diameter of the entrance section
C      of the duct
C
C      DIVIDE....the number of divisions that the
C      entrance flow is split up into due
C      to the fact that the computer can't
C      handle so many equations
C      simultaneously
C
C      SECTION...the section which is being examined;
C      there are "DIVIDE" number of
C      sections in the program.  The lowest
C      section number is the section at the
C      lowest point of the entrance.
C
C      REVISE N, LOOPNDS, ELEMENTS AS NECESSARY....
C      DEPENDENT ON MESH SIZE
C
C      NOTE:  adjust the value of JJJ if the number
C      of elements before the 45 degree turn
C      is different than the number of
C      elements after the 45 degree turn
C      (but before 0 degrees)
C

```

PI=3.14159265359

```

C      These are the values of the parameters:
C
C      S=inertia force/viscous force
C      G=gravity force/viscous force
C
C      NOTE:  NPART/DIVIDE SHOULD BE A WHOLE NUMBER FOR
C      BEST RESULTS
C
C      ISECTST is the section at which the analysis is

```

```

C          being started at
C IPRINT=1 means print all output to screen; if 0,
C          then don't
C
C xFINAL and yFINAL are the final positions of the
C previous particle; these values are to be specified
C only when the analysis is being started at any
C section other than section 1 (ISECTST=1)
C
C *****
C CHANGE INPUT DATA FROM HERE
C *****
C
C S=0.1
C G=0.0
C ENTRSZ=2.0
C N=33
C ELEMENTS=128
C LOOPNDS=23
C NPART=100
C DIVIDE=25
C ISECTST=1
C ISECEND=DIVIDE
C IPRINT=0
C
C *****
C END CHANGES HERE
C *****
C
C PRINT *, 'Number of particles analyzed=', NPART
C WRITE (45, *) S, G, NPART, DIVIDE, dT
C
C IF (NPART.GT.MIN) THEN
C     PRINT *, 'INCREASE MIN'
C     PRINT *, 'NPART=', NPART, '    MIN=', MIN
C     GOTO 237
C ENDIF
C
C Read in the positions and velocities from the mesh
C data
C
C READ (7, *) NNM
C
C IF (NNM.GE.(MINA-1)) THEN
C     PRINT *, 'INCREASE MINA SIZE'
C     PRINT *, 'NNM=', NNM
C     PRINT *, 'MINA=', MINA
C     GOTO 237
C ENDIF

```

```

DO 10 IG=1,NNM
      READ(7,*) NOD(IG)
      READ(7,*) (POS(IG,J), J=1,2)
      READ(7,*) (VEL(IG,J), J=1,2)
10  CONTINUE

PRINT *, ' '
PRINT *, ' '
PRINT *, '*****'
PRINT *, '# of files to compile (DIVIDE)=' ,DIVIDE
PRINT *, 'MIN=' ,MIN, '      MAX=' ,MAX, '      MINA=' ,MINA
PRINT *, '      S=' ,S, '      G=' ,G

C      Loop 283 controls which section is currently being
C      examined

DO 283 ISECT=ISECTST,ISECEND

      SECTION=ISECT

      IF (SECTION.GT.DIVIDE) THEN
        PRINT *, 'ERROR, SECTION>DIVIDE'
        GOTO 237
      ENDIF

PRINT *, '*****'
PRINT *, ' '
PRINT *, ' '
PRINT *, '*****'
PRINT *, 'Currently looking at section ' ,SECTION
PRINT *, '*****'
PRINT *, ' '

C      FILEA is the UNIT number in which the data will be
C      stored in...These SECTIONS only work if the mesh is
C      being divided into 25 sections; Adjust if it will be
C      divided it into more sections by increasing the
C      number of SECTIONS or decreased accordingly.

      IF (SECTION.EQ.1) THEN
        ST=1
        MU=1
        FILEA=457
      ELSEIF (SECTION.EQ.2) THEN
        ST=NPART/DIVIDE+1
        MU=2
        FILEA=458
      ELSEIF (SECTION.EQ.3) THEN
        ST=2*NPART/DIVIDE+1
        MU=3
        FILEA=459
      ELSEIF (SECTION.EQ.4) THEN

```

```
      ST=3*NPART/DIVIDE+1
      MU=4
      FILEA=460
ELSEIF (SECTION.EQ.5) THEN
      ST=4*NPART/DIVIDE+1
      MU=5
      FILEA=461
ELSEIF (SECTION.EQ.6) THEN
      ST=5*NPART/DIVIDE+1
      MU=6
      FILEA=462
ELSEIF (SECTION.EQ.7) THEN
      ST=6*NPART/DIVIDE+1
      MU=7
      FILEA=463
ELSEIF (SECTION.EQ.8) THEN
      ST=7*NPART/DIVIDE+1
      MU=8
      FILEA=464
ELSEIF (SECTION.EQ.9) THEN
      ST=8*NPART/DIVIDE+1
      MU=9
      FILEA=465
ELSEIF (SECTION.EQ.10) THEN
      ST=9*NPART/DIVIDE+1
      MU=10
      FILEA=466
ELSEIF (SECTION.EQ.11) THEN
      ST=10*NPART/DIVIDE+1
      MU=11
      FILEA=467
ELSEIF (SECTION.EQ.12) THEN
      ST=11*NPART/DIVIDE+1
      MU=12
      FILEA=468
ELSEIF (SECTION.EQ.13) THEN
      ST=12*NPART/DIVIDE+1
      MU=13
      FILEA=469
ELSEIF (SECTION.EQ.14) THEN
      ST=13*NPART/DIVIDE+1
      MU=14
      FILEA=470
ELSEIF (SECTION.EQ.15) THEN
      ST=14*NPART/DIVIDE+1
      MU=15
      FILEA=471
ELSEIF (SECTION.EQ.16) THEN
      ST=15*NPART/DIVIDE+1
      MU=16
      FILEA=472
ELSEIF (SECTION.EQ.17) THEN
      ST=16*NPART/DIVIDE+1
```



```

      MU=17
      FILEA=473
ELSEIF (SECTION.EQ.18) THEN
      ST=17*NPART/DIVIDE+1
      MU=18
      FILEA=474
ELSEIF (SECTION.EQ.19) THEN
      ST=18*NPART/DIVIDE+1
      MU=19
      FILEA=475
ELSEIF (SECTION.EQ.20) THEN
      ST=19*NPART/DIVIDE+1
      MU=20
      FILEA=476
ELSEIF (SECTION.EQ.21) THEN
      ST=20*NPART/DIVIDE+1
      MU=21
      FILEA=477
ELSEIF (SECTION.EQ.22) THEN
      ST=21*NPART/DIVIDE+1
      MU=22
      FILEA=478
ELSEIF (SECTION.EQ.23) THEN
      ST=22*NPART/DIVIDE+1
      MU=23
      FILEA=479
ELSEIF (SECTION.EQ.24) THEN
      ST=23*NPART/DIVIDE+1
      MU=24
      FILEA=480
ELSEIF (SECTION.EQ.25) THEN
      ST=24*NPART/DIVIDE+1
      MU=25
      FILEA=481
ELSE
      PRINT *, 'ERROR, NO SECTION NUMBER SPECIFIED'
      GOTO 237
ENDIF

```

C        SPLIT is defined as the diameter of the entrance  
C        section of the duct divided by the total number of  
C        particles entering the duct (+1). This number is  
C        used to determine at which position the particles  
C        are at when they enter the duct, assuming a uniform  
C        distribution of particles at the entrance.

```

SPLIT=ENTRSZ/(100+1)

```

C        Define the initial conditions for all of the  
C        particles in this loop 113...there are NPART initial  
C        conditions, representing one set of initial

C conditions per particle (for NPART total particles).  
 C The entrance flow is taken as parabolic, fully  
 C developed. However, this can be changed by changing  
 C the equation for U(III,0). The dimensions of the  
 C region are such that the lowest portion of the  
 C entrance is at the coordinates x=0.0, y=2.0

YO=-1.0+SPLIT

DO 113 III=1,NPART

    x(III,0)=0.0  
     y(III,0)=YO+3.0  
     Z(III,0)=SQRT(x(III,0)\*\*2+y(III,0)\*\*2)  
     U(III,0)=1.5\*(1-((y(III,0)-3.0)\*\*2))  
     V(III,0)=0.0  
     A(III,0)=U(III,0)  
     B(III,0)=0.0  
     YO=YO+SPLIT  
     IF (y(III,0).EQ.4.0) U(III,0)=0.0  
     IF (y(III,0).EQ.2.0) U(III,0)=0.0

113 CONTINUE

C Now that ALL of the initial conditions have been  
 C defined and are located in the arrays of loop 113,  
 C one particle at a time is examined until it either  
 C exits the duct or is deposited on the duct.

C Loop 114 controls which particle number is being  
 C examined

DO 114 IVI=ST,MU\*NPART/DIVIDE

    DIVIDER=1.0  
     JJJJ=0  
     PRINT \*, ' '  
     PRINT \*, 'Now Analyzing Particle Number', IVI  
     IF (IPRINT.EQ.1) PRINT \*, 'DIVIDER=', DIVIDER  
     WRITE (FILEA,\*) IVI

C The Runge-Kutta 4th order equations are as follows,  
 C for x,y,A,B

    dx/dT=A  
     S\*dx/dT=U-A  
  
     dy/dT=B  
     S\*dy/dT=V-B-G

C The values of the constants for the Runge-  
 C Kutta equations are given the names K1, K2,  
 C K3, K4, K11, K21, K31, K41, K12, K22, K32,  
 C

```

C           K42, K112, K212, K312, K412
C
C           dT (a variable) is the time step after which
C           the particle will move to a new computed
C           location, using the R-K equations
C
C           ZZ is the initial radius of the particle's
C           position; when the radius is less than 2.0
C           or greater than 4.0, the particle is outside
C           of the region of the duct.
C

```

```

ZZ=SQRT(x(IVI,0)**2+y(IVI,0)**2)
IF (ZZ.LE.2.0.OR.ZZ.GE.4.0) THEN
    PRINT *, 'Particle ',IVI,' was deposited'
    PRINT *, 'before ever entering the duct'
    x(IVI,I+1)=x(IVI,I)
    y(IVI,I+1)=y(IVI,I)
    I=-1
    GOTO 23
ENDIF

```

```

C           Loop 12 examines the particle IVI...only that
C           particle is looked at. This loop analyzes one
C           particle at a time. Loop 12 determines when the
C           particle has been deposited/exits. dT is a
C           variable; it is defined by the equation  $dT=dx/Up$ ,
C           where Up is the velocity of the particle in the
C           u-direction and dx is the change in the x-position;
C           take an initial value of  $dT=0.01$ . If  $dx/Up=0.0$ ,
C           then  $dT=dy/Vp$ 
C
C           This analysis is based upon an entrance velocity
C           distribution with the velocity in the y-direction
C           initially equal to 0.0 (V). When this is not the
C           case, the program is stopped.
C

```

```

67      dT=0.01
      dTtotal=0.0
      IF (IPRINT.EQ.1) PRINT *, 'DIVIDER=',DIVIDER

      DO 12 I=0,4000
          IF (V(IVI,0).GT.0.000001) THEN
              PRINT *, 'ERROR...INITIAL V VALUE WAS NOT'
              PRINT *, 'EQUAL TO ZERO'
              PRINT *, 'FOR PARTICLE NUMBER ',IVI
              PRINT *, 'V(',IVI,',0)=' ,V(IVI,0)
              GOTO 237
          ENDIF
      
```

```

C           These next four IF-THEN statements determine
C           whether or not the program will crash due to

```

C parameter specifications not being large enough.  
 C The program is terminated when the parameters are  
 C too small for the analysis.

```

IF (NPART.GT.MIN) THEN
    PRINT *, 'INCREASE MIN'
    PRINT *, 'NPART=', NPART, '    MIN=', MIN
    GOTO 237
ENDIF

IF (NNM.GE.(MINA-1)) THEN
    PRINT *, 'INCREASE MINA SIZE'
    PRINT *, 'NNM=', NNM
    PRINT *, 'MINA=', MINA
    GOTO 237
ENDIF

IF (I.GE.(MAX-1)) THEN
    PRINT *, 'INCREASE MAX SIZE'
    PRINT *, 'I=', I
    PRINT *, 'MAX=', MAX
    PRINT *, 'Current Posistions:  x=', x(IVI,I)
    PRINT *, '                      y=', y(IVI,I)
    PRINT *, '                      z=', z(IVI,I)
    GOTO 237
ENDIF

IF (IVI.GE.(MIN-1)) THEN
    PRINT *, 'INCREASE MIN SIZE'
    PRINT *, 'IVI=', IVI
    PRINT *, 'MIN=', MIN
    GOTO 237
ENDIF

```

C These are the variables which are used to compute  
 C the next A(IVI,I), as defined above

```

K11=dT*(U(IVI,I)-A(IVI,I))/S
K21=dT*(U(IVI,I)-(A(IVI,I)+K11/2))/S
K31=dT*(U(IVI,I)-(A(IVI,I)+K21/2))/S
K41=dT*(U(IVI,I)-(A(IVI,I)+K31))/S

```

C These are the variables which are used to compute  
 C the next x(IVI,I) as defined above

```

K1=dT*A(IVI,I)
K2=dT*(A(IVI,I)+K11/2)
K3=dT*(A(IVI,I)+K21/2)
K4=dT*(A(IVI,I)+K31)

```

C These are the equations to compute the values of

```

C      the next x(IVI,I) and the next A(IVI,I)

      x(IVI,I+1)=x(IVI,I)+(K1+2*K2+2*K3+K4)/6
      A(IVI,I+1)=A(IVI,I)+(K11+2*K21+2*K31+K41)/6

C      These are the variables which are used to compute
C      the next B(IVI,I), as defined above

      K112=dT*(V(IVI,I)-B(IVI,I)-G)/S
      K212=dT*(V(IVI,I)-(B(IVI,I)+K112/2)-G)/S
      K312=dT*(V(IVI,I)-(B(IVI,I)+K212/2)-G)/S
      K412=dT*(V(IVI,I)-(B(IVI,I)+K312)-G)/S

C      These are the variables which are used to compute
C      the next y(IVI,I) as defined above

      K12=dT*B(IVI,I)
      K22=dT*(B(IVI,I)+K112/2)
      K32=dT*(B(IVI,I)+K212/2)
      K42=dT*(B(IVI,I)+K312)

C      These are the equations to compute the values of
C      the next y(IVI,I) and the next B(IVI,I)

      y(IVI,I+1)=y(IVI,I)+(K12+2*K22+2*K32+K42)/6
      B(IVI,I+1)=B(IVI,I)+(K112+2*K212+2*K312+K412)/6

C      The program stops when one of the following
C      conditions are met: (Z is the radius of the
C      particle's position)

      Z(IVI,I+1)=SQRT(x(IVI,I+1)**2+y(IVI,I+1)**2)

C      The particle incorrectly exits through the inlet

      IF (x(IVI,I+1).LT.0.0) THEN
          PRINT *, ' '
          PRINT *, 'Error....x is less than zero'
          PRINT *, 'x=', x(IVI,I+1)
          PRINT *, 'y=', y(IVI,I+1)
          PRINT *, 'z=', z(IVI,I+1)
          PRINT *, 'dT=', dT
          PRINT *, ' '
          GOTO 237

C      The particle hits the lower circular wall

      ELSEIF (x(IVI,I+1).GT.0.0.AND.x(IVI,I+1).LE.2.0.AND
*           .Z(IVI,I+1).LE.2.01.AND.y(IVI,I+1).GT.0.0)
*           THEN
          GOTO 23

C      The particle hits the upper circular wall

```

```

      ELSEIF (x(IVI,I+1).GT.0.0.AND.x(IVI,I+1).LE.4.0.AND
*          .Z(IVI,I+1).GE.3.99.AND.y(IVI,I+1).GT.0.0)
*          THEN
            GOTO 23

      ELSEIF (x(IVI,I+1).GT.0.0.AND.x(IVI,I+1).GT.4.0.AND
*          .Z(IVI,I+1).GE.3.99.AND.y(IVI,I+1).GT.0.0)
*          THEN
            GOTO 23

C      The particle successfully exits the duct through
C      the lower section

      ELSEIF (y(IVI,I+1).LE.-2.0.AND.x(IVI,I+1).GT.2.0.
*          AND.x(IVI,I+1).LT.4.0) THEN
            GOTO 23

C      The particle hits the left vertical section at the
C      exit region

      ELSEIF (x(IVI,I+1).LE.2.0.AND.y(IVI,I+1).GE.-2.0.
*          AND.y(IVI,I+1).LE.0.0) THEN
            GOTO 23

C      The particle hits the right vertical section at the
C      exit region

      ELSEIF (x(IVI,I+1).GE.4.0.AND.y(IVI,I+1).GE.-2.0.
*          AND.y(IVI,I+1).LE.0.0) THEN
            GOTO 23

      ENDIF

C      If the program gets to this point, then the particle
C      is still in the duct.  Velocity computations will be
C      performed as follows...
C
C      From here, the four closest nodes to the element
C      must be identified.
C
C      First determine, based upon the radius of the
C      particle's current position, which nodes are above
C      and below the particle at the entrance region when
C      the particle is in the 90 degree turn of the domain.
C
C      NUMBER is the number of nodes at the entrance

      NUMBER=NOD(NNM)/N
      KUPN=1

      DO 319 KUP=1,NUMBER

```

```

      IF (POS(KUPN,2).LE.Z(IVI,I+1)) THEN
          MINNOD=NOD(KUPN)
      ELSE
          MAXNOD=NOD(KUPN)
          GOTO 321
      ENDIF

      KUPN=KUPN+N

      IF (KUPN.GE.MINA-1) THEN
          PRINT *, 'INCREASE MINA SIZE'
          PRINT *, 'KUPN(LOOP 319)=' , KUPN
          GOTO 237
      ENDIF

      IF (MINNOD.GT.1000) THEN
          PRINT *, ' '
          PRINT *, ' '
          PRINT *, 'MINNOD IS TOO HIGH'
          PRINT *, ' '
          PRINT *, 'CHANGE THE VALUE OF THE PARAM. MIN'
          PRINT *, ' '
          PRINT *, 'MINNOD>NNM'
          PRINT *, 'MINNOD=' , MINNOD
          PRINT *, 'KUPN=' , KUPN
          PRINT *, 'NOD(KUPN)=' , NOD(KUPN)
          PRINT *, 'POS(KUPN,2)=' , POS(KUPN,2)
          PRINT *, 'Z(' , IVI, ' , ' , I+1, ' )=' , Z(IVI,I+1)
          GOTO 237
      ENDIF
319  CONTINUE

321  MINNOD3=MINNOD
      MAXNOD3=MAXNOD

C      If the particle is in the 90 degree turn of the
C      domain, loop 385 will determine which nodes are the
C      four closest nodes to the particle

      DO 385 KJ=1, (LOOPNDS-1)

          IF (POS(MINNOD3,1).LE.x(IVI,I+1).AND.POS
*          (MAXNOD3,2).GE.y(IVI,I+1).AND.POS
*          (MINNOD3+1,2).LE.y(IVI,I+1).AND.POS
*          (MAXNOD3+1,1).GE.x(IVI,I+1)) THEN

              LU(I+1)=MAXNOD3
              RU(I+1)=MAXNOD3+1
              LL(I+1)=MINNOD3
              RL(I+1)=MINNOD3+1
              GOTO 326
          ELSE
              MINNOD3=MINNOD3+1

```

```

                                MAXNOD3=MAXNOD3+1
                                ENDIF
385    CONTINUE

    PHI=PI/4
    MINNOD2=MINNOD

C    When the point is passed the 90 degree turn, then
C    it must be located in the exit vertical section of
C    the duct...Here, first define which nodes the point
C    lies between on the x-axis (where y=0 in loop 325).

    LOOPNDS2=LOOPNDS

    DO 325 KWP=1,N
        IF (POS(LOOPNDS2,1).GT.x(IVI,I+1)) THEN
            MAXNOD4=LOOPNDS2
            MINNOD4=LOOPNDS2-N
            LEFTN=MINNOD4
            RIGHTN=MAXNOD4
            GOTO 361
        ELSE
            LOOPNDS2=LOOPNDS2+N
        ENDIF

        IF (LOOPNDS2.GT.NNM) THEN
            WRITE (FILEA,*) 'ERROR...'
            WRITE (FILEA,*) 'SEE LOOP 325'
            PRINT *, ' '
            PRINT *, ' '
            PRINT *, ' '
            PRINT *, 'LOOP 325 ERROR'
            PRINT *, 'Program Says the Point'
            PRINT *, 'is passed the'
            PRINT *, '90 degree turn '
            PRINT *, 'LOOPNDS2=', LOOPNDS2
            PRINT *, 'LOOPNDS2>NNM'
            PRINT *, 'x(', IVI, ', ', ' ', 'I+1)=', x(IVI,I+1)
            PRINT *, 'y(', IVI, ', ', ' ', 'I+1)=', y(IVI,I+1)
            PRINT *, 'z(', IVI, ', ', ' ', 'I+1)=', z(IVI,I+1)
            PRINT *, 'I+1=', (I+1)
            PRINT *, 'POS(LOOPNDS2-N,1)='
            PRINT *, ' ', POS(LOOPNDS2-N,1)
            PRINT *, 'PROGRAM TERMINATED'
            PRINT *, ' '
            PRINT *, ' '
            PRINT *, ' '
            PRINT *, 'ADJUST PARAMETER MIN '
            PRINT *, 'dT=', dT
            PRINT *, ' '
            PRINT *, ' '
            GOTO 237
        ENDIF
    
```



```

325      CONTINUE

C      At this point, move through the nodes beginning
C      with MINNOD4...increase the value of MINNOD4 up to
C      N; the four closest nodes are found when y(I+1) is
C      greater than the value of MINNOD4's y value (exit
C      vertical section of the duct only).

361      DO 562 III=1,N
           IF (POS(MINNOD4,2).LE.y(IVI,I+1)) THEN
               LL(I+1)=MINNOD4
               LU(I+1)=MINNOD4-1
               RU(I+1)=LU(I+1)+N
               RL(I+1)=RU(I+1)+1

               IF ((LU(I+1)+N).GT.NNM) THEN
                   LU(I+1)=LU(I+1)-N
                   LL(I+1)=LU(I+1)+1
                   RU(I+1)=LU(I+1)+N
                   RL(I+1)=RU(I+1)+1
               ENDIF

               GOTO 326

           ELSE

               MINNOD4=MINNOD4+1

           ENDIF
562      CONTINUE

C      From here, the velocity of the particle must be
C      computed based upon the four closest nodes and how
C      close the particle is to each of those four nodes.
C      Interpolation is performed based upon elements with
C      two circular portions and two straight line
C      portions.

C      RTOP is the radius of the top of the element
C      RBOT is the radius of the bottom of the element
C      RPAR is the radius of the particle's position
C

326      RTOP=SQRT((POS(LU(I+1),1)**2+POS(LU(I+1),2)**2))
          RBOT=SQRT((POS(LL(I+1),1)**2+POS(LL(I+1),2)**2))
          RPAR=SQRT((x(IVI,I+1)**2+y(IVI,I+1)**2))

C      This is the case where the element is located in
C      the 90 degree turn of the mesh...Note the special
C      "if-then" statements for the cases where the mesh
C      has a horizontal or vertical line in it.

          IF (y(IVI,I+1).GT.0.0) THEN

              CI=(RPAR-RBOT)/(RTOP-RBOT)
              XL=(POS(LU(I+1),1)-POS(LL(I+1),1))*CI+POS(LL(I+1),1)

```

```

YL=(POS(LU(I+1),2)-POS(LL(I+1),2))*CI+POS(LL(I+1),2)
XR=(POS(RU(I+1),1)-POS(RL(I+1),1))*CI+POS(RL(I+1),1)
YR=(POS(RU(I+1),2)-POS(RL(I+1),2))*CI+POS(RL(I+1),2)

```

```

UL=(VEL(LU(I+1),1)-VEL(LL(I+1),1))*CI+VEL(LL(I+1),1)
UR=(VEL(RU(I+1),1)-VEL(RL(I+1),1))*CI+VEL(RL(I+1),1)
VL=(VEL(LU(I+1),2)-VEL(LL(I+1),2))*CI+VEL(LL(I+1),2)
VR=(VEL(RU(I+1),2)-VEL(RL(I+1),2))*CI+VEL(RL(I+1),2)

```

```

      IF (XL.EQ.0.0) THEN
        THETA1=1.571
      ELSE
        THETA1=ATAN(YL/XL)
      ENDIF

```

```

      IF (YR.EQ.0.0) THEN
        THETA3=0.0
      ELSE
        THETA3=ATAN(YR/XR)
      ENDIF

```

```

THETA2=ATAN(y(IVI,I+1)/x(IVI,I+1))
PHI1=THETA1-THETA2
PHI2=THETA2-THETA3

```

```

ARCLP=RPAR*PHI1
ARCPR=RPAR*PHI2
ARCLR=ARCLP+ARCPR
ARC4B=RBOT*PHI1
ARCB3=RBOT*PHI2
ARC1T=RTOP*PHI1
ARCT2=RTOP*PHI2

```

```

CIT=ARC1T/(ARC1T+ARCT2)
CIB=ARC4B/(ARC4B+ARCB3)
CIP=ARCLP/(ARCLP+ARCPR)

```

```

XT=(POS(RU(I+1),1)-POS(LU(I+1),1))*
*   CIT+POS(LU(I+1),1)
YT=(POS(RU(I+1),2)-POS(LU(I+1),2))*
*   CIT+POS(LU(I+1),2)
XB=(POS(RL(I+1),1)-POS(LL(I+1),1))*
*   CIB+POS(LL(I+1),1)
YB=(POS(RL(I+1),2)-POS(LL(I+1),2))*
*   CIB+POS(LL(I+1),2)

```

```

UT=(VEL(RU(I+1),1)-VEL(LU(I+1),1))*
*   CIT+VEL(LU(I+1),1)
UB=(VEL(RL(I+1),1)-VEL(LL(I+1),1))*
*   CIB+VEL(LL(I+1),1)
VT=(VEL(RU(I+1),2)-VEL(LU(I+1),2))*
*   CIT+VEL(LU(I+1),2)

```

```

VB=(VEL(RL(I+1),2)-VEL(LL(I+1),2))*
*   CIB+VEL(LL(I+1),2)

```

```

UHORIZ=(UR-UL)*CIP+UL
UVERT =(UT-UB)*CI +UB
U(IVI,I+1)=(UHORIZ+UVERT)/2

```

```

VHORIZ=(VR-VL)*CIP+VL
VVERT =(VT-VB)*CI +VB
V(IVI,I+1)=(VHORIZ+VVERT)/2

```

```

ENDIF

```

```

C   This is the case when the mesh is in the exit
C   vertical section of the duct

```

```

IF (y(IVI,I+1).LT.0.0) THEN

```

```

  YR=y(IVI,I+1)
  YL=y(IVI,I+1)
  XT=x(IVI,I+1)
  XB=x(IVI,I+1)
  XL=POS(LU(I+1),1)
  XR=POS(RU(I+1),1)
  YT=POS(LU(I+1),2)
  YB=POS(LL(I+1),2)

```

```

  CIV=(YL-POS(LL(I+1),2))/(POS(LU(I+1),2)
*    -POS(LL(I+1),2))
  CIH=(XT-POS(LU(I+1),1))/(POS(RU(I+1),1)
*    -POS(LU(I+1),1))

```

```

  UL=(VEL(LU(I+1),1)-VEL(LL(I+1),1))*CIV+
*    VEL(LL(I+1),1)
  UR=(VEL(RU(I+1),1)-VEL(RL(I+1),1))*CIV+
*    VEL(RL(I+1),1)

```

```

  VL=(VEL(LU(I+1),2)-VEL(LL(I+1),2))*CIV+
*    VEL(LL(I+1),2)
  VR=(VEL(RU(I+1),2)-VEL(RL(I+1),2))*CIV+
*    VEL(RL(I+1),2)

```

```

  UT=(VEL(RU(I+1),1)-VEL(LU(I+1),1))*CIH+
*    VEL(LU(I+1),1)
  UB=(VEL(RL(I+1),1)-VEL(LL(I+1),1))*CIH+
*    VEL(LL(I+1),1)

```

```

  VT=(VEL(RU(I+1),2)-VEL(LU(I+1),2))*CIH+
*    VEL(LU(I+1),2)
  VB=(VEL(RL(I+1),2)-VEL(LL(I+1),2))*CIH+
*    VEL(LL(I+1),2)

```

```

  UHORIZ=(UR-UL)*CIH+UL
  UVERT =(UT-UB)*CIH+UB

```

```

      U(IVI, I+1) = (UHORIZ+UVERT) / 2

      VHORIZ = (VR-VL) * CIH + VL
      VVERT = (VT-VB) * CIV + VB
      V(IVI, I+1) = (VHORIZ+VVERT) / 2

    ENDIF

    IF (Y(IVI, I+1).EQ.0.0) THEN
      CIH = (X(IVI, I+1) - POS(LEFTN, 1)) / (POS(RIGHTN, 1)
*        - POS(LEFTN, 1))
      U(IVI, I+1) = (VEL(RIGHTN, 1) - VEL(LEFTN, 1)) * CIH +
*        VEL(LEFTN, 1)
      V(IVI, I+1) = (VEL(RIGHTN, 2) - VEL(LEFTN, 2)) * CIH +
*        VEL(LEFTN, 2)
    ENDIF

C      dT is a variable; it is defined by the equation
C      dT=dx/Up, where Up is the velocity of the particle
C      in the u-direction and dx is the change in the
C      x-position. If dT is equal to zero, then dT=dy/Vp
C      is used.
C
C      DIVIDER is a number used to adjust the value of dT
C      so that the number of iterations will converge to
C      a certain value (in this analysis, 2000-3000
C      iterations were desired).

      dT = ABS((X(IVI, I+1) - X(IVI, I)) / (U(IVI, I+1)))

      IF (dT.EQ.0.0) THEN
        dT = ABS((Y(IVI, I+1) - Y(IVI, I)) / (V(IVI, I+1)))
      ENDIF

      dT = dT / DIVIDER

C      Adjust these statements if number of iterations are
C      too small or too large
C
C      Smaller dTmax gives more iterations
C      Smaller dTmin gives more iterations

      dTmax = 0.1
      IF (dT.GT. dTmax)      dT = dTmax
      dTmin = 0.005
      IF (dT.LT. dTmin)      dT = dTmin

C      Since the particles which initially have a greater
C      y-value than their previous counterparts should not
C      land at a location further downstream than the
C      previous particle, the program will stop when this
C      occurs; usually at the top portion of particles,
C      section 25....the particle is assumed to be

```

C deposited if the radius is greater than 3.98 (less  
C than 4.0 due to round-off errors)

```

dTtotal=dTtotal+dT
IF (IVI.GT.1) THEN
IF (xFINAL.EQ.0.0.AND.yFINAL.EQ.0.0) THEN
    PRINT *, 'xFINAL=yFINAL=0.0'
    PRINT *, 'Enter the values of the previous '
    PRINT *, 'particles final positions, particle #'
    PRINT *, ' ', IVI-1
    PRINT *, 'xFINAL for particle ', IVI-1, ' ='
    READ *, xFINAL
    PRINT *, 'yFINAL for particle ', IVI-1, ' ='
    READ *, yFINAL
ENDIF
ENDIF

zFINAL=SQRT(xFINAL**2+yFINAL**2)
IF (IVI.NE.1) THEN
IF (IVI.GT.50.AND.yFINAL.GT.0.0.AND.zFINAL.GT.
*   3.98) THEN
IF (x(IVI, I+1).GT.xFINAL.OR.y(IVI, I+1).LT.yFINAL)
*   THEN
IF (Z(IVI, I+1).GT.3.98.AND.y(IVI, I+1).GT.0.0.AND.I.
*   GT.0) THEN

IF (IPRINT.EQ.1) THEN
    PRINT *, ' -----'
    PRINT *, 'Particle # ', IVI, ' has been deposited'
    PRINT *, 'by default'
    PRINT *, 'xFINAL=', xFINAL, '      yFINAL=', yFINAL
ENDIF

IF (xFINAL.EQ.0.0.AND.yFINAL.EQ.0.0) THEN
    PRINT *, 'START AT A DIFFERENT SECTION'
    PRINT *, 'BECAUSE xFINAL=yFINAL=0.0'
    GOTO 237
ENDIF

x(IVI, I+1)=x(IVI, I)
y(IVI, I+1)=y(IVI, I)
z(IVI, I+1)=z(IVI, I)

IF (IPRINT.EQ.1) THEN
    PRINT *, ' -----'
ENDIF

GOTO 23

ENDIF
ENDIF
ENDIF
ENDIF

```

C Here the program checks if the number of iterations  
 C (I) are more than a preset maximum limit (currently  
 C at 3000). If this occurs during the first run, the  
 C program decreases the value of DIVIDER, thereby  
 C decreasing the number of iterations, since dT is  
 C proportional to 1/DIVIDER, and larger dT gives less  
 C iterations.

```
IF (I.GT.3000) THEN
IF (IPRINT.EQ.1) THEN
  PRINT *, 'Iterations>3000...Go for another round!'
  PRINT *, 'Reanalyzing Particle Number ',IVI
  PRINT *, 'Iterations (I) were ',I
  PRINT *, 'Current positions are:x=',x(IVI,I+1)
  PRINT *, '                                y=',y(IVI,I+1)
  PRINT *, '                                z=',z(IVI,I+1)
  PRINT *, 'dT=',dT
  PRINT *, ' '
ENDIF
```

```
IF (JJJJ.EQ.1) THEN
  PRINT *, ' '
  PRINT *, ' '
  PRINT *, 'TOO MANY ITERATIONS!!!!'
  PRINT *, 'DIVIDER=',DIVIDER
  PRINT *, 'Decrease DINCRE; DINCRE=',DINCRE
  PRINT *, 'I=',I
  PRINT *, 'dTavg=',dTtotal/I
  GOTO 237
ELSE
  DIVIDER=DIVIDER-0.05
  IF (DIVIDER.LT.0.49) THEN
    PRINT *, 'DIVIDER TOO LOW!'
    GOTO 237
  ENDIF
  PRINT *, 'DIVIDER=',DIVIDER, ' >3000...REDO!!'
  *      dTavg=',dTtotal/I
  GOTO 67
ENDIF
```

```
IF(IPRINT.EQ.1) THEN
  PRINT *, '- - - - -'
  PRINT *, ' '
ENDIF
```

C This statement checks that x is always greater than  
 C 0.0, since at the entrance x=0.0 and the particle  
 C must move forward to make sense physically

```
IF (x(IVI,I+1).LT.0.0) THEN
  PRINT *, 'ERROR!!! x is less than zero'
  GOTO 237
```

```

ENDIF

ENDIF

12    CONTINUE

C      After the particle has been deposited or exits the
C      duct, this loop checks if the number of iterations
C      are less than a preset amount (currently set at
C      2000). If this is the case, then the value of the
C      variable DIVIDER must be increased so that dT
C      (proportional to 1/DIVIDER) will be decreased and
C      the number of iterations will therefore be
C      increased. DIVIDER is increased by an amount
C      DINCRE, which has a smaller and smaller value as
C      the number of iterations become closer and closer
C      to the preset minimum (2000 in this case).
C
C      dTavg is the average value of dT throughout the
C      analysis
C

23    IF (I.LT.2000) THEN
      dTavg=dTtotal/I
986   PRINT *, 'I=', I, ' DIVIDER=', DIVIDER, ' PART#', IVI,
*      ' dTavg=', dTavg
51    IF (IPRINT.EQ.1) THEN
      PRINT *, 'Iterations<2000...Trying Again!'
      PRINT *, 'Iterations (I) were ', I
      PRINT *, 'Reanalyzing Particle Number ', IVI
    ENDIF

      JJJJ=1

C      Since  $dT=dT/DIVIDER$ , to increase the number of
C      iterations, DINCRE should be increased; to decrease
C      the number of iterations, DINCRE should be decreased
C      ( $DIVIDER=DIVIDER+DINCRE$ )

      IF (I.GE.0)          DINCRE=0.01
      IF (I.GE.50)         DINCRE=0.005
      IF (I.GE.90)         DINCRE=0.003
      IF (I.GE.500)        DINCRE=0.001
      IF (I.GE.800)        DINCRE=0.00005
      IF (I.GE.1200)       DINCRE=0.00002
      IF (I.GE.1800)       DINCRE=0.00001

      DIVIDER=DIVIDER+DINCRE

      IF (IPRINT.EQ.1) THEN
        PRINT *, 'Current positions are: x=', x(IVI, I+1)
        PRINT *, ' y=', y(IVI, I+1)
        PRINT *, ' z=', z(IVI, I+1)

```

```

        PRINT *, '                for particle # ', IVI
        PRINT *, '                                dTavg=', dTavg
        PRINT *, 'NEW DIVIDER=', DIVIDER, '      I=', I
        PRINT *, ' - - - - - '
        PRINT *, ' '
    ENDIF

GOTO 67

ENDIF

C      This loop checks to see if the particle has landed
C      further downstream than its predecessor. This may
C      occur when the values of dTavg for two consecutive
C      particles differ by a very large amount. The
C      program is terminated at this point when this
C      occurs, and the values of dT must be checked.

    IF (IVI.GT.1) THEN
    IF (x(IVI,I+1).GT.xFINAL.OR.y(IVI,I+1).LT.yFINAL) THEN
    IF (x(IVI,I+1).LT.4.0) THEN
    IF (y(IVI,I+1).GT.-2.0) THEN
        PRINT *, ' '
        PRINT *, '***Must reanalyze because the particle'
        PRINT *, '***landed further downstream than its*'
        PRINT *, '***predecessor*****'
        PRINT *, ' '
        zFINAL=SQRT((xFINAL**2)+(yFINAL**2))
        PRINT *, 'PREDECESSORS LOCATION (FINAL): '
        PRINT *, '                xpred=', xFINAL
        PRINT *, '                ypred=', yFINAL
        PRINT *, '                zpred=', zFINAL
        PRINT *, 'Current particles location:'
        PRINT *, '                xcurrent=', x(IVI,I+1)
        PRINT *, '                ycurrent=', y(IVI,I+1)
        PRINT *, '                zcurrent=', z(IVI,I+1)
        PRINT *, '                I=', I
        PRINT *, ' '
        PRINT *, 'TERMINATING PROGRAM!!!!'
        PRINT *, ' '
        PRINT *, 'Particle was further downstream'
        PRINT *, 'than its predecessor....END!!'
        GOTO 237
    ENDIF
    ENDIF
    ENDIF
    ENDIF

dTavg=dTtotal/I

C      Here the output is written to the data files which
C      will be later analyzed by the program
C      "particlesout.f".

```



```

WRITE (FILEA,*) x(IVI,0)
WRITE (FILEA,*) y(IVI,0)
WRITE (FILEA,*) U(IVI,0)
WRITE (FILEA,*) V(IVI,0)
WRITE (FILEA,*) x(IVI,I+1)
WRITE (FILEA,*) y(IVI,I+1)
zFINAL=SQRT((xFINAL**2)+(yFINAL**2))
PRINT *,I+1,' Equations Solved for particle ',IVI
PRINT *,'The final positions are:   x=',x(IVI,I+1)
PRINT *,'                               y=',y(IVI,I+1)
PRINT *,'                               z=',z(IVI,I+1)
PRINT *,'                               DIVIDER=',DIVIDER
PRINT *,'                               dTavg=',dTavg
WRITE (FILEA,*) (I+1)

IF (y(IVI,I+1).GE.-2.0) THEN
  PRINT *,' '
  PRINT *,'*****D E P O S I T E D*****'
  PRINT *,' '
ENDIF
xFINAL=x(IVI,I+1)
yFINAL=y(IVI,I+1)
IF (x(IVI,I+1).LT.0.0) THEN
  PRINT *,'ERROR!!!  x is less than zero'
  GOTO 237
ENDIF

114  CONTINUE

283  CONTINUE

100  FORMAT (E12.4,5X,E12.4,5X,E12.4,5X,E12.4)
101  FORMAT (/,'x(I)',15X,'A(I)',15X,'y(I)',15X,'B(I)')
102  FORMAT (80(' '))
103  FORMAT (4(E12.4,5X))
104  FORMAT (/)
105  FORMAT (80(' '))
106  FORMAT (/,'ULU',15X,'ULL',15X,'URU',15X,'URL')
107  FORMAT (/,'VLU',15X,'VLL',15X,'VRU',15X,'VRL')
108  FORMAT (/,'UFINAL',15X,'VFINAL')
110  FORMAT (E12.4,4X,E12.4,5X,E12.4,5X,I5)
111  FORMAT (/,'PARTICLE #',X,'XINIT',11X,'YINIT',
*      17X,'UINIT',12X,'VINIT',10X,'XFINAL',5X,
*      'YFINAL')
112  FORMAT (/,'I',5X,'LEFT UPPER',4X,'RIGHT UPPER',
*      4X,'LEFT LOWER',4X,'RIGHT LOWER')
199  FORMAT (I4,3X,E12.4,3X,E12.4,3X,E12.4,3X,E12.4,
*      3X,E12.4)
285  FORMAT (5(/))
512  FORMAT (I4,3X,E6.4,3X,E6.4,3X,E6.4,3X,E6.4,3X,
*      E6.4,3X,E6.4)

237  END

```

# APPENDIX H

PROGRAM "particlesout.f" WITH OUTPUT "particles.output"

```

C
C   Program "particlesout.f"
C
C   written by Pantaleo Loiacono
C               February 1996
C
C   This program analyzes the output from the program
C   "particles.f"; it determines the particle
C   deposition percentage in a 90 degree duct bend.
C
C   DIMENSION NP(1000),PI(1000,2),VI(1000,2),PF(1000,2)
C   DIMENSION ITN(2000),Z(1000),DEPOSIT(100),DEP(100)
C   DIMENSION PHIP(150),PDEP(100),REALDEP(100)
C   REAL PIE
C
C   OPEN (UNIT=8,FILE='particles.output',STATUS='OLD')
C   OPEN (UNIT=457,FILE='particles1.out',STATUS='OLD')
C   OPEN (UNIT=458,FILE='particles2.out',STATUS='OLD')
C   OPEN (UNIT=459,FILE='particles3.out',STATUS='OLD')
C   OPEN (UNIT=460,FILE='particles4.out',STATUS='OLD')
C   OPEN (UNIT=461,FILE='particles5.out',STATUS='OLD')
C   OPEN (UNIT=462,FILE='particles6.out',STATUS='OLD')
C   OPEN (UNIT=463,FILE='particles7.out',STATUS='OLD')
C   OPEN (UNIT=464,FILE='particles8.out',STATUS='OLD')
C   OPEN (UNIT=465,FILE='particles9.out',STATUS='OLD')
C   OPEN (UNIT=466,FILE='particles10.out',STATUS='OLD')
C   OPEN (UNIT=467,FILE='particles11.out',STATUS='OLD')
C   OPEN (UNIT=468,FILE='particles12.out',STATUS='OLD')
C   OPEN (UNIT=469,FILE='particles13.out',STATUS='OLD')
C   OPEN (UNIT=470,FILE='particles14.out',STATUS='OLD')
C   OPEN (UNIT=471,FILE='particles15.out',STATUS='OLD')
C   OPEN (UNIT=472,FILE='particles16.out',STATUS='OLD')
C   OPEN (UNIT=473,FILE='particles17.out',STATUS='OLD')
C   OPEN (UNIT=474,FILE='particles18.out',STATUS='OLD')
C   OPEN (UNIT=475,FILE='particles19.out',STATUS='OLD')
C   OPEN (UNIT=476,FILE='particles20.out',STATUS='OLD')
C   OPEN (UNIT=477,FILE='particles21.out',STATUS='OLD')
C   OPEN (UNIT=478,FILE='particles22.out',STATUS='OLD')
C   OPEN (UNIT=479,FILE='particles23.out',STATUS='OLD')
C   OPEN (UNIT=480,FILE='particles24.out',STATUS='OLD')
C   OPEN (UNIT=481,FILE='particles25.out',STATUS='OLD')
C   OPEN (UNIT=45,FILE='particles.info',STATUS='OLD')
C
C   PIE=3.14159265359
C
C   * * * * * D A T A   A N A L Y S I S   * * * * *
C   Here the Values of the initial conditions and the

```

C final positions are put into arrays...Dependent on  
C Divisions

READ (45,\*) S,G,NPART,DIVIDE,dT

```
DO 509 ISECTN=1,DIVIDE
  SECTION=ISECTN
  IF (SECTION.EQ.1) THEN
    ST=1
    MU=1
    FILEA=457
  ELSEIF (SECTION.EQ.2) THEN
    ST=NPART/DIVIDE+1
    MU=2
    FILEA=458
  ELSEIF (SECTION.EQ.3) THEN
    ST=2*NPART/DIVIDE+1
    MU=3
    FILEA=459
  ELSEIF (SECTION.EQ.4) THEN
    ST=3*NPART/DIVIDE+1
    MU=4
    FILEA=460
  ELSEIF (SECTION.EQ.5) THEN
    ST=4*NPART/DIVIDE+1
    MU=5
    FILEA=461
  ELSEIF (SECTION.EQ.6) THEN
    ST=5*NPART/DIVIDE+1
    MU=6
    FILEA=462
  ELSEIF (SECTION.EQ.7) THEN
    ST=6*NPART/DIVIDE+1
    MU=7
    FILEA=463
  ELSEIF (SECTION.EQ.8) THEN
    ST=7*NPART/DIVIDE+1
    MU=8
    FILEA=464
  ELSEIF (SECTION.EQ.9) THEN
    ST=8*NPART/DIVIDE+1
    MU=9
    FILEA=465
  ELSEIF (SECTION.EQ.10) THEN
    ST=9*NPART/DIVIDE+1
    MU=10
    FILEA=466
  ELSEIF (SECTION.EQ.11) THEN
    ST=10*NPART/DIVIDE+1
    MU=11
    FILEA=467
  ELSEIF (SECTION.EQ.12) THEN
    ST=11*NPART/DIVIDE+1
```

```
MU=12
FILEA=468
ELSEIF (SECTION.EQ.13) THEN
  ST=12*NPART/DIVIDE+1
  MU=13
  FILEA=469
ELSEIF (SECTION.EQ.14) THEN
  ST=13*NPART/DIVIDE+1
  MU=14
  FILEA=470
ELSEIF (SECTION.EQ.15) THEN
  ST=14*NPART/DIVIDE+1
  MU=15
  FILEA=471
ELSEIF (SECTION.EQ.16) THEN
  ST=15*NPART/DIVIDE+1
  MU=16
  FILEA=472
ELSEIF (SECTION.EQ.17) THEN
  ST=16*NPART/DIVIDE+1
  MU=17
  FILEA=473
ELSEIF (SECTION.EQ.18) THEN
  ST=17*NPART/DIVIDE+1
  MU=18
  FILEA=474
ELSEIF (SECTION.EQ.19) THEN
  ST=18*NPART/DIVIDE+1
  MU=19
  FILEA=475
ELSEIF (SECTION.EQ.20) THEN
  ST=19*NPART/DIVIDE+1
  MU=20
  FILEA=476
ELSEIF (SECTION.EQ.21) THEN
  ST=20*NPART/DIVIDE+1
  MU=21
  FILEA=477
ELSEIF (SECTION.EQ.22) THEN
  ST=21*NPART/DIVIDE+1
  MU=22
  FILEA=478
ELSEIF (SECTION.EQ.23) THEN
  ST=22*NPART/DIVIDE+1
  MU=23
  FILEA=479
ELSEIF (SECTION.EQ.24) THEN
  ST=23*NPART/DIVIDE+1
  MU=24
  FILEA=480
ELSEIF (SECTION.EQ.25) THEN
  ST=24*NPART/DIVIDE+1
  MU=25
```

```

        FILEA=481
      ELSE
        PRINT *, 'ERROR, NO SECTION # SPECIFIED'
        GOTO 237

      ENDIF

C      Read in all of the data; node point, initial
C      positions, initial velocities, final positions,
C      and number of iterations required to perform the
C      particle's analysis.

      DO 510 IREAD=ST,MU*NPART/DIVIDE
        READ (FILEA,*) NP(IREAD)
        READ (FILEA,*) (PI(IREAD,J), J=1,2)
        READ (FILEA,*) (VI(IREAD,J), J=1,2)
        READ (FILEA,*) (PF(IREAD,J), J=1,2)
        READ (FILEA,*) ITN(IREAD)
510    CONTINUE

509    CONTINUE

      WRITE (8,*) 'S=',S,'      G=',G,'      NPART=',NPART
      WRITE (8,*) 'DIVIDE=',DIVIDE,
      WRITE (8,190)
      WRITE (8,105)

      DO 511 IJ=1,NPART
        WRITE (8,200) NP(IJ),PI(IJ,1),PI(IJ,2),
*                VI(IJ,1),VI(IJ,2)
511    CONTINUE

      WRITE (8,104)
      WRITE (8,195)
      WRITE (8,105)

C      Determine the final radius of the particles;
C      particles which have exited the duct will have a
C      final radius of zero

      DO 581 IK=1,NPART
        IF (PF(IK,2).GE.-2.0) THEN
          Z(IK)=SQRT(PF(IK,1)**2+PF(IK,2)**2)
        ELSE
          Z(IK)=0.0
        ENDIF

        WRITE (8,210) NP(IK),ITN(IK),PF(IK,1),
*                PF(IK,2),Z(IK)
581    CONTINUE

C      NOMB is the number of sections in which the
C      circular 90 degree portion of the domain is broken

```

C up into to analyze particle deposition.

```
IPARDEP=0
IL=1
NOMB=16
NN=0
```

C This section of the program examines the curve of  
 C the duct...it consists of 16 pieces. The curved  
 C portion of the duct is split into 16 regions such  
 C that there are 90 degrees/16 or 5.63 degrees  
 C (0.982 rad) in each section of this analysis.  
 C Loop 300 computes the value of PHI based on the  
 C value of JANG; PHI starts out at 90-5.63 degrees.  
 C If PHIP (the value of the particle's angle) is  
 C greater than or equal to PHI, and the particle is  
 C deposited in the 90 degree region, then the  
 C particle is considered to be deposited in that  
 C section. The analysis is continued, decreasing the  
 C value of PHI until it gets to 0.0 degrees.

```
DO 300 JANG=1,NOMB
    IPARDEP=0
    LAST=101

    DO 582 IK=1,NPART
        PHIP(IK)=ATAN(PF(IK,2)/PF(IK,1))
        PHI=PIE/2.0-(PIE/2.0)*(JANG/16.0)

        IF (Z(IK).GT.0.0.AND.PHIP(IK).GE.PHI.AND.
*         PF(IK,2).GE.0.0) THEN
            IPARDEP=IPARDEP+1
            IF (IK.LT.LAST) LAST=IK-1
        ENDIF
    CONTINUE
582
```

C IPARDEP is the total number of particles deposited  
 C in a particular section of the duct. The  
 C deposition is equal to the total number of  
 C particles deposited divided by the total number of  
 C particles at the entrance region times 100.

```
DEPOSIT(IL)=(IPARDEP*100.0/NPART)
DEP(IL)=DEPOSIT(IL)
```

C REALDEP is the deposit amount at that particular  
 C section number...  
 C DEPOSIT is the total deposit amount to this point  
 C (this section and previous sections)

```
IF (LAST.EQ.101) THEN
    LAST=0
```

```

      GOTO 57
ENDIF

```

```

C      A particle can be semi-deposited...that is, if
C      particle 26 is deposited in this section, then
C      particle 25 is semi-deposited in this section,
C      although it's not completely in this section as
C      well. This is found through interpolation and
C      becomes very useful in predicting deposition when
C      the number of particles is increased significantly
C      (e.g. NPART=1000+). EXTRA is the extra portion of
C      deposition in a particular section. It is based
C      upon the last particle's position deposited, (LAST).

```

```

57      EXTRA=(PHIP(LAST+1)-PHI)/(PHIP(LAST+1)-PHIP(LAST))
      IF(JANG.EQ.NOMB) THEN
          AMS=PHIP(LAST+1)-PHI
          EXTRA=AMS/(AMS+ABS(PF(LAST,2)))
          IF (PF(LAST,2).LT.-2.0) EXTRA=0.0
      ENDIF

```

```

      IF (DEP(IL).EQ.100.0) EXTRA=0.0
      IF (DEPOSIT(IL-1).GT.99.0) EXTRA=0.0
      IF (IPARDEP.EQ.0) EXTRA=0.0
      IF (PF(LAST,2).LT.-2.0) EXTRA=0.0
      IF (LAST.EQ.0) EXTRA=0.0
      IF (DEP(IL).EQ.0.0) EXTRA=0.0

```

```

      REALDEP(IL)=DEPOSIT(IL)-DEP(IL-1)+EXTRA
      DEPOSIT(IL)=DEPOSIT(IL)+EXTRA
      PRINT *, 'DEPOSIT(', IL, ') = ', DEPOSIT(IL), '%'
      PDEP(IL)=DEPOSIT(IL)
      IL=IL+1

```

```

300      CONTINUE

```

```

C      This part of the program examines the straight
C      section of the duct, consisting of 5 pieces.

```

```

      DO 310 JSTR=1,5
          LAST=101
          IPARDEP=0
          STRSECT=-(0.4)*JSTR

```

```

C      A particle is considered deposited when its radius
C      is greater than 0.0, and its final y-value is
C      between 0.0 and the value of STRSECT

```

```

          DO 583 KI=1,NPART
              IF (Z(KI).GT.0.0.AND.PF(KI,2).LT.0.0.AND
*                  .PF(KI,2).GT.STRSECT) THEN
                  IPARDEP=IPARDEP+1

```

```

                                IF (KI.LT.LAST) LAST=KI-1
                                ENDIF

583      CONTINUE

                                IF (LAST.EQ.101) LAST=0
                                IF (IL-1.EQ.NOMB) THEN
                                    DEPOSIT(IL-1)=DEPOSIT(IL-1)-EXTRA
                                ENDIF
                                EXTRA=ABS((STRSECT-PF(LAST+1,2))
*                                     /ABS(PF(LAST,2)-PF(LAST+1,2)))
                                DEPOSIT(IL)=(IPARDEP*100.0/NPART)+
*                                     DEPOSIT(NOMB)
                                DEP(IL)=DEPOSIT(IL)

                                IF (DEP(IL).EQ.100.0) EXTRA=0.0
                                IF (IPARDEP.EQ.0) EXTRA=0.0
                                IF (JSTR.EQ.5) EXTRA=0.0
                                IF (PF(LAST,2).LT.-2.0) EXTRA=0.0

C      REALDEP is the deposit amount at that particular
C      section number...DEPOSIT is the total deposit
C      amount to this point (this section and previous
C      sections)

                                REALDEP(IL)=DEPOSIT(IL)-DEP(IL-1)+EXTRA
                                DEPOSIT(IL)=DEPOSIT(IL)+EXTRA
                                PRINT *, 'DEPOSIT(', IL, ') = ', DEPOSIT(IL), ' %'
                                PDEP(IL)=DEPOSIT(IL)
                                IL=IL+1

310      CONTINUE

                                DEPOSIT(16)=PDEP(16)
                                WRITE (8,104)
                                TOTAL=0.0
                                WRITE (8,544)
                                WRITE (8,105)
                                WRITE (8,*) ' '

                                DO 400 IPR=1,IL-1
                                    WRITE (8,543) IPR,REALDEP(IPR),DEPOSIT(IPR)
400      CONTINUE

                                III=NPART/100*(DEPOSIT(16)-EXTRA)
                                WRITE (8,104)
                                WRITE (8,*) 'Total particles deposited'
                                WRITE (8,*) 'were ',III,' particles'
                                WRITE (8,*) ' or ',DEPOSIT(21),' %'

104      FORMAT (3(/))
105      FORMAT (70(' _'))

```



```
190  FORMAT (/,'PARTICLE #',3X,'XINIT',12X,'YINIT',12X,  
*      'UINIT',12X,'VINIT')  
195  FORMAT (/,'PARTICLE #',5X,'ITERATIONS',5X,'XFINAL',  
*      10X,'YFINAL',12X,'Z (IF APPLICABLE)')  
200  FORMAT (I5,5X,E12.4,5X,E12.4,5X,E12.4,5X,E12.4)  
210  FORMAT (I5,10X,I5,5X,E12.4,5X,E12.4,5X,5X,E12.4)  
543  FORMAT (I3,10X,E12.5,10X,E12.5)  
544  FORMAT (/,'LOCATION',5X,'DEP % HERE ONLY',9X,  
*      'TOTAL DEPOSIT %')  
  
237  END
```

```
*****END OF PROGRAM "particlesout.f"*****
```

\*\*\*Typical output from the program "particlesout.f"\*\*\*

S= 5.00000 G= 0.0 NPART= 100  
DIVIDE= 25.0000

PART#	XINIT	YINIT	UNIT	VINIT
1	0.0000E+00	0.2020E+01	0.5882E-01	0.0000E+00
2	0.0000E+00	0.2040E+01	0.1165E+00	0.0000E+00
3	0.0000E+00	0.2059E+01	0.1729E+00	0.0000E+00
4	0.0000E+00	0.2079E+01	0.2282E+00	0.0000E+00
5	0.0000E+00	0.2099E+01	0.2823E+00	0.0000E+00
6	0.0000E+00	0.2119E+01	0.3353E+00	0.0000E+00
7	0.0000E+00	0.2139E+01	0.3870E+00	0.0000E+00
8	0.0000E+00	0.2158E+01	0.4376E+00	0.0000E+00
9	0.0000E+00	0.2178E+01	0.4870E+00	0.0000E+00
10	0.0000E+00	0.2198E+01	0.5352E+00	0.0000E+00
11	0.0000E+00	0.2218E+01	0.5823E+00	0.0000E+00
12	0.0000E+00	0.2238E+01	0.6282E+00	0.0000E+00
13	0.0000E+00	0.2257E+01	0.6729E+00	0.0000E+00
14	0.0000E+00	0.2277E+01	0.7164E+00	0.0000E+00
15	0.0000E+00	0.2297E+01	0.7587E+00	0.0000E+00
16	0.0000E+00	0.2317E+01	0.7999E+00	0.0000E+00
17	0.0000E+00	0.2337E+01	0.8399E+00	0.0000E+00
18	0.0000E+00	0.2356E+01	0.8787E+00	0.0000E+00
19	0.0000E+00	0.2376E+01	0.9164E+00	0.0000E+00
20	0.0000E+00	0.2396E+01	0.9528E+00	0.0000E+00
21	0.0000E+00	0.2416E+01	0.9881E+00	0.0000E+00
22	0.0000E+00	0.2436E+01	0.1022E+01	0.0000E+00
23	0.0000E+00	0.2455E+01	0.1055E+01	0.0000E+00
24	0.0000E+00	0.2475E+01	0.1087E+01	0.0000E+00
25	0.0000E+00	0.2495E+01	0.1118E+01	0.0000E+00
26	0.0000E+00	0.2515E+01	0.1147E+01	0.0000E+00
27	0.0000E+00	0.2535E+01	0.1175E+01	0.0000E+00
28	0.0000E+00	0.2554E+01	0.1202E+01	0.0000E+00
29	0.0000E+00	0.2574E+01	0.1228E+01	0.0000E+00
30	0.0000E+00	0.2594E+01	0.1253E+01	0.0000E+00
31	0.0000E+00	0.2614E+01	0.1276E+01	0.0000E+00
32	0.0000E+00	0.2634E+01	0.1299E+01	0.0000E+00
33	0.0000E+00	0.2653E+01	0.1320E+01	0.0000E+00
34	0.0000E+00	0.2673E+01	0.1340E+01	0.0000E+00
35	0.0000E+00	0.2693E+01	0.1359E+01	0.0000E+00
36	0.0000E+00	0.2713E+01	0.1376E+01	0.0000E+00
37	0.0000E+00	0.2733E+01	0.1393E+01	0.0000E+00
38	0.0000E+00	0.2752E+01	0.1408E+01	0.0000E+00
39	0.0000E+00	0.2772E+01	0.1422E+01	0.0000E+00
40	0.0000E+00	0.2792E+01	0.1435E+01	0.0000E+00
41	0.0000E+00	0.2812E+01	0.1447E+01	0.0000E+00
42	0.0000E+00	0.2832E+01	0.1457E+01	0.0000E+00
43	0.0000E+00	0.2851E+01	0.1467E+01	0.0000E+00
44	0.0000E+00	0.2871E+01	0.1475E+01	0.0000E+00

45	0.0000E+00	0.2891E+01	0.1482E+01	0.0000E+00
46	0.0000E+00	0.2911E+01	0.1488E+01	0.0000E+00
47	0.0000E+00	0.2931E+01	0.1493E+01	0.0000E+00
48	0.0000E+00	0.2950E+01	0.1496E+01	0.0000E+00
49	0.0000E+00	0.2970E+01	0.1499E+01	0.0000E+00
50	0.0000E+00	0.2990E+01	0.1500E+01	0.0000E+00
51	0.0000E+00	0.3010E+01	0.1500E+01	0.0000E+00
52	0.0000E+00	0.3030E+01	0.1499E+01	0.0000E+00
53	0.0000E+00	0.3049E+01	0.1496E+01	0.0000E+00
54	0.0000E+00	0.3069E+01	0.1493E+01	0.0000E+00
55	0.0000E+00	0.3089E+01	0.1488E+01	0.0000E+00
56	0.0000E+00	0.3109E+01	0.1482E+01	0.0000E+00
57	0.0000E+00	0.3129E+01	0.1475E+01	0.0000E+00
58	0.0000E+00	0.3149E+01	0.1467E+01	0.0000E+00
59	0.0000E+00	0.3168E+01	0.1457E+01	0.0000E+00
60	0.0000E+00	0.3188E+01	0.1447E+01	0.0000E+00
61	0.0000E+00	0.3208E+01	0.1435E+01	0.0000E+00
62	0.0000E+00	0.3228E+01	0.1422E+01	0.0000E+00
63	0.0000E+00	0.3248E+01	0.1408E+01	0.0000E+00
64	0.0000E+00	0.3267E+01	0.1393E+01	0.0000E+00
65	0.0000E+00	0.3287E+01	0.1376E+01	0.0000E+00
66	0.0000E+00	0.3307E+01	0.1359E+01	0.0000E+00
67	0.0000E+00	0.3327E+01	0.1340E+01	0.0000E+00
68	0.0000E+00	0.3347E+01	0.1320E+01	0.0000E+00
69	0.0000E+00	0.3366E+01	0.1299E+01	0.0000E+00
70	0.0000E+00	0.3386E+01	0.1276E+01	0.0000E+00
71	0.0000E+00	0.3406E+01	0.1253E+01	0.0000E+00
72	0.0000E+00	0.3426E+01	0.1228E+01	0.0000E+00
73	0.0000E+00	0.3446E+01	0.1202E+01	0.0000E+00
74	0.0000E+00	0.3465E+01	0.1175E+01	0.0000E+00
75	0.0000E+00	0.3485E+01	0.1147E+01	0.0000E+00
76	0.0000E+00	0.3505E+01	0.1118E+01	0.0000E+00
77	0.0000E+00	0.3525E+01	0.1087E+01	0.0000E+00
78	0.0000E+00	0.3545E+01	0.1055E+01	0.0000E+00
79	0.0000E+00	0.3564E+01	0.1022E+01	0.0000E+00
80	0.0000E+00	0.3584E+01	0.9881E+00	0.0000E+00
81	0.0000E+00	0.3604E+01	0.9528E+00	0.0000E+00
82	0.0000E+00	0.3624E+01	0.9164E+00	0.0000E+00
83	0.0000E+00	0.3644E+01	0.8787E+00	0.0000E+00
84	0.0000E+00	0.3663E+01	0.8399E+00	0.0000E+00
85	0.0000E+00	0.3683E+01	0.7999E+00	0.0000E+00
86	0.0000E+00	0.3703E+01	0.7588E+00	0.0000E+00
87	0.0000E+00	0.3723E+01	0.7164E+00	0.0000E+00
88	0.0000E+00	0.3743E+01	0.6729E+00	0.0000E+00
89	0.0000E+00	0.3762E+01	0.6282E+00	0.0000E+00
90	0.0000E+00	0.3782E+01	0.5823E+00	0.0000E+00
91	0.0000E+00	0.3802E+01	0.5352E+00	0.0000E+00
92	0.0000E+00	0.3822E+01	0.4870E+00	0.0000E+00
93	0.0000E+00	0.3842E+01	0.4376E+00	0.0000E+00
94	0.0000E+00	0.3861E+01	0.3870E+00	0.0000E+00
95	0.0000E+00	0.3881E+01	0.3353E+00	0.0000E+00
96	0.0000E+00	0.3901E+01	0.2823E+00	0.0000E+00
97	0.0000E+00	0.3921E+01	0.2282E+00	0.0000E+00

98	0.0000E+00	0.3941E+01	0.1729E+00	0.0000E+00
99	0.0000E+00	0.3960E+01	0.1165E+00	0.0000E+00
100	0.0000E+00	0.3980E+01	0.5882E-01	0.0000E+00

PART #	ITRTNS	XFINAL	YFINAL	Z (RADIUS)
1	2449	0.3669E+01	-0.2006E+01	0.0000E+00
2	2654	0.4026E+01	-0.1942E+01	0.4470E+01
3	2673	0.4017E+01	-0.1191E+01	0.4190E+01
4	2017	0.4012E+01	-0.6926E+00	0.4071E+01
5	2772	0.4017E+01	-0.3521E+00	0.4032E+01
6	2078	0.4027E+01	-0.1113E+00	0.4029E+01
7	2017	0.3991E+01	0.1646E+00	0.3995E+01
8	2065	0.3985E+01	0.3686E+00	0.4002E+01
9	2003	0.3981E+01	0.5529E+00	0.4019E+01
10	2001	0.3968E+01	0.7178E+00	0.4033E+01
11	2001	0.3923E+01	0.8899E+00	0.4022E+01
12	2004	0.3910E+01	0.1020E+01	0.4041E+01
13	2210	0.3839E+01	0.1174E+01	0.4015E+01
14	2004	0.3831E+01	0.1275E+01	0.4038E+01
15	2812	0.3782E+01	0.1389E+01	0.4029E+01
16	2003	0.3753E+01	0.1483E+01	0.4036E+01
17	2004	0.3675E+01	0.1591E+01	0.4005E+01
18	2089	0.3622E+01	0.1678E+01	0.3991E+01
19	2136	0.3619E+01	0.1737E+01	0.4014E+01
20	2742	0.3612E+01	0.1794E+01	0.4033E+01
21	2005	0.3556E+01	0.1865E+01	0.4016E+01
22	2002	0.3535E+01	0.1920E+01	0.4023E+01
23	2005	0.3510E+01	0.1973E+01	0.4027E+01
24	2004	0.3454E+01	0.2032E+01	0.4007E+01
25	2001	0.3425E+01	0.2080E+01	0.4007E+01
26	2007	0.3400E+01	0.2124E+01	0.4009E+01
27	2041	0.3358E+01	0.2170E+01	0.3998E+01
28	2028	0.3342E+01	0.2209E+01	0.4006E+01
29	2005	0.3331E+01	0.2245E+01	0.4017E+01
30	2003	0.3312E+01	0.2281E+01	0.4021E+01
31	2007	0.3263E+01	0.2322E+01	0.4005E+01
32	2003	0.3218E+01	0.2360E+01	0.3991E+01
33	2005	0.3217E+01	0.2390E+01	0.4007E+01
34	2012	0.3201E+01	0.2421E+01	0.4013E+01
35	2004	0.3200E+01	0.2449E+01	0.4030E+01
36	2001	0.3187E+01	0.2479E+01	0.4037E+01
37	2001	0.3171E+01	0.2508E+01	0.4043E+01
38	2004	0.3085E+01	0.2547E+01	0.4000E+01
39	2003	0.3053E+01	0.2577E+01	0.3995E+01
40	2030	0.3026E+01	0.2605E+01	0.3993E+01
41	2055	0.3008E+01	0.2630E+01	0.3996E+01
42	2024	0.3000E+01	0.2656E+01	0.4006E+01
43	2026	0.2960E+01	0.2684E+01	0.3996E+01
44	2091	0.2950E+01	0.2709E+01	0.4006E+01
45	2049	0.2936E+01	0.2734E+01	0.4012E+01

46	2056	0.2934E+01	0.2757E+01	0.4027E+01
47	2031	0.2871E+01	0.2787E+01	0.4001E+01
48	2014	0.2866E+01	0.2811E+01	0.4014E+01
49	1950	0.2835E+01	0.2838E+01	0.4011E+01
50	2607	0.2835E+01	0.2860E+01	0.4027E+01
51	2324	0.2799E+01	0.2886E+01	0.4020E+01
52	2022	0.2772E+01	0.2910E+01	0.4019E+01
53	1953	0.2721E+01	0.2936E+01	0.4003E+01
54	1951	0.2718E+01	0.2958E+01	0.4017E+01
55	1952	0.2715E+01	0.2980E+01	0.4031E+01
56	1950	0.2661E+01	0.3006E+01	0.4014E+01
57	1961	0.2594E+01	0.3032E+01	0.3990E+01
58	2216	0.2575E+01	0.3055E+01	0.3995E+01
59	2052	0.2569E+01	0.3076E+01	0.4008E+01
60	2006	0.2521E+01	0.3100E+01	0.3996E+01
61	1988	0.2512E+01	0.3122E+01	0.4007E+01
62	1952	0.2476E+01	0.3145E+01	0.4002E+01
63	1950	0.2431E+01	0.3169E+01	0.3994E+01
64	1951	0.2400E+01	0.3191E+01	0.3993E+01
65	1956	0.2386E+01	0.3212E+01	0.4002E+01
66	1950	0.2341E+01	0.3236E+01	0.3994E+01
67	1951	0.2305E+01	0.3258E+01	0.3991E+01
68	1952	0.2276E+01	0.3280E+01	0.3992E+01
69	2005	0.2245E+01	0.3300E+01	0.3991E+01
70	2072	0.2226E+01	0.3321E+01	0.3998E+01
71	2010	0.2221E+01	0.3342E+01	0.4012E+01
72	2002	0.2154E+01	0.3365E+01	0.3996E+01
73	2008	0.2150E+01	0.3385E+01	0.4010E+01
74	2008	0.2116E+01	0.3407E+01	0.4010E+01
75	2004	0.2076E+01	0.3429E+01	0.4009E+01
76	2002	0.2039E+01	0.3451E+01	0.4008E+01
77	2005	0.1965E+01	0.3475E+01	0.3992E+01
78	2006	0.1954E+01	0.3495E+01	0.4004E+01
79	2006	0.1936E+01	0.3515E+01	0.4013E+01
80	2007	0.1899E+01	0.3536E+01	0.4014E+01
81	2012	0.1870E+01	0.3557E+01	0.4019E+01
82	2006	0.1825E+01	0.3579E+01	0.4017E+01
83	2005	0.1765E+01	0.3601E+01	0.4010E+01
84	2694	0.1674E+01	0.3625E+01	0.3993E+01
85	2686	0.1634E+01	0.3646E+01	0.3995E+01
86	2852	0.1614E+01	0.3666E+01	0.4005E+01
87	2008	0.1580E+01	0.3686E+01	0.4011E+01
88	2433	0.1523E+01	0.3708E+01	0.4008E+01
89	2004	0.1437E+01	0.3730E+01	0.3998E+01
90	2013	0.1366E+01	0.3752E+01	0.3993E+01
91	2010	0.1312E+01	0.3773E+01	0.3995E+01
92	2026	0.1261E+01	0.3794E+01	0.3998E+01
93	2007	0.1171E+01	0.3816E+01	0.3992E+01
94	2055	0.1101E+01	0.3838E+01	0.3992E+01
95	2200	0.1033E+01	0.3858E+01	0.3994E+01
96	2284	0.9313E+00	0.3880E+01	0.3990E+01

97	2126	0.8440E+00	0.3901E+01	0.3991E+01
98	2005	0.7442E+00	0.3922E+01	0.3992E+01
99	2014	0.6147E+00	0.3943E+01	0.3990E+01
100	2263	0.4764E+00	0.3962E+01	0.3990E+01

LOCATION	DEP % HERE ONLY	TOTAL DEPOSIT %
----------	-----------------	-----------------

---

1	0.00000E+00	0.00000E+00
2	0.33455E+01	0.33455E+01
3	0.48248E+01	0.78248E+01
4	0.61952E+01	0.13195E+02
5	0.77768E+01	0.20777E+02
6	0.10632E+02	0.30632E+02
7	0.11342E+02	0.41342E+02
8	0.11052E+02	0.52052E+02
9	0.11140E+02	0.63140E+02
10	0.94445E+01	0.72444E+02
11	0.74601E+01	0.79460E+02
12	0.54920E+01	0.84492E+02
13	0.40542E+01	0.88054E+02
14	0.26058E+01	0.90606E+02
15	0.28702E+01	0.92870E+02
16	0.22703E+01	0.94270E+02
17	0.21407E+01	0.96141E+02
18	0.12155E+01	0.97215E+02
19	0.10120E+01	0.98012E+02
20	0.54461E+00	0.98545E+02
21	0.10000E+01	0.99000E+02

The total amount of particles deposited  
 was 99 particles  
 or 99.0000 %

# APPENDIX I

## PARTICLE DEPOSITION PERCENTAGE VALUES FOR FIGURE 5.2

Section #	S=0.5	S=0.66	S=1.0	S=5.0	S=10.0	S=100.0	
1	0	0	0	0	1.418	1.5307	
1.5	0.001	0.016	0.128	1.627	2.627	2.682	
2	0.002	0.021	0.364	3.345	4.058	4.352	
2.5	0.024	0.084	0.431	5.262	6.161	6.842	
3	0.049	0.098	0.584	7.824	8.665	9.126	
3.5	0.053	0.107	1.255	10.935	12.159	12.861	
4	0.057	0.134	2.256	13.195	15.08	15.767	
4.5	0.124	0.217	3.428	16.596	19.52	19.042	
5	0.187	0.287	6.265	20.777	23.207	24.19	
5.5	0.192	0.308	11.021	24.778	27.267	29.013	
6	0.198	0.314	16.749	30.632	32.524	34.19	
6.5	0.219	0.348	20.551	35.221	38.552	39.542	
7	0.248	0.547	24.456	41.342	43.732	45.931	
7.5	0.305	0.587	28.453	46.23	48.763	51.293	
8	0.324	0.861	32.444	52.052	55.071	58.709	
8.5	0.458	0.959	36.547	56.822	61.683	65.735	
9	0.647	1.207	40.168	63.14	68.05	72.629	
9.5	0.692	1.456	43.574	68.128	73.148	79.568	
10	0.849	1.656	47.146	72.444	77.844	87.247	
10.5	0.924	1.87	49.561	75.658	82.138	92.217	
11	1.268	2.138	52.971	79.46	85.18	95.089	
11.5	1.384	2.448	55.648	82.285	87.612	96.862	
12	1.958	2.72	59.157	84.492	89.615	97.399	
12.5	2.068	3.045	61.248	86.214	91.219	98.242	
13	2.483	3.392	63.859	88.054	92.457	98.496	
13.5	2.592	3.658	66.315	89.009	93.289	99.038	
14	2.997	4.184	68.212	90.606	94.473	99.222	
14.5	3.024	4.267	70.814	91.783	95.224	99.348	
15	3.812	6.927	72.355	92.87	95.938	99.569	
15.5	5.248	18.624	73.891	93.987	97.087	99.896	
16	9.012	48.156	75.797	94.87	97.928	100	
16.5	9.197	48.245	76.917	95.549	98.169	100	
17	9.245	48.386	78.794	96.141	98.306	100	
17.5	9.506	48.394	80.099	96.849	99.007	100	
18	9.548	48.522	81.023	97.215	99.068	100	
18.5	9.715	48.629	81.829	97.732	99.251	100	
19	9.784	48.799	82.489	98.012	99.556	100	
19.5	9.814	48.811	83.027	98.343	99.862	100	
20	9.821	48.817	83.712	98.545	100	100	
20.5	9.823	48.929	83.893	98.861	100	100	
21	9.846	48.967	84	99	100	100	

# APPENDIX J

VELOCITY DISTRIBUTION FOR THE 128 ELEMENT MESH OF FIGURE 3.9

Node	x-coord.	y-coord.	Value of u	Value of v
1	0.00000E+00	0.20000E+01	0.00000E+00	0.00000E+00
2	0.14270E+00	0.19950E+01	0.00000E+00	0.00000E+00
3	0.28460E+00	0.19800E+01	0.00000E+00	0.00000E+00
4	0.42510E+00	0.19540E+01	0.00000E+00	0.00000E+00
5	0.56350E+00	0.19190E+01	0.00000E+00	0.00000E+00
6	0.69890E+00	0.18740E+01	0.00000E+00	0.00000E+00
7	0.83080E+00	0.18190E+01	0.00000E+00	0.00000E+00
8	0.95850E+00	0.17550E+01	0.00000E+00	0.00000E+00
9	0.10810E+01	0.16830E+01	0.00000E+00	0.00000E+00
10	0.11990E+01	0.16010E+01	0.00000E+00	0.00000E+00
11	0.13100E+01	0.15110E+01	0.00000E+00	0.00000E+00
12	0.14140E+01	0.14140E+01	0.00000E+00	0.00000E+00
13	0.15110E+01	0.13100E+01	0.00000E+00	0.00000E+00
14	0.16010E+01	0.11990E+01	0.00000E+00	0.00000E+00
15	0.16830E+01	0.10810E+01	0.00000E+00	0.00000E+00
16	0.17550E+01	0.95850E+00	0.00000E+00	0.00000E+00
17	0.18190E+01	0.83080E+00	0.00000E+00	0.00000E+00
18	0.18740E+01	0.69890E+00	0.00000E+00	0.00000E+00
19	0.19190E+01	0.56350E+00	0.00000E+00	0.00000E+00
20	0.19540E+01	0.42510E+00	0.00000E+00	0.00000E+00
21	0.19800E+01	0.28460E+00	0.00000E+00	0.00000E+00
22	0.19950E+01	0.14270E+00	0.00000E+00	0.00000E+00
23	0.20000E+01	0.00000E+00	0.00000E+00	0.00000E+00
24	0.20000E+01	-0.20000E+00	0.00000E+00	0.00000E+00
25	0.20000E+01	-0.40000E+00	0.00000E+00	0.00000E+00
26	0.20000E+01	-0.60000E+00	0.00000E+00	0.00000E+00
27	0.20000E+01	-0.80000E+00	0.00000E+00	0.00000E+00
28	0.20000E+01	-0.10000E+01	0.00000E+00	0.00000E+00
29	0.20000E+01	-0.12000E+01	0.00000E+00	0.00000E+00
30	0.20000E+01	-0.14000E+01	0.00000E+00	0.00000E+00
31	0.20000E+01	-0.16000E+01	0.00000E+00	0.00000E+00
32	0.20000E+01	-0.18000E+01	0.00000E+00	0.00000E+00
33	0.20000E+01	-0.20000E+01	0.00000E+00	0.00000E+00
34	0.00000E+00	0.21250E+01	0.35200E+00	0.00000E+00
35	0.15160E+00	0.21200E+01	0.35911E+00	-0.31514E-01
36	0.30240E+00	0.21030E+01	0.36984E+00	-0.61398E-01
37	0.45170E+00	0.20760E+01	0.38020E+00	-0.90083E-01
38	0.59870E+00	0.20390E+01	0.38896E+00	-0.11927E+00
39	0.74260E+00	0.19910E+01	0.38955E+00	-0.14998E+00
40	0.88280E+00	0.19330E+01	0.38538E+00	-0.17919E+00
41	0.10180E+01	0.18650E+01	0.37556E+00	-0.20637E+00
42	0.11490E+01	0.17880E+01	0.36482E+00	-0.23501E+00
43	0.12730E+01	0.17010E+01	0.34640E+00	-0.26095E+00
44	0.13920E+01	0.16060E+01	0.33029E+00	-0.28608E+00



45	0.15030E+01	0.15030E+01	0.30954E+00	-0.31029E+00
46	0.16060E+01	0.13920E+01	0.28737E+00	-0.33056E+00
47	0.17010E+01	0.12730E+01	0.26128E+00	-0.34924E+00
48	0.17880E+01	0.11490E+01	0.23771E+00	-0.36879E+00
49	0.18650E+01	0.10180E+01	0.20802E+00	-0.38416E+00
50	0.19330E+01	0.88280E+00	0.18374E+00	-0.39842E+00
51	0.19910E+01	0.74260E+00	0.15296E+00	-0.41137E+00
52	0.20390E+01	0.59870E+00	0.12517E+00	-0.42006E+00
53	0.20760E+01	0.45170E+00	0.92970E-01	-0.42388E+00
54	0.21030E+01	0.30240E+00	0.67831E-01	-0.42323E+00
55	0.21200E+01	0.15160E+00	0.35584E-01	-0.41757E+00
56	0.21250E+01	0.00000E+00	0.18083E-01	-0.39379E+00
57	0.21250E+01	-0.20000E+00	0.36428E-02	-0.36678E+00
58	0.21250E+01	-0.40000E+00	0.49288E-02	-0.35696E+00
59	0.21250E+01	-0.60000E+00	-0.52317E-04	-0.35173E+00
60	0.21250E+01	-0.80000E+00	0.17891E-02	-0.35028E+00
61	0.21250E+01	-0.10000E+01	-0.58605E-03	-0.34965E+00
62	0.21250E+01	-0.12000E+01	0.67717E-03	-0.35009E+00
63	0.21250E+01	-0.14000E+01	-0.47154E-03	-0.35045E+00
64	0.21250E+01	-0.16000E+01	0.16685E-03	-0.35113E+00
65	0.21250E+01	-0.18000E+01	-0.26216E-03	-0.35160E+00
66	0.21250E+01	-0.20000E+01	0.00000E+00	-0.35200E+00
67	0.00000E+00	0.22500E+01	0.65600E+00	0.00000E+00
68	0.16050E+00	0.22440E+01	0.66328E+00	-0.66277E-01
69	0.32020E+00	0.22270E+01	0.67918E+00	-0.12232E+00
70	0.47830E+00	0.21990E+01	0.69479E+00	-0.17418E+00
71	0.63390E+00	0.21590E+01	0.70162E+00	-0.22507E+00
72	0.78630E+00	0.21080E+01	0.70082E+00	-0.27534E+00
73	0.93470E+00	0.20470E+01	0.69246E+00	-0.32643E+00
74	0.10780E+01	0.19750E+01	0.67654E+00	-0.37508E+00
75	0.12160E+01	0.18930E+01	0.65243E+00	-0.42438E+00
76	0.13480E+01	0.18010E+01	0.62403E+00	-0.46970E+00
77	0.14730E+01	0.17000E+01	0.58946E+00	-0.51323E+00
78	0.15910E+01	0.15910E+01	0.55409E+00	-0.55443E+00
79	0.17000E+01	0.14730E+01	0.51163E+00	-0.59336E+00
80	0.18010E+01	0.13480E+01	0.47098E+00	-0.62841E+00
81	0.18930E+01	0.12160E+01	0.42350E+00	-0.66276E+00
82	0.19750E+01	0.10780E+01	0.37701E+00	-0.69109E+00
83	0.20470E+01	0.93470E+00	0.32513E+00	-0.71787E+00
84	0.21080E+01	0.78630E+00	0.27642E+00	-0.73641E+00
85	0.21590E+01	0.63390E+00	0.22122E+00	-0.75409E+00
86	0.21990E+01	0.47830E+00	0.17322E+00	-0.76157E+00
87	0.22270E+01	0.32020E+00	0.11877E+00	-0.76118E+00
88	0.22440E+01	0.16050E+00	0.78837E-01	-0.74552E+00
89	0.22500E+01	0.00000E+00	0.39226E-01	-0.71964E+00
90	0.22500E+01	-0.20000E+00	0.20191E-01	-0.68696E+00
91	0.22500E+01	-0.40000E+00	0.58400E-02	-0.66560E+00
92	0.22500E+01	-0.60000E+00	0.47072E-02	-0.65959E+00
93	0.22500E+01	-0.80000E+00	-0.56658E-03	-0.65377E+00
94	0.22500E+01	-0.10000E+01	0.75466E-03	-0.65443E+00
95	0.22500E+01	-0.12000E+01	-0.14804E-02	-0.65300E+00
96	0.22500E+01	-0.14000E+01	-0.29662E-03	-0.65505E+00
97	0.22500E+01	-0.16000E+01	-0.98045E-03	-0.65467E+00

98	0.22500E+01	-0.18000E+01	-0.50842E-03	-0.65638E+00
99	0.22500E+01	-0.20000E+01	0.00000E+00	-0.65600E+00
100	0.00000E+00	0.23750E+01	0.91400E+00	0.00000E+00
101	0.16940E+00	0.23690E+01	0.92089E+00	-0.98693E-01
102	0.33800E+00	0.23510E+01	0.93508E+00	-0.17729E+00
103	0.50480E+00	0.23210E+01	0.94622E+00	-0.24636E+00
104	0.66910E+00	0.22790E+01	0.95063E+00	-0.31227E+00
105	0.83000E+00	0.22250E+01	0.94487E+00	-0.37775E+00
106	0.98660E+00	0.21600E+01	0.93047E+00	-0.44269E+00
107	0.11380E+01	0.20840E+01	0.90696E+00	-0.50719E+00
108	0.12840E+01	0.19980E+01	0.87659E+00	-0.57119E+00
109	0.14230E+01	0.19010E+01	0.83712E+00	-0.63202E+00
110	0.15550E+01	0.17950E+01	0.79388E+00	-0.68989E+00
111	0.16790E+01	0.16790E+01	0.74290E+00	-0.74525E+00
112	0.17950E+01	0.15550E+01	0.68951E+00	-0.79709E+00
113	0.19010E+01	0.14230E+01	0.63079E+00	-0.84449E+00
114	0.19980E+01	0.12840E+01	0.57063E+00	-0.88797E+00
115	0.20840E+01	0.11380E+01	0.50424E+00	-0.92675E+00
116	0.21600E+01	0.98660E+00	0.43893E+00	-0.95952E+00
117	0.22250E+01	0.83000E+00	0.36953E+00	-0.98848E+00
118	0.22790E+01	0.66910E+00	0.30237E+00	-0.10088E+01
119	0.23210E+01	0.50480E+00	0.23328E+00	-0.10219E+01
120	0.23510E+01	0.33800E+00	0.17152E+00	-0.10213E+01
121	0.23690E+01	0.16940E+00	0.11279E+00	-0.10102E+01
122	0.23750E+01	0.00000E+00	0.69948E-01	-0.98365E+00
123	0.23750E+01	-0.20000E+00	0.34490E-01	-0.94981E+00
124	0.23750E+01	-0.40000E+00	0.18179E-01	-0.93121E+00
125	0.23750E+01	-0.60000E+00	0.72759E-02	-0.91853E+00
126	0.23750E+01	-0.80000E+00	0.38067E-02	-0.91498E+00
127	0.23750E+01	-0.10000E+01	0.14626E-03	-0.91156E+00
128	0.23750E+01	-0.12000E+01	-0.16833E-03	-0.91254E+00
129	0.23750E+01	-0.14000E+01	-0.12709E-02	-0.91192E+00
130	0.23750E+01	-0.16000E+01	-0.96018E-03	-0.91372E+00
131	0.23750E+01	-0.18000E+01	-0.75936E-03	-0.91342E+00
132	0.23750E+01	-0.20000E+01	0.00000E+00	-0.91400E+00
133	0.00000E+00	0.25000E+01	0.11250E+01	0.00000E+00
134	0.17830E+00	0.24940E+01	0.11300E+01	-0.12599E+00
135	0.35580E+00	0.24750E+01	0.11383E+01	-0.22267E+00
136	0.53140E+00	0.24430E+01	0.11436E+01	-0.30477E+00
137	0.70430E+00	0.23990E+01	0.11425E+01	-0.38190E+00
138	0.87370E+00	0.23420E+01	0.11313E+01	-0.45717E+00
139	0.10390E+01	0.22740E+01	0.11114E+01	-0.53296E+00
140	0.11980E+01	0.21940E+01	0.10815E+01	-0.60772E+00
141	0.13520E+01	0.21030E+01	0.10431E+01	-0.68220E+00
142	0.14980E+01	0.20010E+01	0.99655E+00	-0.75325E+00
143	0.16370E+01	0.18890E+01	0.94320E+00	-0.82205E+00
144	0.17680E+01	0.17680E+01	0.88493E+00	-0.88731E+00
145	0.18890E+01	0.16370E+01	0.81860E+00	-0.94917E+00
146	0.20010E+01	0.14980E+01	0.75109E+00	-0.10041E+01
147	0.21030E+01	0.13520E+01	0.67665E+00	-0.10577E+01
148	0.21940E+01	0.11980E+01	0.60116E+00	-0.11016E+01
149	0.22740E+01	0.10390E+01	0.52016E+00	-0.11437E+01
150	0.23420E+01	0.87370E+00	0.44112E+00	-0.11739E+01

151	0.23990E+01	0.70430E+00	0.35836E+00	-0.12017E+01
152	0.24430E+01	0.53140E+00	0.28212E+00	-0.12137E+01
153	0.24750E+01	0.35580E+00	0.20616E+00	-0.12207E+01
154	0.24940E+01	0.17830E+00	0.14422E+00	-0.12095E+01
155	0.25000E+01	0.00000E+00	0.88836E-01	-0.11879E+01
156	0.25000E+01	-0.20000E+00	0.51847E-01	-0.11629E+01
157	0.25000E+01	-0.40000E+00	0.24539E-01	-0.11398E+01
158	0.25000E+01	-0.60000E+00	0.13453E-01	-0.11329E+01
159	0.25000E+01	-0.80000E+00	0.38778E-02	-0.11236E+01
160	0.25000E+01	-0.10000E+01	0.16907E-02	-0.11247E+01
161	0.25000E+01	-0.12000E+01	-0.15181E-02	-0.11210E+01
162	0.25000E+01	-0.14000E+01	-0.12673E-02	-0.11243E+01
163	0.25000E+01	-0.16000E+01	-0.18747E-02	-0.11224E+01
164	0.25000E+01	-0.18000E+01	-0.10782E-02	-0.11255E+01
165	0.25000E+01	-0.20000E+01	0.00000E+00	-0.11250E+01
166	0.00000E+00	0.26250E+01	0.12890E+01	0.00000E+00
167	0.18730E+00	0.26180E+01	0.12900E+01	-0.14676E+00
168	0.37360E+00	0.25980E+01	0.12920E+01	-0.25635E+00
169	0.55800E+00	0.25650E+01	0.12897E+01	-0.34815E+00
170	0.73950E+00	0.25190E+01	0.12813E+01	-0.43209E+00
171	0.91730E+00	0.24590E+01	0.12633E+01	-0.51401E+00
172	0.10900E+01	0.23880E+01	0.12379E+01	-0.59539E+00
173	0.12580E+01	0.23040E+01	0.12024E+01	-0.67785E+00
174	0.14190E+01	0.22080E+01	0.11582E+01	-0.75759E+00
175	0.15730E+01	0.21010E+01	0.11055E+01	-0.83688E+00
176	0.17190E+01	0.19840E+01	0.10472E+01	-0.91196E+00
177	0.18560E+01	0.18560E+01	0.98057E+00	-0.98447E+00
178	0.19840E+01	0.17190E+01	0.90894E+00	-0.10518E+01
179	0.21010E+01	0.15730E+01	0.83197E+00	-0.11140E+01
180	0.22080E+01	0.14190E+01	0.75065E+00	-0.11705E+01
181	0.23040E+01	0.12580E+01	0.66576E+00	-0.12222E+01
182	0.23880E+01	0.10900E+01	0.57782E+00	-0.12652E+01
183	0.24590E+01	0.91730E+00	0.48838E+00	-0.13019E+01
184	0.25190E+01	0.73950E+00	0.40055E+00	-0.13292E+01
185	0.25650E+01	0.55800E+00	0.31416E+00	-0.13488E+01
186	0.25980E+01	0.37360E+00	0.23518E+00	-0.13553E+01
187	0.26180E+01	0.18730E+00	0.16418E+00	-0.13538E+01
188	0.26250E+01	0.00000E+00	0.10841E+00	-0.13395E+01
189	0.26250E+01	-0.20000E+00	0.63035E-01	-0.13187E+01
190	0.26250E+01	-0.40000E+00	0.35285E-01	-0.13066E+01
191	0.26250E+01	-0.60000E+00	0.17098E-01	-0.12950E+01
192	0.26250E+01	-0.80000E+00	0.79168E-02	-0.12921E+01
193	0.26250E+01	-0.10000E+01	0.18243E-02	-0.12877E+01
194	0.26250E+01	-0.12000E+01	-0.39254E-03	-0.12888E+01
195	0.26250E+01	-0.14000E+01	-0.19371E-02	-0.12872E+01
196	0.26250E+01	-0.16000E+01	-0.18253E-02	-0.12893E+01
197	0.26250E+01	-0.18000E+01	-0.14110E-02	-0.12883E+01
198	0.26250E+01	-0.20000E+01	0.00000E+00	-0.12890E+01
199	0.00000E+00	0.27500E+01	0.14060E+01	0.00000E+00
200	0.19620E+00	0.27430E+01	0.14044E+01	-0.16070E+00
201	0.39140E+00	0.27220E+01	0.13988E+01	-0.27882E+00
202	0.58460E+00	0.26870E+01	0.13882E+01	-0.37620E+00
203	0.77480E+00	0.26390E+01	0.13721E+01	-0.46439E+00

204	0.96100E+00	0.25770E+01	0.13478E+01	-0.54930E+00
205	0.11420E+01	0.25010E+01	0.13148E+01	-0.63445E+00
206	0.13180E+01	0.24140E+01	0.12752E+01	-0.71948E+00
207	0.14870E+01	0.23130E+01	0.12268E+01	-0.80395E+00
208	0.16480E+01	0.22010E+01	0.11705E+01	-0.88634E+00
209	0.18010E+01	0.20780E+01	0.11074E+01	-0.96600E+00
210	0.19450E+01	0.19450E+01	0.10377E+01	-0.10414E+01
211	0.20780E+01	0.18010E+01	0.96092E+00	-0.11133E+01
212	0.22010E+01	0.16480E+01	0.88028E+00	-0.11775E+01
213	0.23130E+01	0.14870E+01	0.79334E+00	-0.12391E+01
214	0.24140E+01	0.13180E+01	0.70390E+00	-0.12908E+01
215	0.25010E+01	0.11420E+01	0.61041E+00	-0.13386E+01
216	0.25770E+01	0.96100E+00	0.51701E+00	-0.13761E+01
217	0.26390E+01	0.77480E+00	0.42349E+00	-0.14095E+01
218	0.26870E+01	0.58460E+00	0.33443E+00	-0.14278E+01
219	0.27220E+01	0.39140E+00	0.25002E+00	-0.14434E+01
220	0.27430E+01	0.19620E+00	0.17799E+00	-0.14431E+01
221	0.27500E+01	0.00000E+00	0.11687E+00	-0.14372E+01
222	0.27500E+01	-0.20000E+00	0.72536E-01	-0.14290E+01
223	0.27500E+01	-0.40000E+00	0.39972E-01	-0.14146E+01
224	0.27500E+01	-0.60000E+00	0.21541E-01	-0.14133E+01
225	0.27500E+01	-0.80000E+00	0.87384E-02	-0.14049E+01
226	0.27500E+01	-0.10000E+01	0.30692E-02	-0.14074E+01
227	0.27500E+01	-0.12000E+01	-0.97855E-03	-0.14028E+01
228	0.27500E+01	-0.14000E+01	-0.18826E-02	-0.14067E+01
229	0.27500E+01	-0.16000E+01	-0.24494E-02	-0.14036E+01
230	0.27500E+01	-0.18000E+01	-0.15165E-02	-0.14072E+01
231	0.27500E+01	-0.20000E+01	0.00000E+00	-0.14060E+01
232	0.00000E+00	0.28750E+01	0.14770E+01	0.00000E+00
233	0.20510E+00	0.28680E+01	0.14716E+01	-0.16742E+00
234	0.40920E+00	0.28460E+01	0.14585E+01	-0.28941E+00
235	0.61110E+00	0.28090E+01	0.14394E+01	-0.38900E+00
236	0.81000E+00	0.27590E+01	0.14154E+01	-0.47822E+00
237	0.10050E+01	0.26940E+01	0.13855E+01	-0.56427E+00
238	0.11940E+01	0.26150E+01	0.13486E+01	-0.65018E+00
239	0.13780E+01	0.25230E+01	0.13045E+01	-0.73623E+00
240	0.15540E+01	0.24190E+01	0.12537E+01	-0.82049E+00
241	0.17230E+01	0.23020E+01	0.11950E+01	-0.90476E+00
242	0.18830E+01	0.21730E+01	0.11300E+01	-0.98457E+00
243	0.20330E+01	0.20330E+01	0.10578E+01	-0.10621E+01
244	0.21730E+01	0.18830E+01	0.97977E+00	-0.11342E+01
245	0.23020E+01	0.17230E+01	0.89715E+00	-0.12013E+01
246	0.24190E+01	0.15540E+01	0.80862E+00	-0.12617E+01
247	0.25230E+01	0.13780E+01	0.71756E+00	-0.13165E+01
248	0.26150E+01	0.11940E+01	0.62286E+00	-0.13630E+01
249	0.26940E+01	0.10050E+01	0.52685E+00	-0.14040E+01
250	0.27590E+01	0.81000E+00	0.43225E+00	-0.14344E+01
251	0.28090E+01	0.61110E+00	0.34106E+00	-0.14600E+01
252	0.28460E+01	0.40920E+00	0.25646E+00	-0.14751E+01
253	0.28680E+01	0.20510E+00	0.18221E+00	-0.14859E+01
254	0.28750E+01	0.00000E+00	0.12162E+00	-0.14880E+01
255	0.28750E+01	-0.20000E+00	0.76105E-01	-0.14846E+01
256	0.28750E+01	-0.40000E+00	0.44454E-01	-0.14840E+01

257	0.28750E+01	-0.60000E+00	0.23354E-01	-0.14786E+01
258	0.28750E+01	-0.80000E+00	0.10795E-01	-0.14792E+01
259	0.28750E+01	-0.10000E+01	0.32999E-02	-0.14759E+01
260	0.28750E+01	-0.12000E+01	-0.35391E-03	-0.14777E+01
261	0.28750E+01	-0.14000E+01	-0.21670E-02	-0.14756E+01
262	0.28750E+01	-0.16000E+01	-0.24028E-02	-0.14776E+01
263	0.28750E+01	-0.18000E+01	-0.17197E-02	-0.14761E+01
264	0.28750E+01	-0.20000E+01	0.00000E+00	-0.14770E+01
265	0.00000E+00	0.30000E+01	0.15000E+01	0.00000E+00
266	0.21400E+00	0.29920E+01	0.14918E+01	-0.16742E+00
267	0.42690E+00	0.29690E+01	0.14721E+01	-0.28880E+00
268	0.63770E+00	0.29310E+01	0.14459E+01	-0.38740E+00
269	0.84520E+00	0.28780E+01	0.14149E+01	-0.47556E+00
270	0.10480E+01	0.28110E+01	0.13796E+01	-0.55955E+00
271	0.12460E+01	0.27290E+01	0.13393E+01	-0.64431E+00
272	0.14380E+01	0.26330E+01	0.12929E+01	-0.72837E+00
273	0.16220E+01	0.25240E+01	0.12408E+01	-0.81210E+00
274	0.17980E+01	0.24020E+01	0.11815E+01	-0.89389E+00
275	0.19650E+01	0.22670E+01	0.11168E+01	-0.97349E+00
276	0.21210E+01	0.21210E+01	0.10453E+01	-0.10490E+01
277	0.22670E+01	0.19650E+01	0.96818E+00	-0.11209E+01
278	0.24020E+01	0.17980E+01	0.88580E+00	-0.11855E+01
279	0.25240E+01	0.16220E+01	0.79925E+00	-0.12470E+01
280	0.26330E+01	0.14380E+01	0.70821E+00	-0.12990E+01
281	0.27290E+01	0.12460E+01	0.61529E+00	-0.13477E+01
282	0.28110E+01	0.10480E+01	0.51956E+00	-0.13853E+01
283	0.28780E+01	0.84520E+00	0.42718E+00	-0.14205E+01
284	0.29310E+01	0.63770E+00	0.33617E+00	-0.14437E+01
285	0.29690E+01	0.42690E+00	0.25297E+00	-0.14670E+01
286	0.29920E+01	0.21400E+00	0.17921E+00	-0.14783E+01
287	0.30000E+01	0.00000E+00	0.11908E+00	-0.14899E+01
288	0.30000E+01	-0.20000E+00	0.75926E-01	-0.14983E+01
289	0.30000E+01	-0.40000E+00	0.44758E-01	-0.14955E+01
290	0.30000E+01	-0.60000E+00	0.24010E-01	-0.15017E+01
291	0.30000E+01	-0.80000E+00	0.11051E-01	-0.14971E+01
292	0.30000E+01	-0.10000E+01	0.35773E-02	-0.15018E+01
293	0.30000E+01	-0.12000E+01	-0.38589E-03	-0.14975E+01
294	0.30000E+01	-0.14000E+01	-0.21519E-02	-0.15015E+01
295	0.30000E+01	-0.16000E+01	-0.25117E-02	-0.14979E+01
296	0.30000E+01	-0.18000E+01	-0.18303E-02	-0.15014E+01
297	0.30000E+01	-0.20000E+01	0.00000E+00	-0.15000E+01
298	0.00000E+00	0.31250E+01	0.14770E+01	0.00000E+00
299	0.22290E+00	0.31170E+01	0.14656E+01	-0.16097E+00
300	0.44470E+00	0.30930E+01	0.14401E+01	-0.27753E+00
301	0.66430E+00	0.30540E+01	0.14076E+01	-0.37207E+00
302	0.88040E+00	0.29980E+01	0.13718E+01	-0.45647E+00
303	0.10920E+01	0.29280E+01	0.13327E+01	-0.53750E+00
304	0.12980E+01	0.28430E+01	0.12900E+01	-0.61771E+00
305	0.14980E+01	0.27430E+01	0.12427E+01	-0.69857E+00
306	0.16900E+01	0.26290E+01	0.11909E+01	-0.77858E+00
307	0.18730E+01	0.25020E+01	0.11337E+01	-0.85711E+00
308	0.20460E+01	0.23620E+01	0.10711E+01	-0.93223E+00
309	0.22100E+01	0.22100E+01	0.10018E+01	-0.10052E+01

310	0.23620E+01	0.20460E+01	0.92721E+00	-0.10736E+01
311	0.25020E+01	0.18730E+01	0.84914E+00	-0.11364E+01
312	0.26290E+01	0.16900E+01	0.76544E+00	-0.11930E+01
313	0.27430E+01	0.14980E+01	0.67865E+00	-0.12446E+01
314	0.28430E+01	0.12980E+01	0.58818E+00	-0.12890E+01
315	0.29280E+01	0.10920E+01	0.49806E+00	-0.13286E+01
316	0.29980E+01	0.88040E+00	0.40750E+00	-0.13596E+01
317	0.30540E+01	0.66430E+00	0.32109E+00	-0.13874E+01
318	0.30930E+01	0.44470E+00	0.23969E+00	-0.14085E+01
319	0.31170E+01	0.22290E+00	0.16951E+00	-0.14300E+01
320	0.31250E+01	0.00000E+00	0.11083E+00	-0.14481E+01
321	0.31250E+01	-0.20000E+00	0.71568E-01	-0.14602E+01
322	0.31250E+01	-0.40000E+00	0.42087E-01	-0.14709E+01
323	0.31250E+01	-0.60000E+00	0.22908E-01	-0.14728E+01
324	0.31250E+01	-0.80000E+00	0.10358E-01	-0.14776E+01
325	0.31250E+01	-0.10000E+01	0.34652E-02	-0.14763E+01
326	0.31250E+01	-0.12000E+01	-0.50200E-03	-0.14787E+01
327	0.31250E+01	-0.14000E+01	-0.20580E-02	-0.14766E+01
328	0.31250E+01	-0.16000E+01	-0.24903E-02	-0.14782E+01
329	0.31250E+01	-0.18000E+01	-0.18323E-02	-0.14763E+01
330	0.31250E+01	-0.20000E+01	0.00000E+00	-0.14770E+01
331	0.00000E+00	0.32500E+01	0.14060E+01	0.00000E+00
332	0.23190E+00	0.32420E+01	0.13927E+01	-0.14868E+00
333	0.46250E+00	0.32170E+01	0.13627E+01	-0.25648E+00
334	0.69080E+00	0.31760E+01	0.13255E+01	-0.34433E+00
335	0.91560E+00	0.31180E+01	0.12870E+01	-0.42281E+00
336	0.11360E+01	0.30450E+01	0.12459E+01	-0.49877E+00
337	0.13500E+01	0.29560E+01	0.12039E+01	-0.57330E+00
338	0.15580E+01	0.28520E+01	0.11571E+01	-0.64869E+00
339	0.17570E+01	0.27340E+01	0.11079E+01	-0.72294E+00
340	0.19480E+01	0.26020E+01	0.10528E+01	-0.79504E+00
341	0.21280E+01	0.24560E+01	0.99523E+00	-0.86578E+00
342	0.22980E+01	0.22980E+01	0.93008E+00	-0.93284E+00
343	0.24560E+01	0.21280E+01	0.86168E+00	-0.99693E+00
344	0.26020E+01	0.19480E+01	0.78736E+00	-0.10536E+01
345	0.27340E+01	0.17570E+01	0.71153E+00	-0.11081E+01
346	0.28520E+01	0.15580E+01	0.62952E+00	-0.11543E+01
347	0.29560E+01	0.13500E+01	0.54696E+00	-0.11983E+01
348	0.30450E+01	0.11360E+01	0.46112E+00	-0.12315E+01
349	0.31180E+01	0.91560E+00	0.37839E+00	-0.12648E+01
350	0.31760E+01	0.69080E+00	0.29511E+00	-0.12875E+01
351	0.32170E+01	0.46250E+00	0.22110E+00	-0.13151E+01
352	0.32420E+01	0.23190E+00	0.15258E+00	-0.13350E+01
353	0.32500E+01	0.00000E+00	0.99829E-01	-0.13618E+01
354	0.32500E+01	-0.20000E+00	0.62793E-01	-0.13829E+01
355	0.32500E+01	-0.40000E+00	0.38239E-01	-0.13905E+01
356	0.32500E+01	-0.60000E+00	0.19689E-01	-0.14028E+01
357	0.32500E+01	-0.80000E+00	0.98243E-02	-0.14021E+01
358	0.32500E+01	-0.10000E+01	0.26219E-02	-0.14083E+01
359	0.32500E+01	-0.12000E+01	-0.60171E-04	-0.14049E+01
360	0.32500E+01	-0.14000E+01	-0.21000E-02	-0.14086E+01
361	0.32500E+01	-0.16000E+01	-0.20516E-02	-0.14048E+01
362	0.32500E+01	-0.18000E+01	-0.17195E-02	-0.14075E+01

363	0.32500E+01	-0.20000E+01	0.00000E+00	-0.14060E+01
364	0.00000E+00	0.33750E+01	0.12890E+01	0.00000E+00
365	0.24080E+00	0.33660E+01	0.12744E+01	-0.13126E+00
366	0.48030E+00	0.33410E+01	0.12405E+01	-0.22661E+00
367	0.71740E+00	0.32980E+01	0.12020E+01	-0.30573E+00
368	0.95080E+00	0.32380E+01	0.11626E+01	-0.37634E+00
369	0.11790E+01	0.31620E+01	0.11222E+01	-0.44469E+00
370	0.14020E+01	0.30700E+01	0.10808E+01	-0.51164E+00
371	0.16170E+01	0.29620E+01	0.10384E+01	-0.57949E+00
372	0.18250E+01	0.28390E+01	0.99179E+00	-0.64626E+00
373	0.20230E+01	0.27020E+01	0.94268E+00	-0.71079E+00
374	0.22100E+01	0.25510E+01	0.88957E+00	-0.77354E+00
375	0.23860E+01	0.23860E+01	0.83299E+00	-0.83486E+00
376	0.25510E+01	0.22100E+01	0.76960E+00	-0.89042E+00
377	0.27020E+01	0.20230E+01	0.70460E+00	-0.94230E+00
378	0.28390E+01	0.18250E+01	0.63531E+00	-0.98935E+00
379	0.29620E+01	0.16170E+01	0.56338E+00	-0.10330E+01
380	0.30700E+01	0.14020E+01	0.48711E+00	-0.10690E+01
381	0.31620E+01	0.11790E+01	0.41248E+00	-0.11023E+01
382	0.32380E+01	0.95080E+00	0.33536E+00	-0.11289E+01
383	0.32980E+01	0.71740E+00	0.26278E+00	-0.11541E+01
384	0.33410E+01	0.48030E+00	0.19197E+00	-0.11757E+01
385	0.33660E+01	0.24080E+00	0.13250E+00	-0.12042E+01
386	0.33750E+01	0.00000E+00	0.81852E-01	-0.12339E+01
387	0.33750E+01	-0.20000E+00	0.52568E-01	-0.12568E+01
388	0.33750E+01	-0.40000E+00	0.29809E-01	-0.12749E+01
389	0.33750E+01	-0.60000E+00	0.16424E-01	-0.12820E+01
390	0.33750E+01	-0.80000E+00	0.67724E-02	-0.12892E+01
391	0.33750E+01	-0.10000E+01	0.23298E-02	-0.12895E+01
392	0.33750E+01	-0.12000E+01	-0.84978E-03	-0.12919E+01
393	0.33750E+01	-0.14000E+01	-0.16134E-02	-0.12900E+01
394	0.33750E+01	-0.16000E+01	-0.20429E-02	-0.12910E+01
395	0.33750E+01	-0.18000E+01	-0.13189E-02	-0.12888E+01
396	0.33750E+01	-0.20000E+01	0.00000E+00	-0.12890E+01
397	0.00000E+00	0.35000E+01	0.11250E+01	0.00000E+00
398	0.24970E+00	0.34910E+01	0.11097E+01	-0.10920E+00
399	0.49810E+00	0.34640E+01	0.10763E+01	-0.18983E+00
400	0.74400E+00	0.34200E+01	0.10375E+01	-0.25753E+00
401	0.98610E+00	0.33580E+01	0.99971E+00	-0.31821E+00
402	0.12230E+01	0.32790E+01	0.96242E+00	-0.37723E+00
403	0.14540E+01	0.31840E+01	0.92450E+00	-0.43466E+00
404	0.16770E+01	0.30720E+01	0.88681E+00	-0.49300E+00
405	0.18920E+01	0.29440E+01	0.84756E+00	-0.55055E+00
406	0.20970E+01	0.28020E+01	0.80433E+00	-0.60564E+00
407	0.22920E+01	0.26450E+01	0.75947E+00	-0.65967E+00
408	0.24750E+01	0.24750E+01	0.70911E+00	-0.71064E+00
409	0.26450E+01	0.22920E+01	0.65756E+00	-0.75929E+00
410	0.28020E+01	0.20970E+01	0.60015E+00	-0.80313E+00
411	0.29440E+01	0.18920E+01	0.54320E+00	-0.84421E+00
412	0.30720E+01	0.16770E+01	0.47914E+00	-0.87931E+00
413	0.31840E+01	0.14540E+01	0.41684E+00	-0.91153E+00
414	0.32790E+01	0.12230E+01	0.34987E+00	-0.93851E+00
415	0.33580E+01	0.98610E+00	0.28727E+00	-0.96411E+00

416	0.34200E+01	0.74400E+00	0.22045E+00	-0.98249E+00
417	0.34640E+01	0.49810E+00	0.16288E+00	-0.10080E+01
418	0.34910E+01	0.24970E+00	0.10596E+00	-0.10299E+01
419	0.35000E+01	0.00000E+00	0.65830E-01	-0.10650E+01
420	0.35000E+01	-0.20000E+00	0.38290E-01	-0.10929E+01
421	0.35000E+01	-0.40000E+00	0.24127E-01	-0.11059E+01
422	0.35000E+01	-0.60000E+00	0.10828E-01	-0.11203E+01
423	0.35000E+01	-0.80000E+00	0.63333E-02	-0.11218E+01
424	0.35000E+01	-0.10000E+01	0.80832E-03	-0.11276E+01
425	0.35000E+01	-0.12000E+01	0.19214E-03	-0.11251E+01
426	0.35000E+01	-0.14000E+01	-0.16539E-02	-0.11277E+01
427	0.35000E+01	-0.16000E+01	-0.11597E-02	-0.11244E+01
428	0.35000E+01	-0.18000E+01	-0.10037E-02	-0.11261E+01
429	0.35000E+01	-0.20000E+01	0.00000E+00	-0.11250E+01
430	0.00000E+00	0.36250E+01	0.91400E+00	0.00000E+00
431	0.25860E+00	0.36160E+01	0.89874E+00	-0.83609E-01
432	0.51590E+00	0.35880E+01	0.86818E+00	-0.14696E+00
433	0.77050E+00	0.35420E+01	0.83367E+00	-0.20108E+00
434	0.10210E+01	0.34780E+01	0.80019E+00	-0.25036E+00
435	0.12670E+01	0.33960E+01	0.76857E+00	-0.29752E+00
436	0.15060E+01	0.32970E+01	0.73720E+00	-0.34448E+00
437	0.17370E+01	0.31820E+01	0.70536E+00	-0.39032E+00
438	0.19600E+01	0.30500E+01	0.67227E+00	-0.43577E+00
439	0.21720E+01	0.29020E+01	0.63936E+00	-0.48069E+00
440	0.23740E+01	0.27400E+01	0.60179E+00	-0.52295E+00
441	0.25630E+01	0.25630E+01	0.56414E+00	-0.56471E+00
442	0.27400E+01	0.23740E+01	0.52063E+00	-0.60174E+00
443	0.29020E+01	0.21720E+01	0.47735E+00	-0.63768E+00
444	0.30500E+01	0.19600E+01	0.42907E+00	-0.66852E+00
445	0.31820E+01	0.17370E+01	0.38106E+00	-0.69787E+00
446	0.32970E+01	0.15060E+01	0.32947E+00	-0.72333E+00
447	0.33960E+01	0.12670E+01	0.27851E+00	-0.74579E+00
448	0.34780E+01	0.10210E+01	0.22495E+00	-0.76342E+00
449	0.35420E+01	0.77060E+00	0.17466E+00	-0.78154E+00
450	0.35880E+01	0.51590E+00	0.12299E+00	-0.79822E+00
451	0.36160E+01	0.25860E+00	0.80199E-01	-0.82222E+00
452	0.36250E+01	0.00000E+00	0.42265E-01	-0.85615E+00
453	0.36250E+01	-0.20000E+00	0.26347E-01	-0.88225E+00
454	0.36250E+01	-0.40000E+00	0.12995E-01	-0.90099E+00
455	0.36250E+01	-0.60000E+00	0.75850E-02	-0.90877E+00
456	0.36250E+01	-0.80000E+00	0.21180E-02	-0.91514E+00
457	0.36250E+01	-0.10000E+01	0.95485E-03	-0.91565E+00
458	0.36250E+01	-0.12000E+01	-0.10094E-02	-0.91717E+00
459	0.36250E+01	-0.14000E+01	-0.82962E-03	-0.91555E+00
460	0.36250E+01	-0.16000E+01	-0.11152E-02	-0.91578E+00
461	0.36250E+01	-0.18000E+01	-0.60038E-03	-0.91406E+00
462	0.36250E+01	-0.20000E+01	0.00000E+00	-0.91400E+00
463	0.00000E+00	0.37500E+01	0.65600E+00	0.00000E+00
464	0.26750E+00	0.37400E+01	0.64506E+00	-0.56138E-01
465	0.53370E+00	0.37120E+01	0.61779E+00	-0.99638E-01
466	0.79710E+00	0.36640E+01	0.59209E+00	-0.13841E+00
467	0.10560E+01	0.35980E+01	0.56573E+00	-0.17344E+00
468	0.13100E+01	0.35140E+01	0.54136E+00	-0.20684E+00



469	0.15580E+01	0.34110E+01	0.51921E+00	-0.24043E+00
470	0.17970E+01	0.32910E+01	0.49682E+00	-0.27409E+00
471	0.20270E+01	0.31550E+01	0.47356E+00	-0.30571E+00
472	0.22470E+01	0.30020E+01	0.44910E+00	-0.33750E+00
473	0.24560E+01	0.28340E+01	0.42339E+00	-0.36728E+00
474	0.26520E+01	0.26520E+01	0.39476E+00	-0.39537E+00
475	0.28340E+01	0.24560E+01	0.36694E+00	-0.42249E+00
476	0.30020E+01	0.22470E+01	0.33489E+00	-0.44782E+00
477	0.31550E+01	0.20270E+01	0.30306E+00	-0.47013E+00
478	0.32910E+01	0.17970E+01	0.26745E+00	-0.49060E+00
479	0.34110E+01	0.15580E+01	0.23318E+00	-0.50815E+00
480	0.35140E+01	0.13100E+01	0.19362E+00	-0.52232E+00
481	0.35980E+01	0.10560E+01	0.16040E+00	-0.53693E+00
482	0.36640E+01	0.79710E+00	0.11971E+00	-0.54814E+00
483	0.37120E+01	0.53370E+00	0.87592E-01	-0.56212E+00
484	0.37400E+01	0.26750E+00	0.49973E-01	-0.57826E+00
485	0.37500E+01	0.00000E+00	0.27009E-01	-0.60876E+00
486	0.37500E+01	-0.20000E+00	0.11625E-01	-0.63361E+00
487	0.37500E+01	-0.40000E+00	0.96430E-02	-0.64441E+00
488	0.37500E+01	-0.60000E+00	0.21185E-02	-0.65450E+00
489	0.37500E+01	-0.80000E+00	0.31483E-02	-0.65589E+00
490	0.37500E+01	-0.10000E+01	-0.54757E-03	-0.65900E+00
491	0.37500E+01	-0.12000E+01	0.70401E-03	-0.65749E+00
492	0.37500E+01	-0.14000E+01	-0.89821E-03	-0.65834E+00
493	0.37500E+01	-0.16000E+01	-0.13996E-03	-0.65647E+00
494	0.37500E+01	-0.18000E+01	-0.17064E-03	-0.65692E+00
495	0.37500E+01	-0.20000E+01	0.00000E+00	-0.65600E+00
496	0.00000E+00	0.38750E+01	0.35200E+00	0.00000E+00
497	0.27640E+00	0.38650E+01	0.34400E+00	-0.27449E-01
498	0.55150E+00	0.38360E+01	0.32771E+00	-0.50263E-01
499	0.82370E+00	0.37860E+01	0.31382E+00	-0.70596E-01
500	0.10920E+01	0.37180E+01	0.29811E+00	-0.90184E-01
501	0.13540E+01	0.36310E+01	0.28490E+00	-0.10714E+00
502	0.16100E+01	0.35250E+01	0.27229E+00	-0.12567E+00
503	0.18570E+01	0.34010E+01	0.26103E+00	-0.14318E+00
504	0.20950E+01	0.32600E+01	0.24776E+00	-0.16015E+00
505	0.23220E+01	0.31020E+01	0.23578E+00	-0.17673E+00
506	0.25380E+01	0.29290E+01	0.22016E+00	-0.19158E+00
507	0.27400E+01	0.27400E+01	0.20737E+00	-0.20720E+00
508	0.29290E+01	0.25380E+01	0.19060E+00	-0.22032E+00
509	0.31020E+01	0.23220E+01	0.17611E+00	-0.23468E+00
510	0.32600E+01	0.20950E+01	0.15777E+00	-0.24629E+00
511	0.34010E+01	0.18570E+01	0.14093E+00	-0.25716E+00
512	0.35250E+01	0.16100E+01	0.12065E+00	-0.26616E+00
513	0.36310E+01	0.13540E+01	0.10227E+00	-0.27368E+00
514	0.37180E+01	0.10920E+01	0.81595E-01	-0.28099E+00
515	0.37860E+01	0.82370E+00	0.63770E-01	-0.28785E+00
516	0.38360E+01	0.55150E+00	0.40538E-01	-0.29279E+00
517	0.38650E+01	0.27640E+00	0.26098E-01	-0.30333E+00
518	0.38750E+01	0.00000E+00	0.36740E-02	-0.32292E+00
519	0.38750E+01	-0.20000E+00	0.54526E-02	-0.33855E+00
520	0.38750E+01	-0.40000E+00	-0.61894E-03	-0.34727E+00
521	0.38750E+01	-0.60000E+00	0.17542E-02	-0.35095E+00

522	0.38750E+01	-0.80000E+00	-0.11490E-02	-0.35290E+00
523	0.38750E+01	-0.10000E+01	0.54016E-03	-0.35319E+00
524	0.38750E+01	-0.12000E+01	-0.92796E-03	-0.35317E+00
525	0.38750E+01	-0.14000E+01	0.96913E-04	-0.35260E+00
526	0.38750E+01	-0.16000E+01	-0.49748E-03	-0.35221E+00
527	0.38750E+01	-0.18000E+01	0.76556E-04	-0.35189E+00
528	0.38750E+01	-0.20000E+01	0.00000E+00	-0.35200E+00
529	0.00000E+00	0.40000E+01	0.00000E+00	0.00000E+00
530	0.28540E+00	0.39900E+01	0.00000E+00	0.00000E+00
531	0.56930E+00	0.39590E+01	0.00000E+00	0.00000E+00
532	0.85030E+00	0.39090E+01	0.00000E+00	0.00000E+00
533	0.11270E+01	0.38380E+01	0.00000E+00	0.00000E+00
534	0.13980E+01	0.37480E+01	0.00000E+00	0.00000E+00
535	0.16620E+01	0.36390E+01	0.00000E+00	0.00000E+00
536	0.19170E+01	0.35110E+01	0.00000E+00	0.00000E+00
537	0.21630E+01	0.33650E+01	0.00000E+00	0.00000E+00
538	0.23970E+01	0.32020E+01	0.00000E+00	0.00000E+00
539	0.26190E+01	0.30230E+01	0.00000E+00	0.00000E+00
540	0.28280E+01	0.28280E+01	0.00000E+00	0.00000E+00
541	0.30230E+01	0.26190E+01	0.00000E+00	0.00000E+00
542	0.32020E+01	0.23970E+01	0.00000E+00	0.00000E+00
543	0.33650E+01	0.21630E+01	0.00000E+00	0.00000E+00
544	0.35110E+01	0.19170E+01	0.00000E+00	0.00000E+00
545	0.36390E+01	0.16620E+01	0.00000E+00	0.00000E+00
546	0.37480E+01	0.13980E+01	0.00000E+00	0.00000E+00
547	0.38380E+01	0.11270E+01	0.00000E+00	0.00000E+00
548	0.39090E+01	0.85030E+00	0.00000E+00	0.00000E+00
549	0.39590E+01	0.56930E+00	0.00000E+00	0.00000E+00
550	0.39900E+01	0.28540E+00	0.00000E+00	0.00000E+00
551	0.40000E+01	0.00000E+00	0.00000E+00	0.00000E+00
552	0.40000E+01	-0.20000E+00	0.00000E+00	0.00000E+00
553	0.40000E+01	-0.40000E+00	0.00000E+00	0.00000E+00
554	0.40000E+01	-0.60000E+00	0.00000E+00	0.00000E+00
555	0.40000E+01	-0.80000E+00	0.00000E+00	0.00000E+00
556	0.40000E+01	-0.10000E+01	0.00000E+00	0.00000E+00
557	0.40000E+01	-0.12000E+01	0.00000E+00	0.00000E+00
558	0.40000E+01	-0.14000E+01	0.00000E+00	0.00000E+00
559	0.40000E+01	-0.16000E+01	0.00000E+00	0.00000E+00
560	0.40000E+01	-0.18000E+01	0.00000E+00	0.00000E+00
561	0.40000E+01	-0.20000E+01	0.00000E+00	0.00000E+00

## REFERENCES

- Akin, J.E.: *Finite Elements for Analysis and Design*, Academic Press, California, 1994.
- Chandrupatla, T.R., and A.D. Belegundu: *Introduction to Finite Elements in Engineering*, Prentice Hall, New Jersey, 1991.
- Chen, R.Y., H.C. Chiou, and D. Sun: "Deposition of Particles in a Convergent Channel," *Powder Technology*, vol. PTE087/1, pp.83-86, 1996.
- Emanuel, G.: *Analytical Fluid Dynamics*, CRC Press, Florida, 1994
- Fox, R.W., and A.T. McDonald: *Introduction to Fluid Mechanics*, 4th ed., John Wiley & Sons, New York, 1992.
- Gutfinger, C., and D. Pnueli: *Fluid Mechanics*, Cambridge University Press, New York, 1992.
- Hesketh, H.E.: *Fine Particles in Gaseous Media*, 2nd ed., Lewis Publishers, 1986.
- Reddy, J.N.: *An Introduction to the Finite Element Method*, 2nd ed., McGraw-Hill, New York, 1993.
- Ross, C.T.F.: *Finite Element Programs for Axisymmetric Problems in Engineering*, John Wiley & Sons, New York, 1984.
- Warsi, Z.U.A., *Fluid Dynamics: Theoretical and Computational Approaches*, CRC Press, Florida, 1993.